SOLID PHASE MICROEXTRACTION IN AQUEOUS SAMPLE ANALYSIS

by

Wennan Zhao

A thesis
presented to the University of Waterloo
in fulfillment of the
thesis requirement for the degree of
Doctor of Philosophy
in
Chemistry

Waterloo, Ontario, Canada, 2008

AUTHOR'S DECLARATION

I hereby declare that I am the sole author of this thesis. This is a true copy of the thesis, including any required final revisions, as accepted by my examiners.

I understand that my thesis may be made electronically available to the public.

Abstract

This thesis presents enhanced analytical methods developed for complex aqueous sample analysis based on solid phase microextraction (SPME).

First, the laboratory evaluation of the kinetic calibration approach in aqueous sample analysis using SPME is discussed. A modified SPME device, Polydimethylsiloxane (PDMS) rod passive sampler, was developed and the kinetic calibration method based on the standard preloaded in the extraction phase was applied to determine the time-weighted average (TWA) concentration of organic pollutants in water.

Later, the SPME technique was used to investigate the complex interactions between the organic pollutants and humic organic matter (HOM) present in the aqueous samples. The kinetics of the SPME approach in complex aqueous samples was studied. The concentration of freely dissolved analytes and the total concentration of the target analytes in the sample matrix were determined by SPME sampling. The usefulness of the SPME approach for binding studies was further demonstrated by determining the sorption coefficient, a useful parameter for studying the bioavailability of the organic pollutants in the environment.

In addition, the commercial Computational Fluid Dynamics (CFD) software COMSOL Multiphysics was used to predict the kinetics of analyte extraction and flow pattern under different experimental conditions using the SPME technique. A good agreement between the prediction and the experimental data confirms the advantages of the CFD application for experimental optimization thus minimizing the need of extensive experiments.

Acknowledgements

I would like to deeply thank my supervisor, Dr. Janusz Pawliszyn, for providing me the opportunity to work on this interesting and challenging project. His guidance and support encouraged me to go through all the difficulties and to complete my study.

I thank the members of my committee, Dr. George Dixon, Dr. Dan Thomas and Dr. Carey Bissonnette for their advice and efforts during the years of graduate research.

I am very grateful to Dr. Gangfeng Ouyang and Dr. Yong Chen for their encouragement and valuable suggestions in my research.

I would like to express my sincere thanks to Dr. Mehran Alaee from Environment Canada for his collaboration work in field sampling in Hamilton Harbour. I appreciate the help from Technical Operations Services Research Support Branch at Environment Canada in deploying and retrieving the samplers.

I would also like to express my thanks to all the group members for their help and friendship, especially Aiping Wang, Victor Ma, Zhipei Qin, Leslie Bragg, Ying Gong, Dr. Shokouh Hosseinzadeh, Allen Wang, Dr. Simon Zhou, Dr. Lucie Setkova, Dr. Dawei Lou, Dr. Xinyu Liu, Dr. Anca-Maria Tugulea, Dr. Heather Lord, Melissa Morley, Francois Breton, Dr. Vadoud Niri, Dr. In Yong Eom, Dr. Tao Bo, Dr. Zhaoguo Tong, Dr. Liu Zhen, Dr. Marcel Musteata, and Dr. Yan Wang.

I would like to thank my parents, my husband Jianqiang and my son Michael for their love, support and encouragement.

Dedication

I dedicate this thesis to my parents, my husband Jianqiang, and my son Michael for their love, encouragement and understanding.

Table of Contents

List of Figures

List of Tables

Chapter 1
Introduction

1.1 Water Contamination and Quality Control

Water pollution is a large set of adverse effects upon water bodies (lakes, rivers, oceans, groundwater) caused by human activities (e. g. industrial activities, agriculture, traffic, heating etc.) and natural phenomena (e. g. volcanic activity, storms, earthquakes etc.). Organic pollutants originating from diverse sources are found in all natural waters and water supplies. The dissemination of organic compounds after discharge into the aquatic environment is determined by its partition between the water, sediment and atmospheric phases, and by its potential for accumulation in biota. Persistent Organic Pollutants (POPs), such as polycyclic aromatic hydrocarbons (PAHs), are chemical substances that persist in the environment, bioaccumulate through the food web, and have great potential for harmful effects on humans and the environment. [1] Such analytes can be acutely toxic and cause severe illness or death following direct consumption of a sufficient dose. Continuous long-term, low-level intake of these organic chemicals through water can cause chronic difficulties. Consequently, water pollution by persistent organic pollutants (POPs) has caused considerable worldwide concern. The importance of environmental assessment and pollution control to protect and upgrade environmental quality has led to the necessity and demand for research into and monitoring of pollutants in aqueous systems.

1.2 Conventional Sampling Methods for Water Samples

Water analysis deals with various types of aqueous samples, such as ground and surface water, rain water, and municipal and industrial waste water. These various kinds of water differ not only in the types of pollutants encountered, but also in the level of contamination. Though

challenging, it is critical for environmental chemists to identify and quantify the organic contaminants in the aquatic systems, and to assess the biological hazards associated with these compounds.[2]

The analytical procedure for determining the presence and concentration of organic contaminants in water has several steps: sampling, sample preparation, separation, detection and identification, quantification, and validation. Sampling technique is an important aspect in the water monitoring because it influences all subsequent steps. Based on the length of sampling time, sampling procedures can be categorized as spot (grab) sampling or time-weighted average (TWA) sampling for short-term or continuous long-term monitoring of organic pollutants in water, respectively.

1.2.1 Spot Sampling

The most utilized technique for water analysis is spot sampling followed by laboratory-based extraction and determination of the compounds of interest.[3-5] Because persistent organic pollutants are commonly present in water in parts per billion (ppb), parts per trillion (ppt), and even lower levels, grab samples most often need to be pre-concentrated prior to analysis. The most frequently applied techniques for aqueous sample preparation are liquid-liquid extraction (LLE) and solid phase extraction (SPE).

LLE is very simple and straightforward, and continues to play an important role in water analysis. However, there are a number of drawbacks associated with LLE. It is time-consuming and difficult to automate, and thus hardly suitable for the routine analysis of a large number of water samples. The consumption of large quantities of solvents and the environmental and health hazards of these solvents are further disadvantages of LLE.

A comprehensive overview of the development of solid phase extraction (SPE) is presented by Liska.[6] The solid phase extraction has several advantages over liquid-liquid extraction: (1) decreased use of (toxic) organic solvents; (2) shorter analysis times; (3) ease of automation; and (4) suitability for field analysis. In addition, many sorbents are available for SPE to achieve selective

retention of specific analytes or interferents. However, sorbents suffer from high carryover values, and batch-to-batch sorbent variation leads to poor reproducibility in SPE compared with LLE.[7]

In spot samping using LLE and SPE, the measured level is only representative of contaminant levels at the moment of sampling. Therefore it may fail to account for episodic contamination events and has considerable temporal limitations when assessing contaminant concentrations.

1.2.2 Time-Weighted Average (TWA) Sampling

In time-weighted average (TWA) sampling, the analyte concentration is integrated over the time of sampling.[8] TWA sampling can overcome the problems with spot sampling mentioned above. It is less sensitive to accidental extreme variations in organic pollutant concentration, thus giving more accurate information for the long-term monitoring of environmental pollutants.

There are two approaches for collecting integrated or TWA samples. The first involves taking a large number of grab samples over the interval of interest, and averaging the concentrations. Equation 1.1 shows how average analyte concentration can be determined in this way:

$$\overline{C} = \frac{C_1 t_1 + C_2 t_2 + C_3 t_3 + ... + C_n t_n}{t_1 + t_2 + t_3 + ... + t_n} = \frac{\sum_{i=1}^{n} C_i t_i}{\sum_{i=1}^{n} t_i} \qquad \text{Equation 1.1}$$

where $\overline{C}$ is the TWA concentration, and C_i is the analyte concentration observed in time period t_i. By increasing the sampling frequency, a more accurate picture of time-integrated pollutant levels can be obtained. However, obtaining a TWA concentration using this method is time-consuming and expensive. Alternatively, the TWA concentration can be obtained from a single sample if the mass loading of the analyte of interest is directly proportional to the analyte concentration for the entire time period of interest. This latter method is highly recommended for its simplicity and cost-effectiveness.

Two strategies – active and passive sampling – can be used to determine the TWA concentration with a single sampler. Active sampling utilizes pumps to force the sample flow through a solid- or liquid-collecting medium trap where analytes are absorbed or adsorbed, at a constant sampling rate.[9] The mass loading rate of a waterborn analyte onto a sorbent using active sampling is shown in equation 1.2:

$$\frac{n}{t} = R \times \overline{C} \qquad \text{Equation 1.2}$$

where n is the amount of analyte sorbed during sampling time t, R is the pump sampling flow rate (volume/time), and $\overline{C}$ is the TWA concentration during the sampling time. Although active sampling methods are generally believed to be more accurate, active samplers are complicated and expensive because flow meters, pumps and a power supply are required during monitoring.

Thus, passive sampling techniques are the more attractive option for the long-term monitoring of organic pollutants in water as they eliminate power requirements and significantly reduce the costs of analysis.[9-13] The currently available passive samplers for water sampling are either based on permeation or diffusion:[8] solvent-filled devices,[14-16] semi-permeable membrane devices (SPMDs), [9] passive in-situ concentration/extraction samplers (PISCES), [17] and sorbent-filled devices.[18] SPMDs are currently the most widely used passive samplers for water analysis in the field due to their ease of deployment and high sensitivity. However, the sample-treatment procedure associated with SPMDs is very time-consuming.[13]

1.3 Solid Phase Microextraction (SPME)

Pawliszyn and co-workers introduced SPME as a new sampling and sample preparation method in the early 1990s.[19] It was developed to address the need for rapid sampling and sample preparation in the laboratory and in the field.[20] It offered many advantages over conventional analytical methods by combining sampling, isolation, and enrichment into one step and by directly

transferring analytes into a standard gas or liquid chromatography, thus minimizing loss of analyte due to multi-step processes. For a number of applications, the simplicity and convenience of operation of SPME make it a superior alternative to more established techniques. Since its inception, SPME has been widely used for monitoring organic pollutants in water.[21-23]

1.3.1 Introduction to SPME

The most widely used technique of sampling with solid phase microextraction consists of exposing a small amount of extracting phase (fiber coating) to the sample for a predetermined amount of time. The principle of SPME is based on the interactions of analytes between the sample matrix and the fiber coating via absorption or adsorption (depending on the nature of the coatings). The transport of analytes from the sample matrix to the fiber coating occurs immediately after contact between the two phases (Figure 1-1).

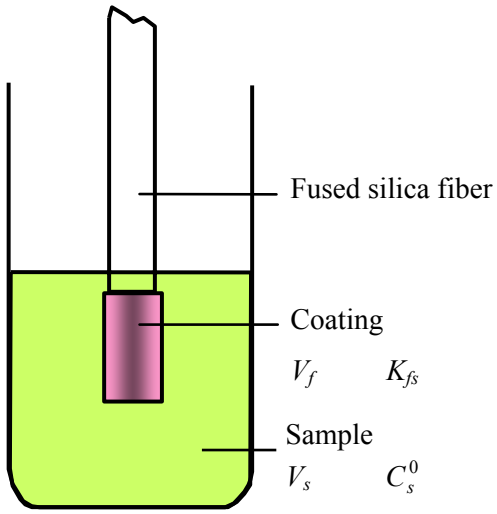

Figure 1-1 Sample preparation with SPME. V_f, volume of fiber coating; K_{fs}, fiber/sample distribution coefficient; V_s, sample volume; C_s^0, initial concentration of analyte in the sample matrix.

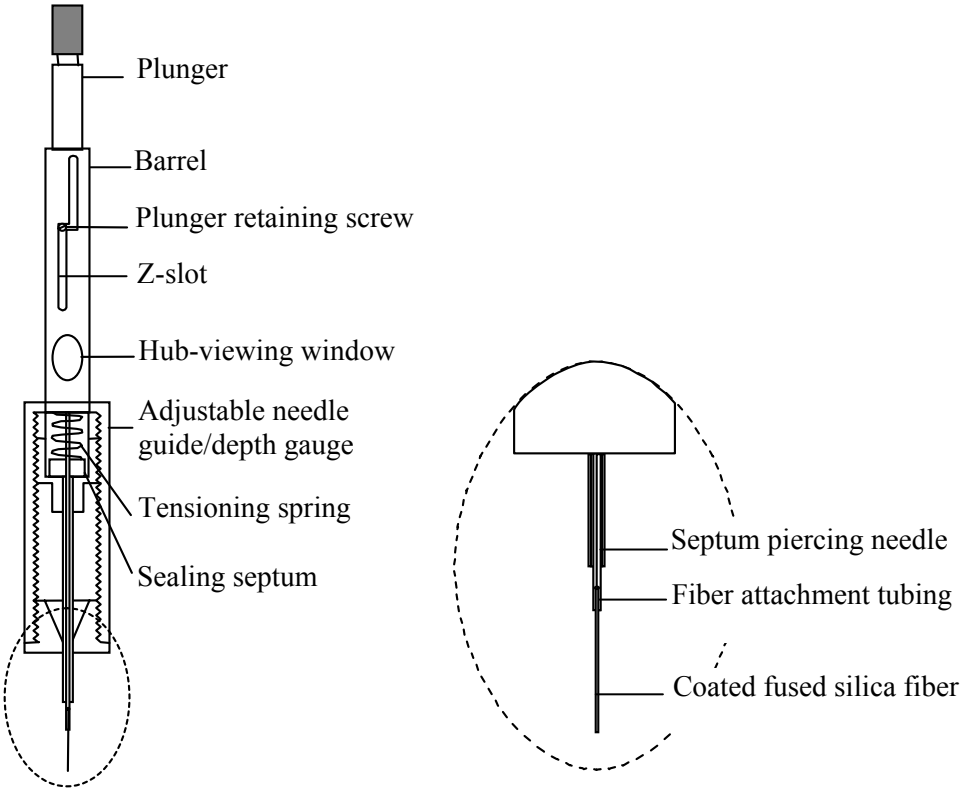

Figure 1-2 Design of the first commercial SPME device made by Supelco.

Figure 1-2 illustrates the commercial SPME device made by Supelco. Moving the plunger allows for exposure of the fiber during extraction and desorption and for its protection inside the needle during storage and penetration of the septum.

1.3.2 Kinetics

The kinetics of the extraction process determines the speed of extractions. Kinetic theory identifies extraction rate "bottlenecks" in solid phase microextraction and therefore indicates strategies for increasing the speed of extractions. All diffusion is assumed to behave according to Fick's law. The theory assumes that there is no interaction between analytes and vial surfaces or fiber core. Factors such as thermal expansion, swelling, and analyte/analyte interactions are also assumed to be negligible. The direct extractions of analytes from a homogeneous water sample into a fiber's

liquid polymer phase coating are discussed under three different conditions: (1) perfect agitation; (2) static solution; and (3) practical agitation.

1.3.2.1 Perfect Agitation

During perfect agitation, the aqueous phase moves very rapidly with respect to the fiber. Therefore all the analyte molecules present in the sample have equal exposure to the fiber coating. Since the coating is always in contact with fresh solution, the speed of the absorption process is determined entirely by the diffusion of the analyte in the polymer coating. Under perfect agitation, the equilibration time, t_e, defined as the time required to extract 95% of the equilibrium amount of an analyte from the sample, corresponds to:[24]

$$t_e = t_{95\%} = \frac{2(r_o - r_i)^2}{D_f} \qquad \text{Equation 1.3}$$

where r_i is fiber coating inner radius, r_o is fiber coating outer radius, $(r_o - r_i)$ is the fiber coating's thickness, and D_f is the analyte diffusion coefficient in the fiber coating.

1.3.2.2 Static Solution

In contrast to perfect agitation, significantly longer extraction times are expected for static solutions because the analytes must diffuse not only through the fiber coating but also through an ever-broadening analytes-depleted layer of water. In this case, the mass transfer of analytes from the progressively thicker depleted layer to the fiber coating determines overall extraction speed.

1.3.2.3 Practical Agitation

The experimental conditions attainable in a real system are intermediate between the perfectly agitated and perfectly static models. Independent of agitation level in the system, there is always a thin layer of unstirred water around the fiber. Fluid movement gradually increases as the distance from the fiber surface increases until it corresponds to the bulk flow in the sample. To model

mass transport under practical agitation conditions, the gradation in fluid motion and convection of molecules in the space surrounding the fiber surface can be simplified as a boundary layer in which no convection occurs and perfect agitation in the bulk of the fluid everywhere else. The thickness of the boundary layer is determined by the viscosity of the fluid and the agitation conditions.

When the extraction rate is determined by the diffusion in the boundary layer, equilibration time can be estimated from the equation below:[20]

$$t_e = t_{95\%} = \frac{3\delta_s K_{fs}(r_o - r_i)}{D_s} \qquad \text{Equation 1.4}$$

where δ_s is the thickness of the boundary layer surrounding the fiber coating, K_{fs} is the analyte's distribution coefficient between fiber and sample.

According to equation 1.4, equilibration time is proportional to the coating and boundary layer thickness. The sensitivity of the technique can be improved by increasing the coating thickness. However, a significant increase in the extraction time will occur. Decreasing the boundary layer thickness will accelerate the extraction process and result in short equilibrium time.

1.3.3 Calibration in SPME

In addition to traditional calibration methods like external calibration, internal calibration and standard addition, there are to date several calibration approaches developed for SPME (Figure 1-3).

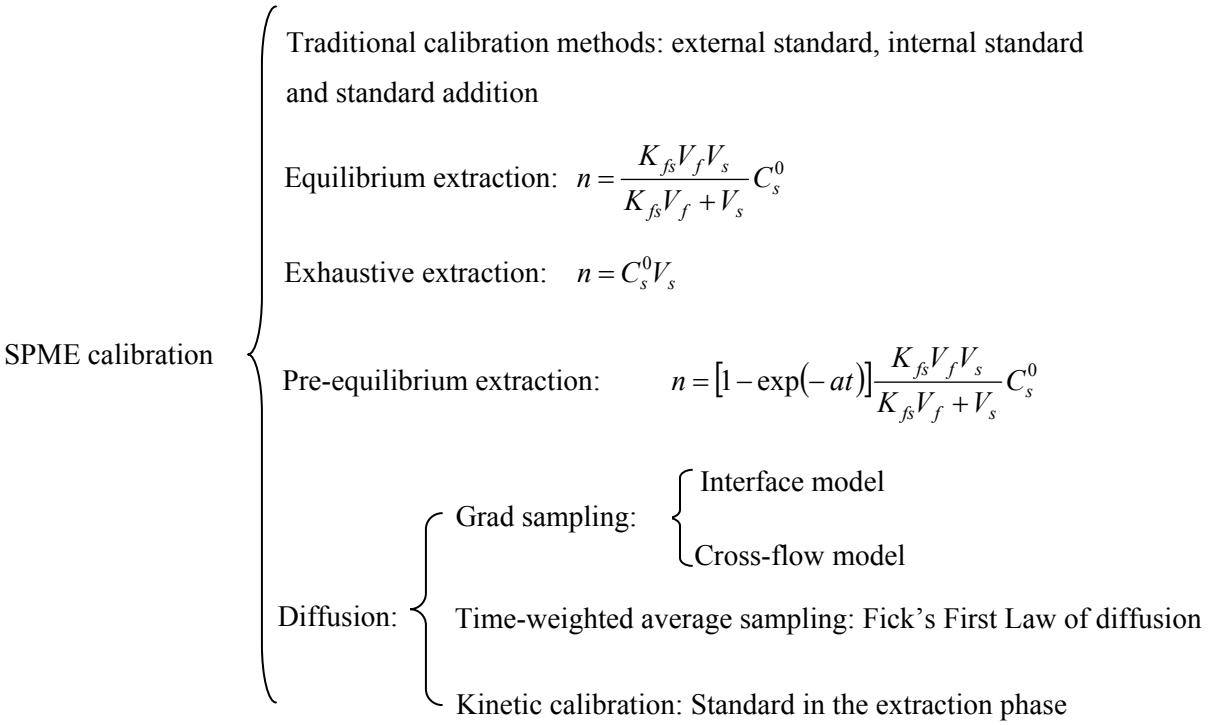

Figure 1-3 Calibration methods in SPME.

1.3.3.1 Equilibrium Extraction

If extraction time is long enough, a concentration equilibrium is established between the sample matrix and the extraction phase. Equilibrium extraction is the most frequently used quantification method for SPME. Equilibrium conditions in a two-phase system including extraction phase and aqueous matrix can be described according to the law of mass conservation (equation 1.5):

$$C_s^0V_s = C_f^\infty V_f + C_s^\infty V_s \qquad \text{Equation 1.5}$$

where C_s^0 is the initial concentration of a given analyte in the sample, V_s is the sample volume, V_f is the fiber coating volume, and C_f^∞ and C_s^∞, are the equilibrium concentrations of the analyte in the fiber and the sample matrix, respectively. The fiber/sample matrix distribution coefficient K_{fs} is defined as,

$$K_{fs} = C_f^{\infty} \big/ C_s^{\infty}$$ Equation 1.6

By combining and rearranging equations 1.5 and 1.6, the mass of the analyte absorbed by the fiber, $n = C_f^{\infty} V_f$, can be described as: [25]

$$n = \frac{K_{fs} V_f C_s^0 V_s}{K_{fs} V_f + V_s}$$ Equation 1.7

Equation 1.7 indicates that the amount of analyte extracted onto the fiber coating is directly proportional to the analyte concentration in the sample. This is the analytical basis for quantification using SPME.

When the sample volume is large (i.e. $V_s >> K_{fs} V_f$), the amount of analyte extracted becomes independent of sample volume, and can be described simply by equation 1.8:

$$n = K_{fs} C_s^0 V_f$$ Equation 1.8

In this equation, the amount of the extracted analyte corresponds directly to its concentration in the sample matrix; in addition, it is independent of sample volume, which points out the usefulness of the approach for field sampling, when sample volume is unknown. In practice, there is no need to collect a defined sample prior to analysis, as the fiber can be exposed directly to the ambient air, water, production stream, etc. When the sample collection step is eliminated, the whole analytical process is accelerated and errors associated with analyte loss through decomposition or adsorption on the sampling container walls are prevented.

Equation 1.8 also illustrates another characteristic of SPME useful for field sampling: the concentration of target analytes can be determined from the amount of the analytes on the fiber under extraction equilibrium by knowing the distribution coefficients of the analytes between the fiber coating and the sample matrix. This is a very desirable characteristic for field application, as

quantification is possible without external calibration, which in turn allows for a faster analysis process.

1.3.3.2 Exhaustive Extraction

When sample volume is very small, and the distribution coefficient of the analyte between the fiber coating and the sample matrix is very large ($V_s << K_{fs}V_f$), as occurs when sampling of semi-volatile organic compounds (semi-VOCs) in small volumes of a sample matrix, equation 1.7 can be simplified to:

$$n = C_s^0 V_s \qquad \text{Equation 1.9}$$

Equation 1.9 implies that all of the analytes in the sample matrix are extracted onto the fiber coating. Therefore, the analyte concentration in the sample can be easily calculated with the amount of analyte extracted by the fiber coating and the volume of the sample.

Calibration for exhaustive extraction is very simple, but not often used in SPME because it is only suitable for small sample volumes and very large distribution coefficient. A cooling fiber device, by which the distribution coefficient is significantly increased through simultaneous heating of the sample matrix and cooling of the fiber coating, provides an opportunity to extract the total amount of analyte in a sample. [26]

1.3.3.3 Pre-equilibrium Extraction

When a SPME fiber is exposed to the sample matrix, transport of the analyte from the sample matrix to the fiber coating occurs. In SPME, the time required to reach extraction equilibrium, which ranges from minutes to hours, is dependent on the agitation conditions, the physicochemical properties of the analytes and fiber coating, and the physical dimensions of the sample matrix and the fiber coating. Equilibrium extraction results in the highest sensitivity in SPME, as the amount of analyte extracted onto the fiber coating is maximized when equilibrium is reached. If sensitivity is not

a major concern in the analysis, reducing extraction time is desirable. In addition, the equilibrium extraction approach is not practical for solid porous coatings, due to the displacement effect at high concentrations. In these circumstances, extraction can be interrupted before the equilibrium is reached.

The kinetics of analytes absorption onto a liquid fiber coating in SPME was proposed by Ai in 1997, based on a diffusion-controlled mass transfer process: [27, 28]

$$n = \left[1 - \exp(-at)\right] \frac{K_{fs} V_f V_s}{K_{fs} V_f + V_s} C_s^0 \qquad \text{Equation 1.10}$$

where a is time constant representing how fast an equilibrium can be reached. This depends on the extraction phase and sample volumes, the mass transfer coefficients, the distribution coefficients, and the surface area of the extraction phase. When extraction time is long enough, equation 1.10 becomes equation 1.7, characterizing equilibrium extraction. If equilibrium is not reached, this dynamic model indicates that a linearly proportional relationship still exists between the amount of analyte extracted onto the fiber (n) and the initial analyte concentration in the sample matrix (C_s^0). This relationship indicates that SPME quantification is feasible before concentration equilibrium is reached, providing agitation conditions, sampling time, and temperature are held constant.

1.3.3.4 Diffusion-based Calibration

Diffusion is the transport of a chemical substance in a material system consisting of two or more components, from area of higher concentration in the given phase towards those of lower concentration or, in non-ideal mixtures, of lower activity. [29] In recent years, several diffusion-based calibration methods have been developed for the quantification of SPME, such as the interface model, the cross-flow model, and the kinetic calibration of absorption and desorption.

1.3.3.4.1 Interface Model

Koziel *et al.* developed a rapid air sampling methodology using adsorptive SPME coatings and controlled air convection conditions. A theoretical model for rapid extraction was formulated based on the diffusion through the interface surrounding the fiber (Figure 1-4): [30]

$$C_s^0 = \frac{n \ln((r_o + \delta_s)/r_o)}{2\pi D_g L t} \qquad \text{Equation 1.11}$$

where C_s^0 is the analyte concentration in the bulk air, n is the amount of analyte extacted by the fiber coating during time t, L is the length of fiber coating, D_g is the gas-phase molecular diffusion coefficient, r_o is the fiber coating outer radius, δ_s is the thickness of the boundary layer surrounding the fiber coating,

The thickness of the boundary layer can be estimated by use of equation 1.12, an empirical equation adapted from heat transfer theory:

$$\delta_s = 9.52(r_o / \mathrm{Re}^{0.62} Sc^{0.38}) \qquad \text{Equation 1.12}$$

where Re is the Reynolds number ($\mathrm{Re} = 2ur_o / v$), u is the linear flow velocity, v is the kinetic viscosity, and Sc is the Schmidt number (Sc = v/D_g).

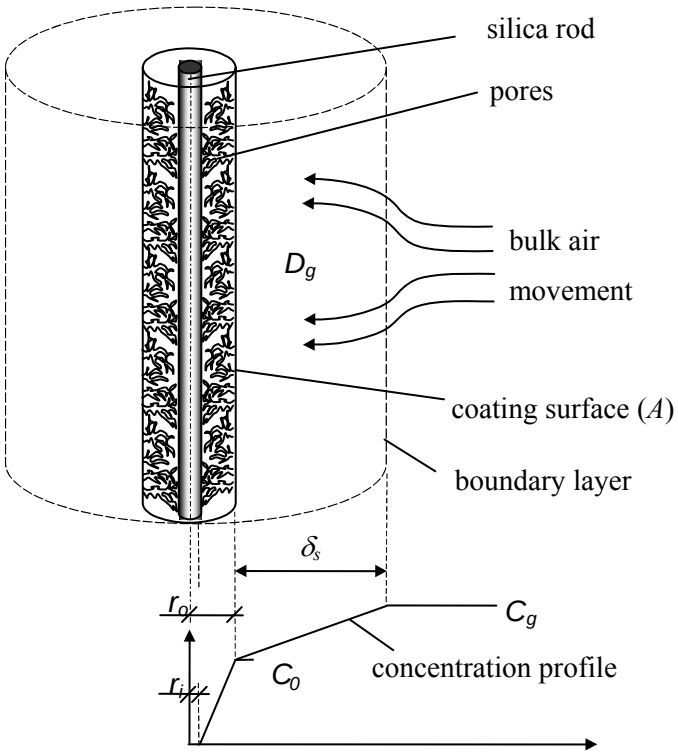

Figure 1-4 Schematic diagram of the diffusion-based calibration model for cylindrical geometry.

Analyte concentration in the bulk of the matrix is regarded as constant when a short sampling time is used and convection results in a constant analyte supply. Sample volume is much greater than the volume of the interface, and the extraction process does not affect the bulk concentration. Analyte concentration on the coating surface is far from saturation and can be assumed to be negligible when sampling time is short and the analyte concentration in the sample is relatively low. The interface model has also been used successfully to predict mass uptake in rapid water sampling.[31] However, the assumption of a uniform boundary layer is not always valid. In addition, calculating the thickness of the boundary layer still depends on an empirical equation, which introduces additional errors.

1.3.3.4.2 Cross-flow Model

To improve the accuracy of analyte concentration prediction, Chen *et al.* proposed another diffusion-based calibration model - the cross-flow model.[32] The concentration of the target analyte can be calculated by equation 1.13:

$$C_s^0 = \frac{n}{\bar{h}At} = \frac{nd}{ERe^b Sc^{1/3} AD_s t} \qquad \text{Equation 1.13}$$

where A is the surface area of the fiber, n is the mass uptake onto the fiber during the sampling time t, D_s is the diffusion coefficient of the analyte molecule in the sample matrix, $\bar{h}$ is the average mass-transfer coefficient, Re is the Reynolds number, and Sc is the Schmidt number. The constants E and b, dependent on the Reynolds number, are available from the literature. The cross-flow model has proved to be more practical and accurate in aqueous sample analysis than the interface model.[32]

1.3.3.4.3 Fick's First Law of Diffusion

The Fick's first law of diffusion was applied to calibrate the SPME TWA sampling device (Figure 1-5, a).[33] Unlike conventional sampling with SPME, the fiber is retracted a known distance into its needle housing during the sampling period. Analyte molecules access the fiber coating only by means of diffusion through the static air/water gap between the opening and the fiber coating. Thus, the amount of analyte accumulated during the sampling time can be predicted by considering Fick's first law of diffusion (Figure 1-5, b). If the sorbent is a "zero sink" for the target analytes, then the concentration of the target analytes in the sample can be calculated with equation 1.14.

$$\bar{C} = \frac{nZ}{AD_s t} \qquad \text{Equation 1.14}$$

where $\bar{C}$ is the TWA concentration of the target analytes in air or water during the sampling time t, Z is the diffusion path length, A is the cross-sectional area of the needle, D_s is the diffusion coefficient of the target analytes in air or water, and n is the amount of analytes extracted by the fiber during time

t. This geometric arrangement is very simple, capable of generating a response proportional to the integral of the analyte concentration over time and space. The disadvantage of this device is its low sampling rate, which corresponds to extremely long sampling time at low analyte concentration.

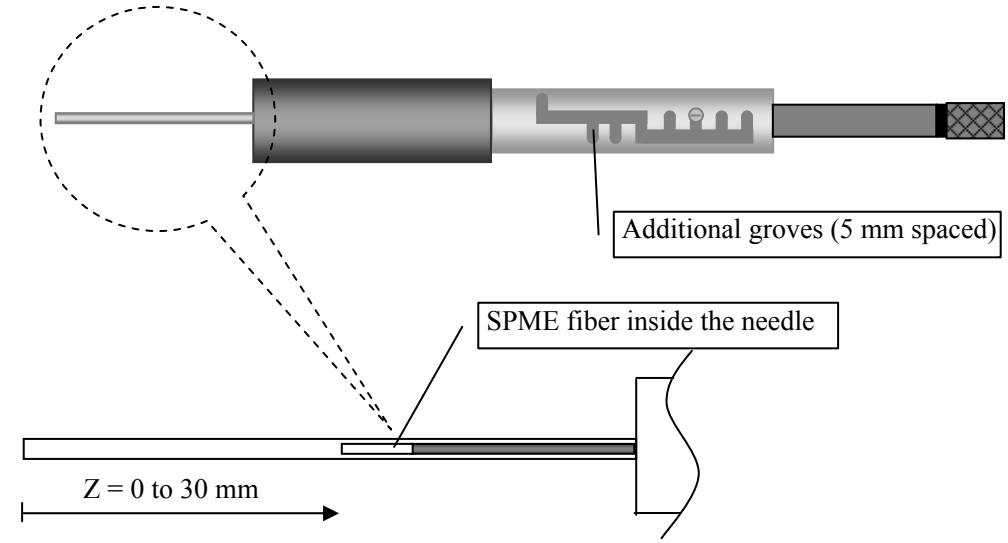

(a)

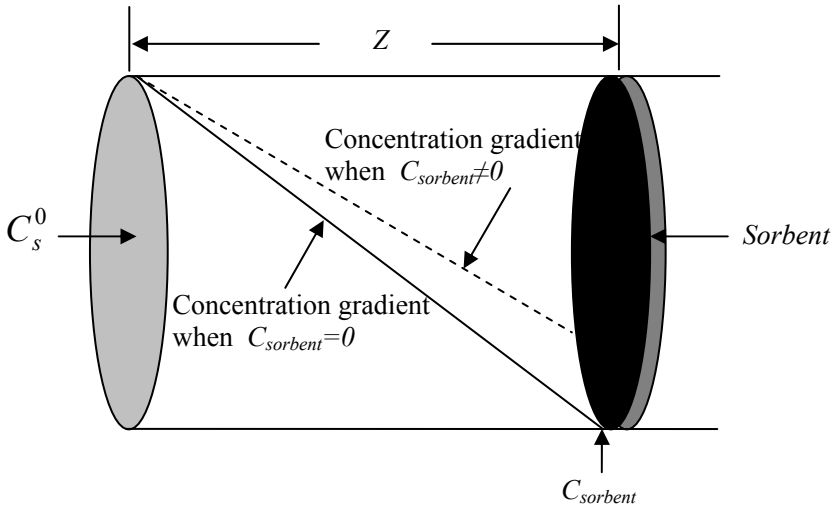

(b)

Figure 1-5 Use of SPME for in-needle time-weighted average sampling: (a) adaptation of commercial SPME manual extraction holder; (b) schematic diagram of fiber retracted SPME device and concentration gradient.

1.3.3.5 Kinetic Calibration

The absorption of analyte from the sample matrix into a SPME liquid coating can be described by equation 1.15: [27, 28]

$$\frac{n}{n_e} = 1 - \exp(-at) \qquad \text{Equation 1.15}$$

where n is the amount of the extracted analyte at time t, n_e is the amount of extracted analyte at equilibrium, and the time constant a is dependent on the volumes of the extraction phase and sample, the mass transfer coefficients, the distribution coefficients, and the surface area of the extraction phase.

Based on the above model, Chen *et al.* demonstrated the isotropy of absorption and desorption of analyte in the SPME liquid fiber coating, and the kinetic calibration method for SPME was proposed.[34, 35] Kinetic calibration, also called the in-fiber standardization technique, uses the desorption of the standards, which are pre-loaded in the extraction phase of fiber coating, to calibrate the extraction of analytes. The method was also validated for in-vial analysis (Equation 1.16). [35, 36]

$$\frac{n}{n_e} + \frac{Q - q_e}{q_0 - q_e} = 1 \qquad \text{Equation 1.16}$$

where n is the amount of analyte extracted by SPME fiber at sampling time t, n_e is the amount of analyte extracted by the SPME fiber at equilibrium, q_0 is the amount of pre-loaded standard in the extraction phase, q_e is the amount of standard remaining in the extraction phase at equilibrium, and Q is the amount of standard remaining in the extraction phase after its exposure to the sample matrix over a given sampling time t.

1.3.4 SPME Method Development

The development of a new SPME method usually involves the following steps:

- Selection of fiber coating
- Selection of extraction mode
- Selection of agitation technique
- Sample volume optimization
- Extraction time optimization
- Extraction conditions optimization
- Determination of desorption conditions
- Selection of calibration method
- Method validation

A number of fiber coating types, differing in polarity, thickness of stationary phase, and coating length are commercially available, either in manual or autosampler versions. Fiber coatings use either absorption (liquid coatings) or adsorption (solid coatings) mechanisms to extract analytes from samples. Single-phase polydimethylsiloxane (PDMS) and polyacrylate (PA) fibers belong to the absorption-type coating group. Mixed-phase fibers, such as PDMS/divinylbenzene (DVB), Carbowax (CW)/DVB, Carboxen (CAR)/PDMS, and the "sandwich" fiber DVB/CAR/PDMS, use an adsorption mechanism when isolating target analytes from the sample. CW/template resin (TPR) is a special CW/polyDVB fiber designed to reduce the molecular weight discrimination of analytes in HPLC applications. Typically, the chemical nature of the target analyte determines the type of coating to be used. A simple rule holds for liquid polymers: "like dissolves like". Fibers with a thicker coating extract higher amounts of analytes, but require more time to reach equilibrium.

SPME offers three extraction-mode options: direct extraction, headspace extraction, and membrane-protected SPME. Extraction mode selection is based on the sample matrix composition, analyte volatility, and analyte affinity to the matrix. Direct immersed SPME (DI-SPME) is more suitable for clean liquid samples, Headspace SPME (HS-SPME) is recommended for complex liquid samples if the target compounds are sufficiently volatile.

In aqueous sample analysis, agitation of the sample assists in the mass transport between the sample and the fiber. Effective stirring allows for shorter extraction times to achieve either equilibrium or satisfactory sensitivity in non-equilibrium extractions. Various agitation techniques can be applied in SPME methods, depending on the type of application: (1) magnetic stirring, (2) intrusive stirring, (3) needle vibration, (4) moving vial (vortex stirring), (5) flow-through stirring, or (6) sonication.

When sample volume is large, the amount of analyte extracted is an insignificant portion of the total amount of analyte in the system. Therefore, analyte concentration in the sample remains constant during extraction, resulting in optimum sensitivity and better precision because the variation in sample volume does not affect the amount of analyte extracted. When sample volume is small, a substantial depletion of sample concentration occurs during extraction, resulting in loss of sensitivity and precision.

In most cases, sample extraction becomes the time-limiting step in a SPME procedure. Therefore, selecting the optimium extraction time is one of the critical steps in the SPME method development. An optimal approach to SPME requires allowing the system to reach equilibrium between the sample and fiber coating. When equilibrium time is excessively long, shorter extraction times can be used. In such cases, extraction time must be strictly controlled to ensure good precision.

Modifying extraction conditions affects both the sensitivity and equilibrium time. Increasing the extraction temperature can significantly reduce the equilibration time, but simultaneously

decreases the distribution coefficient value. The presence of the matrix influences the distribution coefficients and the equilibrium times. Matrix modifications, such as pH or ionic strength adjustment of the sample solution, can, in some circumstances, be used to improve the sensitivity of the method.

Most SPME applications have been developed using gas chromatography. By applying gas chromatographic analysis, desorption time is determined by the temperature of the injector and the linear flow rate of the carrier gas around the fiber. Theoretically, desorption times are very short, as the diffusion coefficients of analytes in the coating increase and the gas/coating distribution coefficients rapidly decrease with rising temperature. In practice, however, desorption temperature is determined by the thermal stability of the coating. It is advisable to use high desorption temperatures in order to speed up desorption. However, applying excessive heat adversely affects longevity of the coating and results in bleeding of the polymer, rendering separation and quantification difficult.

Standard calibration procedures can be used with SPME. The SPME calibration technique suitability depends on the application, the number of samples to be analysed, and the availability of the MS instrument in laboratory when applying the isotopically labeled internal standard.

To validate the method, quantitation results may be compared with certified values obtained for standard reference materials with similar matrix and target analytes. Alternately, they may be compared with officially-accepted techniques for analyzing target samples and analytes. Finally, inter-laboratory studies are frequently performed to validate a method.

1.3.5 SPME in Aqueous Sample Analysis

1.3.5.1 Applications

The SPME technique, using on-site or off-site analytical approaches, has been widely used for the analysis of environmental pollutants in water samples. It is portable, accurate, reproducible, simple to deploy, and re-usable.

Hundreds of papers addressing environmental aqueous sample analysis with SPME have been published in recent years. Table 1-1 illustrates some of the aqueous environment applications of SPME in the analysis of benzene, toluene, ethylbenzene and xylene (BTEX), and polycyclic aromatic hydrocarbons (PAHs), which are reported and summarized by Ouyang et. al. [37]

Table 1-1 Recent applications of SPME in aqueous environmental sample analysis of BTEX and PAHs

Analytes	Extraction method	Fiber/Capillary	Detection	Refs
BTEX	HS	CAR/PDMS	GC/FID	38, 39
BTEX	HS	PPY-coated gold wire	GC/FID	40
BTEX	HS	PDMS/DVB/CAR	GC/FID	41
BTEX	HS	PDMS/DVB	GC/MS	42
PAHs	DI, ultrasound treatment	PDMS	GC/MS	43
PAHs	In-tube SPME	PDMS-coated capillary	HPLC	44
PAHs	DI	PDMS	HPLC/FLD	45
PAHs	In-tube SPME	PDMS-coated capillary	GC/MS	46
PAHs	In-tube SPME	PPY-coated capillary	HPLC/UV	47
PAHs	Static water sampling	PDMS, fiber retracted device	GC/MS	33
PAHs	HS	PPY-DS	GC/MS, FID	48

1.3.5.2 Complex Aqueous Sample Analysis

The transport, bioavailability, and finally the fate of hydrophobic organic compounds (HOCs) in the environment are strongly affected by their interactions with humic organic matter (HOM), which is ubiquitous in the natural world.

Freely dissolved analyte concentration is an important parameter in environmental chemistry, pharmacology, and toxicology. The free concentration of an organic pollutant is the driving force in its transport, distribution, and bioaccumulation in the environment. Binding or partition of chemicals to dissolved organic carbon, sediment, or proteins may reduce the free concentration and thus the bioavailability or effectiveness of the chemical. Therefore, it is important to understand the extent of binding or partitioning of the chemical of interest to the binding matrix in environmental, pharmacological and toxicological analysis. Much effort has been focused on measuring sorption coefficients and binding constants. These constants can be determined by measuring the concentrations of either the bound or the free form.

SPME is proposed as an alternative, more efficient technique for extracting and concentrating target compounds from a complex matrix in order to determine their free concentration. [49, 50] By measuring the free dissolved concentration of target compound, the bioavailablity of the target compound, as well as its sorption coefficient, can be determined.

1.4 Thesis Objective

The overall objective of this thesis is to develop enhanced laboratory and field methods using SPME in order to monitor organic pollutants in aqueous samples.

Chapter 2 deals with the laboratory evaluation of the kinetic calibration approach in aqueous sample analysis using SPME.

A new SPME sampler, the PDMS rod sampler, was developed for TWA aqueous sampling. Laboratory and field validations of this new sampler are presented in Chapter 3, as well as the use of kinetic calibration to determine target analyte concentrations in aqueous samples.

In Chapter 4 and 5, efforts are made to demonstrate that the SPME technique can be used to study the sorption of hydrophobic organic compounds to dissolved organic matter in aqueous samples. Experimental work and theoretical consideration of SPME extraction in a complex aqueous sample matrix are discussed.

Chapter 6 investigates an alternative tool which uses numerical simulation to study the extraction characteristics of SPME in aqueous samples.

Finally, Chapter 7 summarizes the overall conclusions of the research work presented here, and makes recommendations for future considerations.

References

(1) Kumar, H. D.; Hader, D.-P. *Global Aquatic and Atmospheric Environment*; Springer-Verlag Berlin: Heidelberg, Germany, 1999.

(2) Tabor, W. *In Situ Evaluation of Biological Hazards of Environmental Pollutants*; Plenum: New York, 1990.

(3) Barcelo, D.; Chiron, S.; Lacorte, S.; Martinez, E.; Salau, J. S.; Hennion, M. C. *Trends Anal. Chem.* **1994**, *13*, 352.

(4) Barcelo, D. *J. Chromatogr.* **1993**, *643*, 117.

(5) House, W. A. *Int. J. Environ. Anal. Chem.* **1994**, *57*, 207.

(6) Liska, I. *J. Chromatogr. A.* **2000**, *885*, 3.

(7) Dix, K. D.; Fritz, J. S. *Anal. Chim. Acta.* **1990**, *236*, 43.

(8) Kot, A.; Zabiegala, B.; Namiesnik, J. *Trends Anal. Chem.* **2000**, *19*, 446.

(9) Huckins, J. N.; Tubergen, M. W.; Manuweera, G. K. *Chemosphere* **1990**, *20*, 533.

(10) Namiesnik, J.; Zabiegala, B.; Kot-Wasik, A.; Partyka, M.; Wasik, A. *Anal. Bioanal. Chem.* **2005**, *381*, 279.

(11) Vrana, B.; Allan, I. J.; Greenwood, R.; Mills, G. A.; Dominiak, E.; Svensson, K.; Knutsson, J.; Morrison, G. *Trends Anal. Chem.* **2005**, *24*, 845.

(12) Gorecki, T.; Pawliszyn, J. *Anal. Chem.* **1995**, *67*, 3265.

(13) Gorecki, T.; Namiesnik, J. *Trends Anal. Chem.* **2002**, *21*, 276.

(14) Kot-Wasik, A. *Chem. Anal. (Warsaw)* **2004**, *49*, 691.

(15) Sodergren, A. *Environ. Sci. Technol.* **1987**, *21*, 855.

(16) Peterson, S. M. A., S. C.; Batley, G. E.; Coade, G.. *Chem. Spec. Bioavailab.* **1995**, *7*, 83.

(17) Litten, S.; Mead, B.; Hassett, J. *Environ. Toxicol. Chem.* **1993**, *12*, 639.

(18) DiGlano, F. A.; Elliot, D.; Leith, D. *Environ. Sci. Technol.* **1988**, *22*, 1365.

(19) Arthur, C. L.; Pawliszyn, J. *Ana.l Chem.* **1990**, *62*, 2145.

(20) Pawliszyn, J. *Solid Phase Microextraction: Theory and Practice*; Wiley-VCH: New York, 1997.

(21) Eisert, R.; K., L. *J. Chromato. A.* **1996**, *733*, 143.

(22) Eisert, R. P., J. *Crit. Rev. Anal. Chem.* **1997**, *27*, 103.

(23) Pawliszyn, J. *Applications of Solid Phase Microextraction*; Royal Society of Chemistry: Cambridge, 1999.

(24) Louch, D.; Motlagh, S.; Pawliszyn, J. *Anal. Chem.* **1992**, *64*, 1187.

(25) Gorecki, T. *Analyst* **1997**, *122*, 1079.

(26) Zhang, Z.; Pawliszyn, J. *Anal. Chem.* **1995**, *67*, 34.

(27) Ai, J. *Anal. Chem.* **1997**, *69*, 1230.

(28) Ai, J. *Anal. Chem.* **1997**, *69*, 3260.

(29) Erdey-Gruz, T. *Transport Phenomena in Aqueous Solution*; John Wiley & Sons: New York, 1974.

(30) Koziel, J.; Jia, M.; Pawliszyn, J. *Anal. Chem.* **2000**, *72*, 5178.

(31) Sukola, K.; Koziel, J.; Augusto, F.; Pawliszyn, J. *Anal. Chem.* **2001**, *73*, 13.

(32) Chen, Y.; Koziel, J. A.; Pawliszyn, J. *Anal. Chem.* **2003**, *75*, 6485.

(33) Ouyang, G.; Chen, Y.; Pawliszyn, J. *Anal. Chem.* **2005**, *77*, 7319.

(34) Chen, Y.; O'Reilly, J.; Wang, Y.; Pawliszyn, J. *Analyst* **2004**, *129*, 702.

(35) Chen, Y.; Pawliszyn, J. *Anal. Chem.* **2004**, *76*, 5807.

(36) Wang, Y.; O'Reilly, J.; Chen, Y.; Pawliszyn, J. *J. Chromatogr. A.* **2005**, *1072*, 13.

(37) Ouyang, G.; Pawliszyn, J. *Anal. Bioanal. Chem.* **2006**, *386*, 1059.

(38) Cho, H. J.; Baek, K.; Lee, H. H.; Lee, S. H.; Yang, J. W. *J. Chromato. A.* **2003**, *988*, 177.

(39) Brondi, S. H. G.; Lancas, F. M. *J. Environ. Sci. Heal. B* **2005**, *40*, 513.

(40) Djozan, D.; Pournaghi-Azar, M. H.; Bahar, S. *Chromatographia* **2004**, *59*, 595.

(41) Almeida, C. M. M.; Boas, L. V. *J. Environ. Monit.* **2004**, *6*, 80.

(42) Arambarri, I.; Lasa, M.; Garcia, R.; Millan, E. *J. Chromtogr. A* **2004**, *1033*, 193.

(43) Psillakis, E.; Ntelekos, A.; Mantzavinos, D.; E., N.; Kalogerakis, N. *J. Environ. Monit.* **2003**, *5*, 135.

(44) Bagheri, H.; Salemi, A. *Chromatographia* **2004**, *59*, 501.

(45) Chen, H.-W. *Analytical Sciences* **2004**, *20*, 1383.

(46) Globig, D.; Weickhardt, C. *Anal. Bioanal. Chem.* **2005**, *381*, 656.

(47) Wu, J.; Pawliszyn, J. *Anal. Chem.* **2001**, *73*, 55.

(48) Mohammadi, A.; Yamini, Y.; Alizadeh, N. *J. Chromato. A.* **2005**, *1063*, 1.

(49) Hsu, Y. L.; Rose, S.; Furton, K. G., Orlando, FL 2002; ANYL.

(50) Krogh, M.; Johansen, K.; Tonnesen, F.; Rasmunssen, K. E. *J. Chromato. B* **1995**, *673*, 299.

Chapter 2
Laboratory Evaluation of Kinetic Calibration in Solid Phase Microextraction

2.1 Introduction

SPME has been widely used in a variety of disciplines for the analysis of flavours and fragrances, food, forensics and toxicology, environmental and pharmaceutical and clinical samples since its inception in 1990. [1-6] To date, the calibration methods developed for SPME include: equilibrium extraction, [7] pre-equilibrium extraction, [8] exhaustive extraction, [2] diffusion controlled calibration [9, 10] and the most recently developed form of kinetics calibration, which is based on the desorption of an internal standard in the extraction phase to calibrate the extraction of the target analyte. [11] This was later named the in-fiber standardization calibration approach. [12] Internal standard calibration is very useful, particularly when the instrument or technique response is not stable (drifts) or sample loss during the experiment is a concern. Furthermore, it also compensates for the matrix effect, which can improve the accuracy and precision of the analysis. [13] While the traditional approach requires delivery of the standard to the sample matrix, it is not practical in many circumstances, such as sampling in an open system like air or water or various *in-vivo* investigations. As an alternative, the in-fiber internal standardization has been proposed and the kinetics of this technique has been demonstrated. [11, 12, 14] It was found that the desorption of analytes from a SPME fiber into an agitated sampling matrix is a mirror reflection process to the absorption of the analytes onto the SPME fiber from the sample matrix under the same agitation conditions. This therefore allows for the calibration of absorption using desorption. The calibration was accomplished by exposing a SPME fiber, preloaded with a standard, to an agitated sample matrix, during which desorption of the standard and absorption of analytes occurred simultaneously. When the standard is

the isotopically labelled analogue of the target analyte (similar physicochemical properties of the standard and analyte), the information from the desorption process, i.e., time constant *a*, could be directly used to estimate the concentration of the target analyte. When the standard varied from the target analyte, the mass transfer coefficient, or time constant *a*, of the analyte could be extrapolated from that of the standard. [12] These theoretical predictions are well supported by experimental findings in in-vial investigations for both SPME[14] and LPME (liquid-phase microextraction).[15]

This calibration approach facilitates the full integration of sampling, sample preparation, and sample introduction, especially for on-site and *in-vivo* investigations, where the addition of a standard to the sample matrix, or control of the velocity of the sample matrix, is very difficult. The objective of the current study was to develop suitable standard loading techniques that are fast, simple and reproducible for compounds with different properties. Furthermore, the standard loading technique combined with the in-fiber standardization calibration method was applied to the BTEX analysis of a milk sample. The application was fully automated with a CTC CombiPal autosampler.

2.2 Theoretical Considerations

The kinetics of the extraction process with traditional SPME was proposed by Ai for quantification. [8] A dynamic SPME model based on a diffusion-controlled mass transfer process was developed:

$$\frac{n}{n_e} = 1 - \exp(-at) \qquad \text{Equation 2.1}$$

where n is the amount of analyte extracted by SPME fiber at time t, n_e is the amount of analyte extracted by the SPME fiber at equilibrium, and a is a constant that is dependent on the volumes of the fiber coating and sample, mass transfer coefficients, distribution coefficients and the surface area of the fiber.

The challenge for this pre-equilibrium quantification method is to determine the value of constant *a*. The kinetic process of the desorption of analytes from a SPME fiber has been studied and it was found that the desorption of analytes from a SPME fiber into an agitated sampling matrix is a mirror reflection process of the absorption of the analytes onto the SPME fiber from the sample matrix under the same agitation conditions, and this allows for the calibration of absorption using desorption. [12]

For field sampling analyses, the desorption kinetics can be expressed as: [12]

$$\frac{Q}{q_0} = \exp(-at) \qquad \text{Equation 2.2}$$

where Q is the amount of standard remaining in the extraction phase after sampling time t and q_0 is the amount of pre-added standard in the extraction phase. The mirror reflection characteristic of the absorption and desorption can be demonstrated:

$$\frac{n}{n_e} + \frac{Q}{q_0} = 1 \qquad \text{Equation 2.3}$$

Based on the kinetic models described as equations 2.1-2.3, n_e can be obtained by two methods, either by: (1) performing the absorption and desorption alternatively under the same experimental conditions, time constant *a* can be calculated using equation 2.2 and substituted the constant into equation 2.1 to determine n_e; or by (2) performing the desorption and absorption simultaneously and n_e can be directly calculated from equation 2.3.

For the in-vial analysis when the sampling volume is limited, the following equation can be used to describe the kinetics of the desorption of the standard from the PDMS fiber, when the equilibrium of desorption is achieved: [14]

$$\frac{Q-q_e}{q_0-q_e}=\exp(-at) \qquad \text{Equation 2.4}$$

where q_e is the amount of standard remaining in the extraction phase at equilibrium. When constant *a* possesses the same value for the absorption of the target analytes and the desorption of the pre-loaded standards (which are selected to have similar physicochemical properties to the target analytes), the sum of and $\frac{n}{n_e}$ and $\frac{Q-q_e}{q_0-q_e}$ should be 1 at any desorption/absorption time.

$$\frac{n}{n_e}+\frac{Q-q_e}{q_0-q_e}=1 \qquad \text{Equation 2.5}$$

The equilibrium extraction using SPME is the most well-established quantification approach for a three-phase headspace extraction in a vial, and is described as:

$$n_e=\frac{K_{fs}V_fV_s}{K_{fs}V_f+K_{hs}V_h+V_s}C_s^0 \qquad \text{Equation 2.6}$$

where K_{fs} and K_{hs} are the extraction phase (fiber coating)/sample and headspace/sample distribution coefficients of the analyte, V_f and V_s represent the volume of the fiber coating and the sample matrix, respectively, and C_s^0 is the initial concentration of the analyte in the sample matrix.

After equilibrium is reached, the amount of standard that remains on the fiber coating q_e can be calculated similarly, as illustrated:

$$q_e=\frac{K'_{fs}V_f}{K'_{fs}V_f+K'_{hs}V_h+V_s}q_0 \qquad \text{Equation 2.7}$$

where K'_{fs} and K'_{hs} are the extraction phase (fiber coating)/sample and headspace/sample distribution coefficient of the standard.

Substituting equation 2.7 into equation 2.5 results in equation 2.8:

$$n_e = \frac{q_0 n\left(K'_{h's} V_h + V_s\right)}{(K'_{fs} V_f + K'_{hs} V_h + V_s)(q_0 - Q)} \qquad \text{Equation 2.8}$$

When the standard and analyte have the same physicochemical properties ($K'_{fs} = K_{fs}$ and $K'_{hs} = K_{hs}$, equation 2.6 and equation 2.8 can be combined to:

$$C_s^0 = \frac{q_0 n\left(K_{hs} V_h + V_s\right)}{K_{fs} V_s V_f (q_0 - Q)} \qquad \text{Equation 2.9}$$

For in-vial two-phase system without headspace, the initial concentration of the analyte in the sample matrix, C_s^0, can be calculated as:

$$C_s^0 = \frac{q_0 n}{K_{fs} V_f (q_0 - Q)} \qquad \text{Equation 2.10}$$

By preloading a certain amount of standard, q_0, onto the PDMS fiber, and exposing the fiber to the vial that contains the sample matrix for a defined period , *n*, the amount of analyte extracted by the sampler, and *Q*, the amount of standard remaining in the sampler, can be determined. The initial concentration of analyte in the sample matrix, C_s^0, can then be calculated using equation 2.9 or 2.10.

2.3 Experimental Section

2.3.1 Materials and Reagents

HPLC grade methanol and acetone were obtained from BDH (Toronto, ON, Canada). Benzene, [$^2H_6$]benzene (benzene-d_6), toluene, [$^2H_8$]toluene (toluene-d_8), ethylbenzene, and *o*-xylene (HPLC grade, 99+%) were purchased from Sigma-Aldrich (Mississauga, ON, Canada). Naphthalene, fluorene, anthracene, fluoranthene, pyrene and decachlorobiphenyl were purchased from Supelco

(Bellefonte, PA, USA). The silicone vacuum pumping oil was supplied by BOC Edwards (Wilmington, MA, USA). Pure water was obtained using a Barnstead/Thermodyne NANO-pure ultrapure water system (Dubuque, IA, USA). The SPME holder and 100 μm PDMS fiber were also obtained from Supelco. Ten or 20 mL sample vials were used for the automated analyses with magnetic crimp caps and PTFE coated silicone septa (Supelco). All gases were supplied by Praxair (Kitchener, ON, Canada) and were of ultra high purity. The milk sample was obtained from a local supermarket store. All preparations involving BTEX, PAHs and decachlorobiphenyl were carried out in a ventilated fume hood.

2.3.2 Instrument

The investigations were performed on two instruments: the Varian (Mississauga, ON, Canada) 3800 gas chromatograph coupled with a Saturn 2000 MS system, controlled by a computer using Varian Saturn Workstation software (Version 5.51), or a FID (flame ionization detection) detector using Star Chromatography Workstation (Version 5.31). Both the Varian GC-MS and GC-FID were fit with a SPB-5 fused silica column (30 m, 0.25 mm I.D., 0.25 μm film thickness) from Supelco (Mississauga, ON, Canada). Automated analysis was performed with a CTC CombiPal Autosampler (Zwingen, Switzerland) using the associated Cycle Composer software (Version 1.4.0). The PAL was equipped with a SPME fiber holder, a temperature controlled six-vial agitator tray and a fiber conditioning device.

The loading methods study was performed almost exclusively on the GC-FID. The 1093 injector was set at 250 $^{\circ}$C. FID was used at 300 $^{\circ}$C and the hydrogen, high-purity air and make-up gas (nitrogen) flows were set at 30, 300 and 25 mL/min, respectively. For the BTEX analysis, the column was initially set at 40 $^{\circ}$C for 1 min and then ramped at 20 $^{\circ}$C /min to 120 $^{\circ}$C, for a total run time of 5

min. For the analysis of PAHs, the column was initially set at 40 °C for 1 min and then increased at 20 °C /min to 250 °C, for a total run time of 11.5 min.

The application of this approach to a retail milk sample was conducted on the Saturn 3800GC/2000 ITMS system. Helium was used as the carrier gas, with a flow rate of 1 mL/min. The 1079 injector was set at 250 °C. The column temperature programming that was used for the GC-FID analyses was also followed for the BTEX analysis. The MS system was operated in the electron ionization (EI) mode and tuned to perfluorotributylamine (PFTBA). A mass scan from 40 to 120 was acquired and quantification was performed using *m/z* 78 for benzene, *m/z* 84 for benzene-d_6, *m/z* 98 for toluene-d_8 and *m/z* 91 for toluene, ethylbenzene and *o*-xylene.

2.4 Results and Discussion

2.4.1 Standard Loading Techniques Study

The amount of standard that is loaded onto the fiber coating should be at a level that is not too high, compared to the analyte extraction amount at equilibrium and not too low to cause detection problems. For compounds with different volatilities, the extraction amount of the same fiber coating under the same condition would occur in a wide range, due to the different physicochemical properties encountered. To obtain a standard loading method that is fast, reproducible and can be performed automatically, different loading techniques were studied. The other objective of this study was to evaluate the use the same standard generator vials for hundreds of loadings, to determine whether good reproducibility could still be achieved. Repetitive use of the vial would be useful for the automation of this analytical approach, particularly when a large number of samples are analyzed.

In this study, four standard loading approaches were evaluated, including: (a) headspace extraction of the standard dissolved in a solvent or silicone vacuum pumping oil; (b) headspace extraction of pure standard in a vial; (c) direct extraction in a standard solution; and (d) direct transfer

of the standard solution from the syringe to the fiber. The schemes are demonstrated in Figure 2-1. The final approach was achieved by depositing 1 μL of a standard solution onto the SPME fiber and waiting for the volatilization of the solvent in the ambient air prior to transfer to the GC injector for desorption. The four approaches were tested for compounds that possess different volatilities, including BTEX, PAHs and decachloribiphenyl.

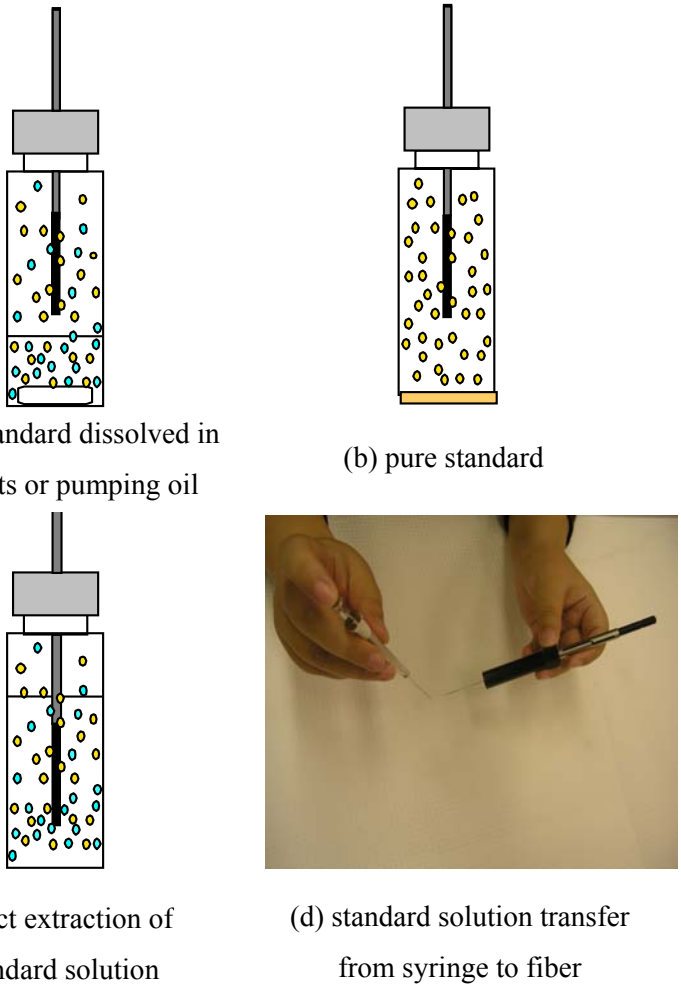

(a) pure standard dissolved in solvents or pumping oil

(b) pure standard

(c) direct extraction of standard solution

(d) standard solution transfer from syringe to fiber

Figure 2-1 Different standard loading techniques.

For the diffusion controlled extraction, the extracted amount on the fiber coating at time *t* before reaching equilibrium could be described with the following equation, assuming that the sample concentration is constant: [9]

$$n = \frac{B_3 D_s A}{\delta_s} C_s^0 t \qquad \text{Equation 2.11}$$

where B_3 is the geometric factor, D_s is the diffusion coefficient of the analyte, A is the surface area of the extraction phase and C_s^0 is the bulk concentration. The thickness of the boundary layer δ_s is a function of the agitation conditions.

Equation 2.11 indicates that the extracted mass of a certain compound is proportional to the area of the extraction phase, the bulk concentration, the diffusion coefficient of the analytes and the extraction time and inversely proportional to δ_s. To adjust the pre-loaded amount of the standard onto the fiber, the bulk concentration, the extraction time, the agitation conditions, as well as the temperature, which will affect the diffusion coefficient, can be adjusted accordingly.

2.4.1.1 Volatile Compounds

The development of an appropriate loading method for volatile compounds was performed using BTEX as the loading standards. Large amounts of the standards were loaded onto the fiber coating by the headspace extraction of pure standards in a vial even within very short extraction time. As mentioned in the previous study, [14] pumping oil can significantly reduce the amount of standards in the vial headspace due to the lower distribution coefficient that exists between the headspace and pumping oil. In this study, 1 μL of BTEX was diluted in 4 g of pumping oil in a 20 mL vial. The extraction temperature was kept at 30 °C. Table 2-1 provides a comparison of the BTEX extraction amounts at different extraction times. Ten loadings were pursued for each loading time tested for

these experiments. Using this approach, each loading cycle of 30 s extraction withdrew only 0.010%, 0.009%, 0.006% and 0.005% of BTEX from the standard generation vial, respectively, which means that the same vial can be reused hundreds of times without significant loss of the standards in the vial. An acceptable and reproducible loading of the fiber by exposure to the headspace of the standard generation vial was obtained using this method. The reproducibility observed for the 30 s extraction was very good, with RSDs < 0.9%. The RSDs for the other extraction times were mostly lower than 3%. The amount of standard loaded onto the fiber can be easily adjusted by changing the initial standard concentration in the pumping oil or the extraction time before the equilibrium is reached.

Table 2-1 Standard loading of BTEX by headspace extraction from pumping oil at different extraction times

Extraction time (second)	Extraction amount (ng) (RSD (%), n = 10)			
	Benzene	Toluene	Ethylbenzene	*o*-Xylene
3	42.8 (2.1)	34.8 (3.9)	21.2 (2.4)	17.7 (3.2)
6	55.1 (1.8)	45.4 (1.1)	28.1 (2.0)	23.5 (2.1)
9	64.1 (1.6)	52.3 (0.9)	33.1 (1.6)	27.4 (0.3)
15	74.0 (1.2)	61.9 (1.2)	39.5 (1.3)	34.1 (2.5)
30	90.2 (0.8)	78.8 (0.7)	52.2 (0.6)	45.3 (0.9)

Direct extractions in 100 ppm standard BTEX methanolic solutions were conducted. The extraction time was set for 3 s, 6 s, 9 s, 15 s, 30 s, 45 s and 60 s, at an incubation temperature of 30°C. The experimental results are shown in Table 2-2. The results indicated that this approach is also applicable for the loading of volatile compounds. The RSDs are mostly lower than 3% for 10 loading cycles. As the extraction time increased, more standards were extracted.

The syringe-fiber transfer approach was performed for the loading of BTEX. Compared to the direct injection of 1 μL 100 ppm standard solution to GC, the BTEX amount left on the fiber coating after the evaporation of solvent was less than 10% for the syringe-fiber transfer approach due to the high volatility of BTEX. The results confirm that this approach is not suitable for volatile compounds.

Table 2-2 Standard loading of BTEX by direct extraction from standard solution at different extraction times

Extraction time (second)	Extraction amount (ng) (RSD (%), n = 10)			
	Benzene	Toluene	Ethylbenzene	*o*-Xylene
3	7.7 (3.0)	13.4 (3.4)	14.0 (4.5)	14.3 (3.3)
6	9.4 (1.9)	16.5 (1.8)	28.1 (1.3)	23.5 (1.4)
9	10.1 (1.7)	18.5 (1.5)	19.4 (1.4)	20.1 (1.8)
15	11.8 (1.4)	22.0 (1.4)	24.0 (1.2)	25.2 (1.6)
30	13.7 (2.2)	26.4 (1.8)	29.7 (0.8)	31.6 (1.0)
45	13.9 (3.0)	27.8 (1.5)	32.2 (1.2)	34.7 (1.0)
60	13.9 (0.9)	28.3 (0.4)	33.6 (1.3)	36.5 (1.9)

2.4.1.2 Semi - volatile Compounds

Five PAHs with a wide range of volatility were selected to study the loading approach for semi-volatile compounds, including naphthalene, fluorene, anthracene, fluoranthene and pyrene. The aforementioned loading methods that are suitable for BTEX also work for naphthalene. However, the headspace extraction of pyrene dissolved in pumping oil will only extract a limited amount due to its low volatility, although the RSD is as good as 1.5% for 10 loading cycles with agitation and

incubation at 50 °C. Therefore, instead of dissolving the standard in the pumping oil, the pure solid compounds were put in a 20 mL vial that was used as the standard generator. 20 mg of pure pyrene was put in a 20 mL vial to load the standard by headspace extraction of 10 min. This approach resulted in almost 3 times greater amount of pyrene extracted than when the pyrene was dissolved in pumping oil. The RSD value also decreased from 1.5% to 0.9%. Figure 2-2 illustrates the headspace extraction profile of solid pyrene. It is observed that equilibrium has not been reached even after 8 hours of extraction. Before reaching equilibrium, the extraction amount can be increased by increasing the extraction time.

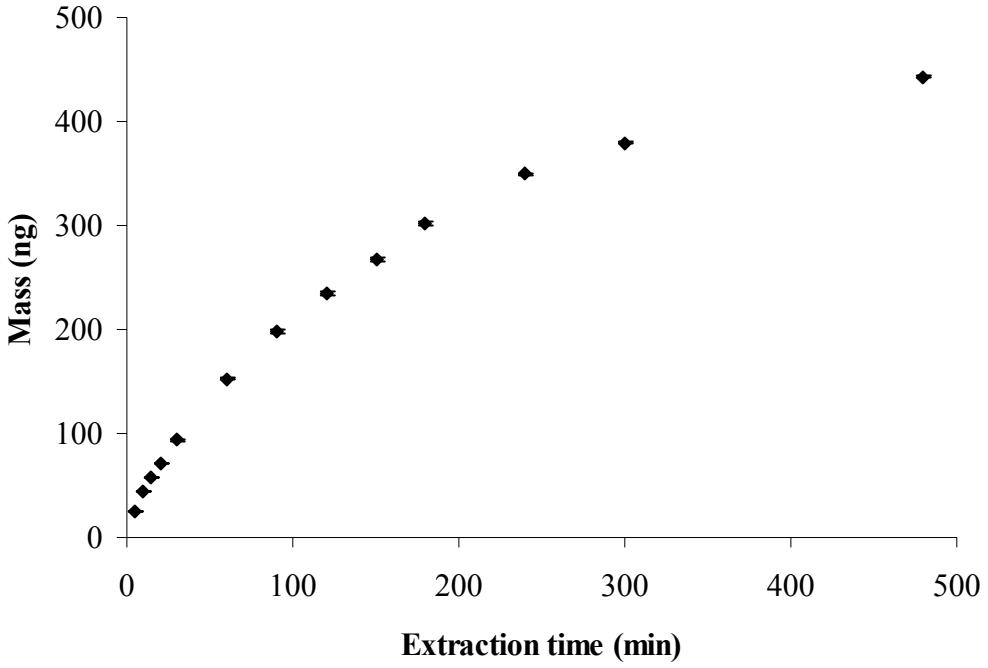

Figure 2-2 Extraction profile of solid pyrene containing in a vial (n=5).

The headspace extraction of solid fluorene provided a RSD of 1.9% with 100 loading cycles. The effect of the amount of standard in the vial and temperature on the standard loading was further

evaluated using fluorene as the standard. It was found that the extraction amount was almost the same for three different starting amounts (10, 20 and 40 mg samples), with the same extraction time, which was expected because the headspace concentration does not change with the amount of the solid. Nevertheless, it was found that temperature has a significant effect on the extraction amount. It is illustrated in Table 2-3 that by increasing the temperature from 40 °C to 60 °C, the extraction amount increased almost three times, which contributed to an increase in the diffusion coefficient D_s as stated in equation 2.11 and the higher concentration of standard in the headspace at higher temperature. The same method was applied to naphthalene, which resulted in a very high loading amount, even with an extraction time as short as 1 min. This illustrates that the headspace extraction of a solid pure sample is more feasible for those PAHs that possess a lower volatility.

Table 2-3 Temperature effect on the headspace extraction of fluorene

Temperature (°C)	Extraction amount (ng)	RSD (%) (n = 6)
40	33.7	0.6
50	62.4	1.1
60	103.3	1.9

For low volatility compounds like pyrene, syringe-fiber technique was also studied. The loss of the standard from the fiber due to evaporation would be limited, and this was confirmed by exposing the fiber to a flowing gas for different exposure times—no significant loss was observed. The syringe-fiber transfer method was evaluated by transferring 1 μL of 100 ppm standard methanolic solution onto a SPME fiber. The fiber was then desorbed in the GC injector after the volatilization of the solvent. The results indicated that the transfer efficiencies were approximately 95% compared to the direct injection of 1 μL of the standard solution into the GC injector. At 4%

RSD for 6 replicate experiments, the reproducibility was acceptable especially when the great advantage of the syringe-fiber transfer approach is considered: it can be performed easily without agitation and exact timing. This approach offers some promise for low volatility standards with a good reproducibility and the loading amount can be easily adjusted by the concentration of the standard solution.

Direct extraction of a standard methanolic solution was conducted simultaneously with five PAHs, including naphthalene, fluorene, anthracene, fluoranthene and pyrene. The fiber was exposed to the 100 ppm standard methanolic solution for 15 s at an incubation temperature of 50 $^{\circ}$C. The extraction was conducted under both static and agitated conditions, to study the effect of the boundary layer. The experimental results are shown in Table 2-4. The RSD values for the two sets of experiments were around 5% for 10 loading cycles. It was found that the extraction amount was greater with agitation than under static conditions, which can be attributed to the faster mass transfer rate associated with the thinner boundary layer at the agitation condition.

Table 2-4 Standard loading of five PAHs by direct extraction from standard solution with and without agitation

	Without agitation (n = 10)		With agitation (n = 10)	
Compound	Amount (ng)	RSD (%)	Amount (ng)	RSD (%)
Naphthalene	36.2	5.1	43.4	2.8
Fluorene	30.2	5.4	43.1	4.0
Anthracene	21.2	5.8	35.8	5.1
Fluoranthene	17.0	6.1	33.5	5.9
Pyrene	18.0	5.9	33.5	5.4

It is concluded from this study that due to the different volatilities of compounds, the standard loading approach must be adjusted correspondingly. For compounds with higher volatility, like naphthalene, the most suitable loading method is the same as for volatile compounds like BTEX. However, the headspace extraction of pure compounds in the vial is more suitable for compounds with medium volatility like fluorene. The direct extraction method, which proved to be the most universal approach, is applicable for all of the PAHs studied, achieving RSDs in the range of 3-6%. For low volatility compounds, another applicable standard loading approach is to directly transfer the standard solution from the syringe to the fiber with RSD less than 4%.

2.4.1.3 Compounds with Low Volatility

Decachlorobiphenyl is a compound with low volatility and high molecular weight. The extraction amount is less than 10 ng for 5 hr headspace extraction of 100 ppm standard acetone solution. The reproducibility is also poor which has a RSD of 11% for five replicate loadings. Therefore, the headspace extraction is not suitable for the loading of this compound. The methods used to load pyrene onto a fiber coating were applied to decachlorobiphenyl, which include the direct extraction of the standard solution and syringe-fiber transfer. Sixty seconds direct extraction of decachlorobiphenyl standard solution offers about 6 times higher extraction amount comparing to 5 hours headspace extraction. The reproducibility was also highly improved with the RSD as low as 1.2% for five replicate loadings. For the syringe-fiber transfer, different concentrations of the standard solution were evaluated (10 ppm, 50 ppm and 100 ppm).

Table 2-5 Standard loading of decachlorobiphenyl by syringe-fiber transfer

Concentration of standard solution (ng/μL)	Loading amount using syringe-fiber transfer (ng)	RSD (%) (n = 5)
10	9.7	2.6
50	48.1	0.9
100	94.8	0.7

The results illustrated in Table 2-5 indicated that the transfer efficiencies were around 95% compared to the direct injection of 1 μL of the standard solution into the GC injector, regardless of the concentration of the standard solution. The results supported the previous observations that the direct extraction and syringe-fiber transfer approach are suitable for the loading of compounds with low volatility.

2.4.2 Application

To test the developed standard loading method and demonstrate the feasibility of the internal standardization calibration method, experiments were conducted to quantify BTEX concentrations in a spiked milk sample with GC-MS analysis. The experiment was conducted fully automated by the CTC autosampler, including the standard loading, sample transfer and agitation, sample extraction and fiber desorption in the GC injector. The mirror reflection characteristic of the absorption of the analytes from the sample matrix to the fiber coating and desorption from the fiber coating to the sample matrix was first demonstrated in this study.

Initially, the absorption and desorption were performed alternatively under the same experimental conditions. Figure 2-3 presents n/n_e and $(Q-q_e)/(q_0-q_e)$ calculated from the extraction profile and desorption profile of BTEX accordingly. The extraction profile was obtained by

exposing a 100 μm PDMS fiber to the headspace of a 10 mL vial containing 3 mL of milk that was spiked with 3 μl of a 100 ppm standard BTEX methanolic solution for different extraction times. The desorption profile of BTEX was achieved by exposing the standard loaded fiber to the headspace of a 3 mL pure milk sample. The extraction and desorption profile illustrate that the extraction and desorption of BTEX reached equilibrium in less than 3 min. The results also illustrate that as the volatility of the standard increases, the desorption equilibrium is achieved more quickly.

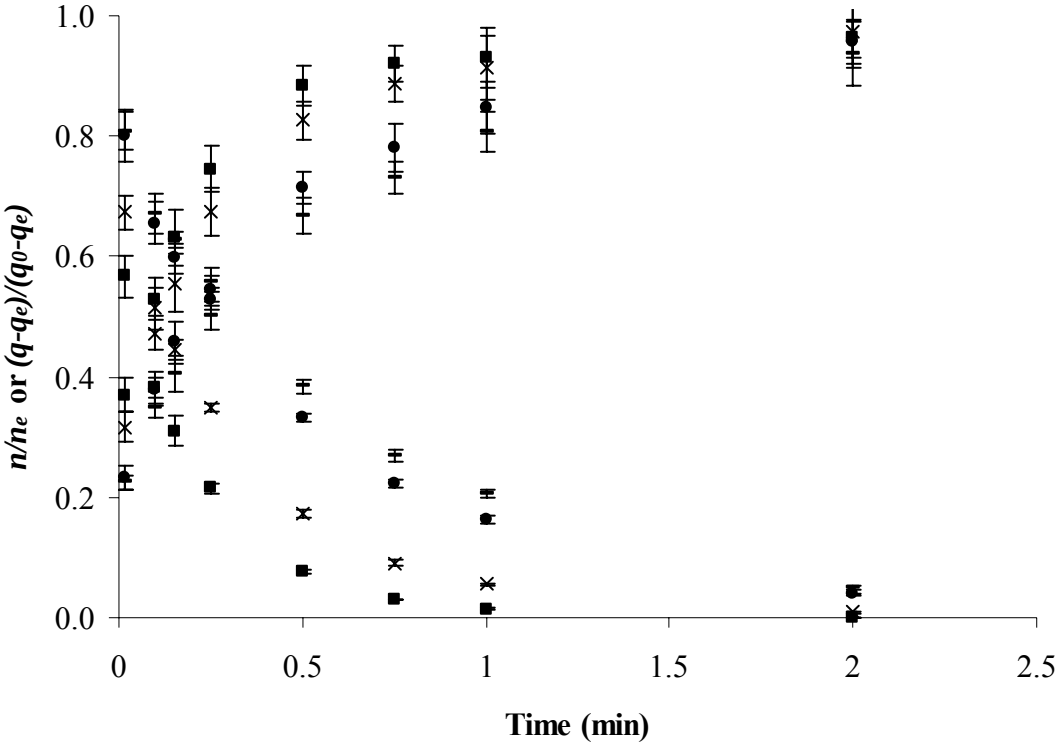

Figure 2-3 Absorption and desorption profiles of BTEX at 25 °C. Benzene(■); toluene (×); ethylbenzene (●) and *o*-xylene (▬).

Table 2-6 Time constant *a* for the absorption and desorption of benzene and toluene

Compound	Time constant *a* (R^2) (min^{-1})	
	Absorption	Desorption
Benzene	3.68 ± 0.56 (0.999)	3.71 ± 0.15 (0.999)
Toluene	2.63 ± 0.39 (0.999)	2.54 ± 0.12 (0.999)

According to equations 2.1 and 2.4, the time constants *a* calculated based on the absorption and desorption of benzene and toluene at 25 °C are listed in Table 2-6. The results illustrate that the time constant *a* for the absorption and desorption are very close, demonstrating the mirror reflection characteristic of the absorption of analytes from the sample matrix and desorption of analytes from the fiber coatings.

Subsequently, the desorption of benzene-d_6 and toluene-d_8 and the absorption of benzene and toluene were determined simultaneously. The pre-loaded PDMS fiber (benzene-d_6 and toluene-d_8) was exposed to the headspace of the spiked BTEX milk solution for different exposure times. The profiles of the absorption of analytes and desorption of deuterated benzene and toluene are shown in Figure 2-4. Duplicate experiments were conducted at each time point. The results demonstrate the mirror reflection characteristic of the absorption and desorption processes: the sum of n/n_e and $(Q-q_e)/(q_0-q_e)$ at any time is close to 1, which illustrates that the absorption of analytes from the sample matrix can be calibrated by the desorption of the standard on the fiber. Nevertheless, it needs to be pointed out that the sum of n/n_e and $(Q-q_e)/(q_0-q_e)$ does fall short of 1 at most of the times, which can be ascribed to the difference of the physicochemical properties of deuterated benzene and toluene from those of benzene and toluene.

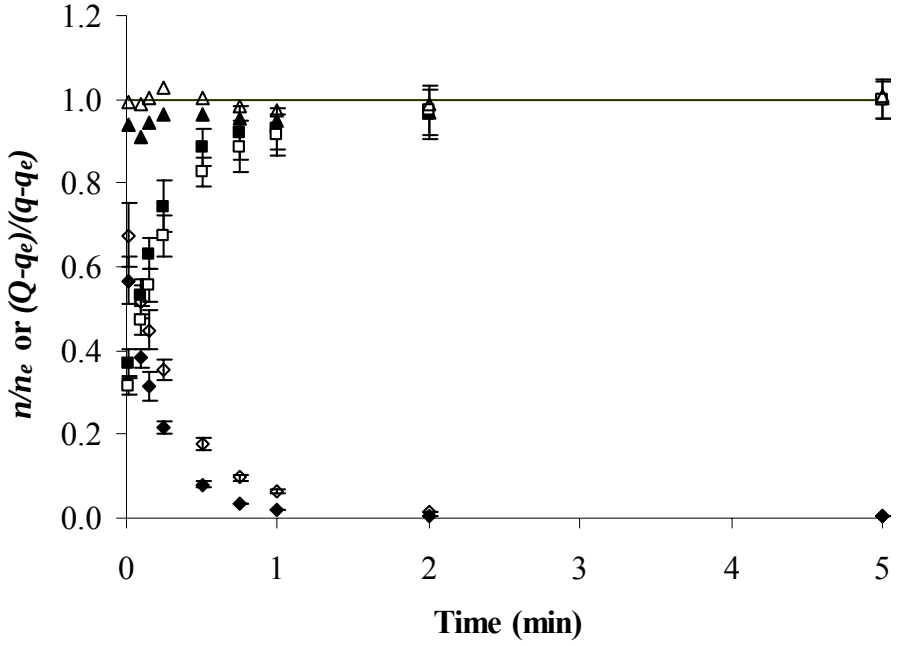

Figure 2-4 Absorption and desorption profiles in SPME. Simultaneous absorption of benzene (■) and toluene (□) and desorption of benzene-d_6 (◆) and toluene-d_8 (◇); (▲) and (Δ), the sum of n/n_e and $(Q-q_e)/(q_0-q_e)$ for benzene and toluene.

To test the in-fiber standardization method, the technique was used to quantify BTEX in a spiked milk sample and compare the result with external calibration. K_{hs} and K_{fs} used in the in-fiber standardization method were obtained using the same method discussed by Ouyang et. al. [15] The recoveries from milk spiked with 3 μL of a 100 ppm BTEX methanolic solution were calculated against a standard prepared in water with external calibration and the in-fiber standardization approach, and the results are presented in Table 2-7. The results illustrate that the recovery calculated using the external calibration is much lower than the in-fiber standardization method, indicating that the kinetic calibration technique can successfully compensate for the matrix effect and produce more accurate results.

Table 2-7 Calculated recoveries of BTEX in a milk sample with external calibration and in-fiber standardization method

Compound	Relative recovery (%) (RSD (%), n = 3)	
	External calibration	In-fiber standardization
Benzene	49.4 (2.3)	96.5 (4.7)
Toluene	32.5 (2.8)	98.1 (4.8)

2.5 Conclusion

The techniques that are used to load internal standards with different physicochemical properties onto a non-porous SPME fiber coating have been described. The loading techniques are fast and reproducible. Moreover, the same standard generation vial can be used for hundreds of analyses, which is essential for the processing of a large number of samples. The standard loading technique and the in-fiber standardization calibration were successfully applied to the analysis of a spiked milk sample, considered a complex matrix, and the results demonstrated that the in-fiber standardization approach effectively compensates for the matrix effect. The analysis can be performed fully automated by a CTC autosampler, which is more accurate and efficient.

References

(1) Arthur, C. L.; Pawliszyn, J. *Anal. Chem.* **1990**, *62*, 2145.

(2) Pawliszyn, J. *Solid Phase Microextraction: Theory and Practice*; Wiley-VCH: New York, 1997.

(3) Pawliszyn, J. *Applications of Solid Phase Microextraction*; Royal Society of Chemistry: Cambridge, 1999.

(4) Pawliszyn, J., Ed. *Sampling and Sample Preparation for Field and Laboratory*; Elsevier: Amsterdam, 2002.

(5) Ouyang, G.; Pawliszyn, J. *Trends Anal. Chem.* **2006**, *25*, 692.

(6) Ouyang, G.; Pawliszyn, J. *Anal. Bioanal. Chem.* **2006**, *386*, 1059.

(7) Louch, D.; Motlagh, S.; Pawliszyn, J. *Anal. Chem.* **1992**, *64*, 1187.

(8) Ai, J. *Anal. Chem.* **1997**, *69*, 1230.

(9) Koziel, J.; Jia, M.; Pawliszyn, J. *Anal. Chem.* **2000**, *72*, 5178.

(10) Chen, Y.; Koziel, J. A.; Pawliszyn, J. *Anal. Chem.* **2003**, *75*, 6485.

(11) Chen, Y.; O'Reilly, J.; Wang, Y.; Pawliszyn, J. *Analyst* **2004**, *129*, 702.

(12) Chen, Y.; Pawliszyn, J. *Anal. Chem.* **2004**, *76*, 5807.

(13) Haefelfinger, P. *J. Chromatogr.* **1981**, *218*, 73.

(14) Wang, Y.; O'Reilly, J.; Chen, Y.; Pawliszyn, J. *J. Chromatogr. A.* **2005**, *1072*, 13.

(15) Ouyang, G.; Zhao, W.; Pawliszyn, J. *Anal. Chem.* **2005**, *77*, 8122.

Chapter 3
Time-Weighted Average Water Sampling Using PDMS Rod Sampler

3.1 Introduction

Water contamination is a global environmental problem. However, monitoring environmental pollutants in water is still a challenge for the analytical chemist. [1] One of the most important steps in water contamination analysis is the sampling of water itself. [2] Generally water sampling relies on spot sampling at prescribed periods of time. However, this approach only gives a snapshot of the situation at the time of sampling and has considerable temporal and spatial limitations when assessing contaminant concentrations. Time-integrative sampling, in contrast, enables the determination of time-weighted average aqueous contaminant concentrations over extended sampling periods, which is suitable for the long-term monitoring. For the long-term monitoring of organic pollutants in water, two strategies can be used: active sampling and passive sampling.

Active sampling utilizes pumps to force the sample flow through a solid- or liquid- collecting medium trap where analytes are absorbed or adsorbed, at a constant rate of the sampling.[3] The mass loading rate of a waterborn analyte onto a sorbent with active sampling is shown in equation 3.1:

$$\frac{n}{t} = R \times \overline{C} \qquad \text{Equation 3.1}$$

where n is the mass of analyte sorbed during sampling time t, R is the pump sampling flow rate (volume/time) and $\overline{C}$ is the average analyte concentration (mass/volume) for the sampling time. Although active sampling is the most common and conventional technique used, it has several disadvantages, including the high costs, since a pump is required and a relatively large number of

samples must be collected from one location for the entire duration of sampling when a TWA concentration is required.

Passive sampling techniques are more attractive, compared to active sampling approaches for the long-term monitoring of organic pollutants in water, since the latter eliminate power requirements and significantly reduce the costs of analysis.[1, 3-6] Passive sampling was first introduced in 1973. [7, 8] There are three main trends related to the design of passive sampling technology, which include the needs to: (1) miniaturize the sampling devices, (2) broaden the types of target analytes that can be analyzed, and (3) couple passive samplers to biological assays, to identify the presence of toxicologically relevant compounds. [9] Currently available passive samplers for water analysis are based on either permeation or diffusion, [10] which include semipermeable membrane devices (SPMDs), [3] solvent-filled devices, [11-13] passive in situ concentration/extraction samplers (PISCES), [14] and sorbent-filled devices, [15] SPMDs are currently the most widely used types of passive samplers for field water analysis due to its high sensitivity and bioavailability. [3, 16-18] However, the main disadvantage of the SPMD technique is the complex procedures required to recover the accumulated analytes from the collection media. [19]

Since its inception in 1990, SPME has been successfully applied to a wide variety of applications, including the analysis of food, forensics and toxicology, environmental and pharmaceutical samples. [20-22] SPME was also developed as an equilibrium passive field sampling technique for the on-site monitoring of organic pollutants in air, water and soil gas. [22-25] However, this type of SPME device is unsuitable for long-term monitoring of contaminants in the environment because the results obtained with this device are only comparable with those obtained by grab sampling. SPME can also be used as a TWA passive sampling technique. Initially, SPME TWA passive sampler for air sampling was developed in Pawliszyn's group.[26-28] Subsequently, the device was modified and applied for TWA sampling in water. [29] Unlike conventional sampling with SPME,

the fiber is retracted a known distance into its needle during the sampling period in the SPME TWA passive sampler. Thus, this method is referred to as a fiber-in-needle SPME device. [29] The advantage of this device is that the analyte molecules access the fiber coating only by means of diffusion through the static air or water gap between the opening and fiber coating, so the mass uptake can be predicted by Fick's law of diffusion. The concentrations of target analytes in the sample can be directly calculated by the amount of analytes extracted by the SPME fiber. However, the disadvantage of this device for passive water sampling is that the sampling rate is low, because of the small surface area/diffusion path ratio, combined with low diffusivity and solubility of analyte molecules in the diffusion medium (water). Thus, the sampling time is long particularly if the target analytes are found at very low concentrations in the sampling environment.

A number of fiber coatings have been developed for a range of applications in SPME. Polydimethylsiloxane (PDMS), a liquid polymer coating, is the most commonly used sorbent because of its inertness, stability and reproducibility. [30] Different configurations of SPME using the PDMS sorption methods were developed over the past twenty years, which include coating the interior of vessels, [31] ultra thick film open tubular trap (OTT), [32] stir-bar sorptive extraction (SBSE), [33, 34] packed sorption tubes, [35] the large size sorption probe (LSP) [36] and membrane-enclosed sorptive coating (MESCO). [37, 38] Several of these implementations are shown in Figure 3-1.

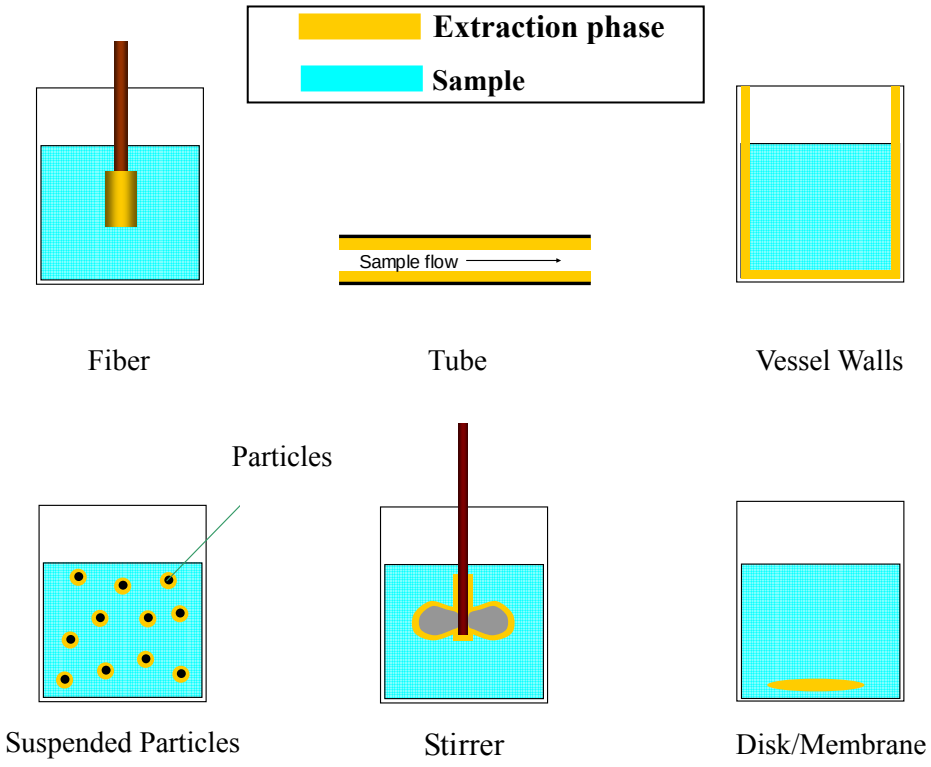

Figure 3-1 Configurations of SPME.

The main reason for developing these alternative approaches is to enhance sensitivity by using larger volume of the extraction phase (PDMS) and improving the kinetics of the mass transfer between sample and fiber coating by increasing the surface to volume ratio of the extraction phase. In this study, a new SPME passive sampler, PDMS rod, was developed for field water analysis.

To date, there are several calibration approaches developed for SPME. Conventional direct SPME is performed by exposing a fiber coated with a liquid polymeric coating to a sample matrix until equilibrium is reached between the fiber coating and the sample matrix. The amount of analyte extracted onto the fiber is linearly proportional to its initial concentration in the sample matrix. [20] In 1997, a pre-equilibrium extraction method for quantification with SPME was proposed, which is based on limited sample volume. [39] The weakness for this pre-equilibrium quantification method is that the constant *a* must be known.

Based on this method, Chen and Pawliszyn further studied the kinetic process of the desorption of analytes from a SPME fiber and found that the desorption of the analytes from the fiber into an agitated sampling matrix is a mirror reflection process to the absorption of the analytes onto the fiber from the sample matrix under the same agitation conditions [40]. Therefore, a new calibration method was proposed, which used the desorption of the standards pre-loaded in the extraction phase, to calibrate the extraction of the analytes. This kinetics calibration method later was known as the in-fiber standardization technique and successfully applied to in-vial investigations for both SPME [41] and liquid-phase microextraction (LPME). [42] In 1991, an "internal reference compound" [43] or "internal standard" [44] concept was introduced for control of the recovery in microdialysis. The approach was later named retrodialysis. [45, 46] The relative recovery of the drug of interest in the tissue is determined by the degree of loss of the calibrator from the perfusion solution during the entire experiment. [47] The ratio of the recovery between the drug and the calibrator is determined by experiment since recoveries are dependent on the perfusate flow rate. In SPMD, using performance reference compound (PRC) as an internal standard was first introduced to monitor the biofouling effect. [48] Later some efforts have been made to calculate the sampling rate in order to estimate the analyte concentration using the release rate of PRC. [49] However, the results showed poor precision and accuracy likely due to the complexity of the SPMD structure and experimental procedures. Most recently PRC has been adopted to adjust the sampling rate by exposure adjustment factor (EAF) which was derived by separate studies performed in the laboratory. [50] The analyte concentration was not exactly calibrated in their work. The results of Vrana and Schuurmann also confirmed that the use of the laboratory-derived calibration data for the estimation of analytes concentrations in the ambient environment is limited unless flow-sensitive performance reference compounds are used. [51]

This study demonstrates a novel approach to calculate the analyte concentration directly using the internal standard preloaded in the extraction phase. There is no need to experimentally

determine the sampling rate or EAF in laboratory prior to the field sampling, which results in much simpler practical approach to obtaining the TWA data.

The PDMS rod sampler, combined with on-rod standardization technique which was similar to the in-fiber standardization method, was tested in the laboratory with a flow-through system and was later used to measure the TWA concentrations of PAH in Hamilton Harbour. The results of the laboratory and field experiments demonstrated that, with the on-rod standardization technique, the PDMS rod can be used as a TWA passive sampler to monitor organic pollutants in water.

3.2 Theory

When a PDMS rod that is preloaded with a standard is exposed to the sample matrix in the field sampling, the absorption of analyte and desorption of standard occur simultaneously. A 2D axisymmetic structure of the rod is illustrated in Figure 3-2.

The 2D axisymmetic structure was applied since there was no angular gradient present. The absorption process follows Fick's first law of diffusion:

$$J \equiv \frac{1}{A}\frac{dn}{dt} = -D_s \frac{dC^s}{dx} = -D_f \frac{dC^f}{dx} \qquad \text{Equation 3.2}$$

where J is the mass flux of the analyte from the sample matrix to the rod, A is the surface area of the rod, n is the amount of the analyte extracted during sampling time t, D_s and D_f are diffusion coefficients of the analyte in the sample matrix and the rod, respectively. C^s and C^f are the concentrations of the analyte in the boundary layer and the rod, respectively. A linear concentration gradient in the boundary layer and the rod is assumed:

$$\frac{1}{A}\frac{dn}{dt} = \frac{D_s}{\delta_s}(C_s - C_s^{'}) = \frac{D_f}{\delta_f}(C_f - C_f^{'}) \qquad \text{Equation 3.3}$$

where δ_s and δ_f are the thickness of the boundary layer and radius of the rod, respectively. C_s is the concentration of the analyte in the sample matrix and $C_s^{'}$ is the concentration of the analyte in the boundary layer at the interface of the boundary layer and rod. C_f is the concentration of the analyte in the rod at the interface of the rod and boundary layer, $C_f^{'}$ is the concentration of the analyte at the axis of the rod.

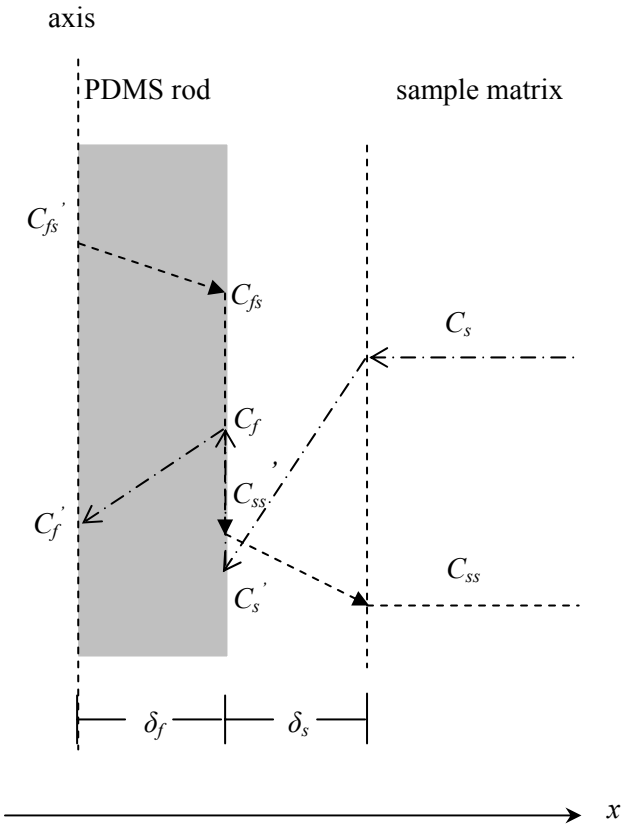

Figure 3-2 Schematic of the calibration of the extraction of target analyte by the desorption of a standard from a PDMS rod to an aqueous media in field sampling.

In the field sampling, the microextraction by the rod will not affect the concentration of analyte in the sample matrix, and thus,

$$C_s = C_s^0 \qquad \text{Equation 3.4}$$

Assuming the partition equilibrium can be quickly reached at the interface of the rod and the boundary layer:

$$K_{fs} = \frac{C_f}{C_s^{'}} \quad \Rightarrow \quad C_s^{'} = \frac{C_f}{K_{fs}} \qquad \text{Equation 3.5}$$

K_{fs} is the distribution coefficient of the analyte between the rod and the sample matrix. Let $h_s = \frac{D_s}{\delta_s}$, $h_f = \frac{D_f}{\delta_f}$, where h_s and h_f are mass transfer coefficients in the boundary layer and the rod, respectively. Equation 3.3 can be rewritten as

$$\frac{1}{A}\frac{dn}{dt} = h_s(C_s^0 - \frac{C_f}{K_{fs}}) = h_f(C_f - C_f^{'}) \qquad \text{Equation 3.6}$$

A linear concentration gradient is assumed in the rod,

$$n = V_f \frac{(C_f + C_f^{'})}{2} \qquad \text{Equation 3.7}$$

Combining equation 3.6 and 3.7

$$C_f = \frac{K_{fs}(2nh_f + h_s V_f C_s^0)}{V_f(2K_{fs}h_f + h_s)} \qquad \text{Equation 3.8}$$

Substitution of equation 3.8 into equation 3.6 gives

$$C_f - C_f^{'} = \frac{2K_{fs}h_s C_s^0}{2K_{fs}h_f + h_s} - \frac{2h_s n}{V_f(2K_{fs}h_f + h_s)} \qquad \text{Equation 3.9}$$

Substitution of equation 3.9 into equation 3.6 gives

$$\frac{1}{A}\frac{dn}{dt} = h_f(C_f - C_f^{'}) = h_f[\frac{2K_{fs}h_sC_s^0}{2K_{fs}h_f + h_s} - \frac{2h_sn}{V_f(2K_{fs}h_f + h_s)}] \quad \text{Equation 3.10}$$

Let

$$a = \frac{2Ah_fh_s}{V_f(2K_{fs}h_f + h_s)} \quad \text{Equation 3.11}$$

$$b = \frac{2AK_{fs}h_fh_sC_0}{2K_{fs}h_f + h_s} \quad \text{Equation 3.12}$$

Equation 3.10 is simplified as

$$\frac{dn}{dt} = b - an \quad \text{Equation 3.13}$$

The solution to equation 3.13 is

$$n = \frac{b}{a}[1 - \exp(-at)] \quad \text{Equation 3.14}$$

With

$$\frac{b}{a} = K_{fs}V_fC_0 = n_e \quad \text{Equation 3.15}$$

where n_e is the amount of the analyte extracted in the rod when the system reaches equilibrium.

Equation 3.14 becomes

$$\frac{n}{n_e} = 1 - \exp(-at) \quad \text{Equation 3.16}$$

The desorption of the standard preloaded onto the rod follows Fick's first law of diffusion too:

$$\frac{1}{A}\frac{dq}{dt} = -h_{ss}(C_{ss} - C_{ss}^{'}) = -h_{fs}(C_{fs} - C_{fs}^{'}) \qquad \text{Equation 3.17}$$

where q is the amount of the standard desorbed from the rod during sampling time t, C_{ss} is the concentration of the standard in the sample matrix and $C_{ss}^{'}$ is the concentration of the standard in the boundary layer at the interface of the boundary layer and rod. C_{fs} is the concentration of the standard in the rod at the interface of the rod and boundary layer, $C_{fs}^{'}$ is the concentration of the standard at the axis of the rod. h_{ss} and h_{fs} are mass transfer coefficients of the standard in the boundary layer and the rod, respectively.

The concentration of the standard in the sample matrix is negligible, which means $C_{ss} \approx 0$. Assuming the partition equilibrium can also be quickly reached at the interface of the rod and the boundary layer for the standard:

$$K_{fs}^{'} = \frac{C_{fs}}{C_{ss}^{'}} \quad \Rightarrow \quad C_{ss}^{'} = \frac{C_{fs}}{K_{fs}^{'}} \qquad \text{Equation 3.18}$$

$K_{fs}^{'}$ is the distribution coefficient of the standard between the rod and the sample matrix. Equation 3.17 can be rewritten as

$$\frac{1}{A}\frac{dq}{dt} = -h_{ss}(-\frac{C_{fs}}{K_{fs}^{'}}) = -h_{fs}(C_{fs} - C_{fs}^{'}) \qquad \text{Equation 3.19}$$

Since there is a linear concentration gradient in the rod,

$$q_0 - q = V_f \frac{C_{fs} + C_{fs}^{'}}{2}$$ Equation 3.20

where q_0 is the amount of the standard initially loaded onto the rod before exposure of the rod to the sample matrix.

Combining equation 3.19 and equation 3.20

$$C_{fs} = \frac{2K_{fs}^{'} h_{fs} (q_0 - q)}{V_f (2K_{fs}^{'} h_{fs} + h_{ss})}$$ Equation 3.21

Substitution of equation 3.21 into equation 3.19

$$\frac{1}{A}\frac{dq}{dt} = -h_{fs}(C_{fs} - C_{fs}^{'}) = \frac{2Ah_{fs}h_{ss}(q_0 - q)}{V_f (2K_{fs}^{'} h_{fs} + h_{ss})}$$ Equation 3.22

Let

$$a^{'} = \frac{2Ah_{fs}h_{ss}}{V_f (2h_{fs}K_{fs}^{'} + h_{ss})}$$ Equation 3.23

Equation 3.22 is simplified as

$$\frac{dq}{dt} = a^{'}(q_0 - q)$$ Equation 3.24

The solution to equation 3.24 is

$$q = q_0[1 - \exp(-a^{'}t)]$$ Equation 3.25

Let $Q = q_0 - q$, equation 3.26 becomes

$$\frac{Q}{q_0} = \exp(-a^{'}t)$$ Equation 3.26

Q is the amount of the standard left on the rod after sampling time t. The constant a in equation 3.11 for the absorption of analyte has the same definition as constant a' in equation 3.23 for the desorption of the standard. In other words, the value of constant a and a' should be the same for both absorption and desorption under the same experimental condition when the distribution coefficient and mass transfer coefficient for both analyte and standard are the same. With the same value of constant a, the isotropy of the absorption and desorption is demonstrated, which has been proved by Chen and Pawliszyn for PDMS fiber using the isotopically labelled analogue as the standard: [40]

$$\frac{n}{n_e} + \frac{Q}{q_0} = 1 \qquad \text{Equation 3.27}$$

Combining equations 3.15 and 3.27, the concentration of analyte in the sample matrix C_0 can be calculated with equation 3.28:

$$C_s^0 = \frac{n}{K_{fs} V_f \left(1 - \frac{Q}{q_0}\right)} \qquad \text{Equation 3.28}$$

The above equation indicates that by pre-loading a certain amount of standard, q_0, onto a sampler, such as a PDMS rod, and exposing the sampler into a sample matrix for a definite time, then, n, the amount of analyte extracted by the sampler and Q, the amount of standard remaining in the sampler, can be determined. Consequently, the averaged concentration of the target analyte in the sample matrix, C_s^0, can be calculated by equation 3.28.

3.3 Experimental Section

3.3.1 Chemical and Supplies

HPLC grade methanol was obtained from BDH (Toronto, Canada). Naphthalene, acenaphthene, fluorene, anthracene, fluoranthene and pyrene were purchased from Supelco (Bellefonte, PA, USA). [$^2H_{10}$]Pyrene (pyrene-d_{10}) and [$^2H_{10}$]fluoranthene (fluoranthene-d_{10}) were purchased from Sigma-Aldrich (Mississauga, Canada). Deionized water was obtained using a Barnstead/Thermodyne NANO-pure ultrapure water system (Dubuque, IA, USA). The PDMS rods, SPME holder and 100 μm PDMS fibers were obtained from Supelco (Oakville, Canada). All preparations involving PAHs were carried out in a ventilated fume hood.

3.3.2 Instrument

A Saturn 3800GC/2000 ITMS system (Varian Associate, Sunnyvale, CA, USA) was used for the PAHs analyses. The GC-MS was equipped with a 1079 Programmable Temperature Vaporizing Injector and coupled to a SPB-5 column (30 m, 0.25 mm I.D., 0.25 μm film thickness) (Supelco, Mississauga, Canada). To obtain better sample transfer efficiency, a SPI liner (2.4 mm I.D. × 4.6 mm O.D. × 54 mm) was used. [51] Helium was used as the carrier gas at a flow rate of 1 mL/min. The 1079 injector was set at 250 °C when the PDMS fiber was used. When performing the PDMS rod desorption in the liner, the injector temperature was programmed to an initial temperature of 40 °C and then ramped to 250 °C at a rate of 100 °C/min. The rod was kept in the injector until the end of the GC analysis. For both the analysis of the PDMS rod and the SPME fiber, the column temperature was maintained at 40 °C for 2 min and then programmed to increase at a rate of 30 °C/min to 250 °C, held for 5 min and increased at a rate of 30 °C/min to 280 °C, and held for 15 min. The total run time was 30 min. The MS system was operated in the electron ionization (EI) mode, and tuned to

perfluorotributylamine (PFTBA). A mass scan from 40 to 300 was acquired, and the base peak of each compound was selected and integrated.

3.3.3 Flow-through System

The schematic diagram of the laboratory flow-through system for the generation of the standard aqueous solution is shown in Figure 3-3. The system for the generation of the standard PAH aqueous solution has been previously described. [52] It consisted of a permeation chamber, a mixing and sampling chamber (it was used to deploy the PDMS rod sampler here) and a sampling cylinder and chamber (sampling cylinder is used for determining the effect of different linear velocity of the water). Water was filled in a 12 L glass reservoir and delivered by an ISO-1000 digital pump (Chrom. Tech., Apple Valley, MN, USA). The flow rate was set at 1 mL/min. Each DispoDialyzer (Spectrum Laoboratories, Rancho Dominguez, CA, USA) was partially filled with pure standards and DI water and reached saturation state before deploying in the permeation chamber. The dissolved analyte inside the DispoDialyzer diffused through the membrane of the DispoDialyer and were carried through the system by the water flow. As the solids (PAHs) and liquid (water) coexist inside the DispoDialyzer, the concentrations of analyte inside the DispoDialyzer will remain constant (saturated concentration) if the temperature remains constant. The temperature of the permeation chamber was controlled at 30 ± 1 $^{\circ}$C by a temperature controller (Omega, Stamford, CT, USA), to minimize the effect of the temperature on the flow-through system. With the constant water flow rate maintained in the system, the diffusion of analyte molecules from inside of the DispoDialyzer to the outside water will reach steady state, creating constant analytes concentrations.

The PAH concentrations in the flow-through system were determined by SPME direct extraction. Ten milliliters of the effluent was collected in a 10 mL vial capped with a phenolic screw cap and PTFE-coated silicone septa (Supelco), and a 0.8 cm PTFE coated stirring bar (Supelco) was

used to agitate the solution at a speed of 1000 rpm (VWR Scientific). The extraction lasted for 30 min, followed by fiber desorption in the GC injector. The concentration for each compound in the system was calibrated using external calibration (direct extraction of DI water spiked with different concentrations in 10 mL viail). The concentrations of PAHs in the flow-through system was monitored every three days to check the stability of the system. The PAH concentrations in the system fluctuated within ± 20% from day to day monitoring over 3 months. The averaged concentrations of the target compounds in the flow-through system during the current experimental period are presented in Table 3-1.

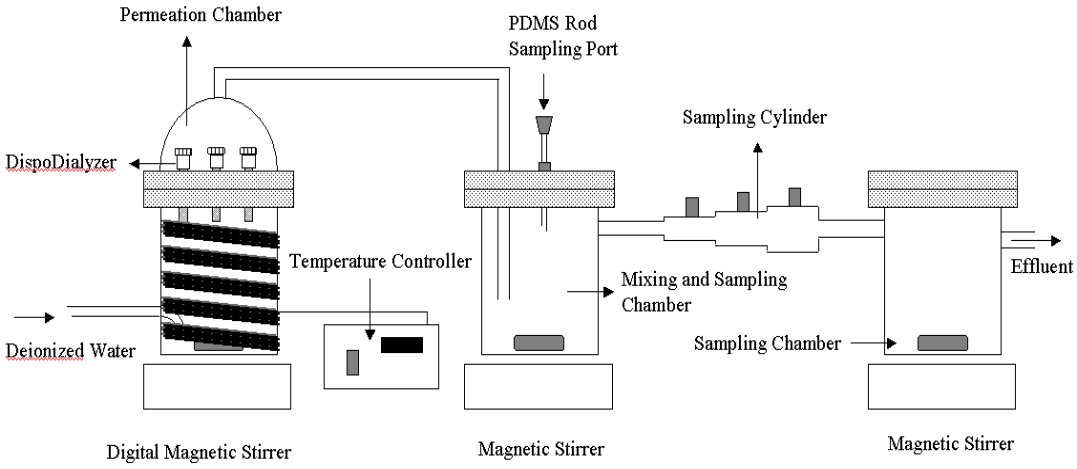

Figure 3-3 Schematic diagram of the flow – through system.

Table 3-1 Averaged PAH concentrations in the flow – through system (n = 3)

Compound	Concentration (μg/L)
Naphthalene	14.9 ± 0.3
Acenaphthene	7.7 ± 0.3
Fluorene	5.2 ± 0.1
Anthracene	0.6 ± 0.1
Fluoranthene	1.4 ± 0.1
Pyrene	1.0 ± 0.1

3.3.4 Field Trial

During the field sampling in Hamilton Harbour (Canada), the PDMS rod passive samplers were set at three different depths at the sample location: surface water at a depth of 1 m, middle water at a depth of 11 m, and bottom water, at a depth of 21 m. Three PDMS rods were deployed at each depth to study the reproducibility. The duration of the sampling was one month. After one month, the samplers were removed from the sampling location and transported to the laboratory at University of Waterloo for same-day analysis. The PDMS rods were gently cleaned with deionized water, quickly dried with a lint-free tissue and then transferred to the GC injector port for desorption.

3.4 Results and Discussion

3.4.1 Loading of the Standard

The pure PDMS rod, which was used as the TWA passive sampler in the current study, is 1 cm long with a diameter of 1 mm. The 1 cm length, which corresponds to about 7.85 μL of PDMS, was chosen for the studies with the consideration of the dimension of the inlet liner of GC injector

and the 10 mL vial that was used in the standard loading step. The PDMS rod was conditioned at 250 °C for 4 h prior to its first use and baked out for 2 h regularly after several extractions were performed. The blank run of the same PDMS rod analyzed between two consecutive extractions illustrated that there was no carryover of the target PAHs on the rod following the previous desorption.

The first challenge in this study was to develop a fast, simple and reproducible method to load the standard to the PDMS rod. Development of an appropriate method was performed using deuterated pyrene as the loading standard. The headspace extraction of the target analyte dissolved in solvent or pumping oil was not suitable for the current study due to the low volatility of deuterated pyrene as discussed earlier. In order to load an appropriate amount of target analyte with high reproducibility, the loading was conducted by placing the rod directly in the standard solution with agitation.

To adjust the pre-loaded amount of the standard onto the rod, the surface area of the rod, the concentration of the standard solution and the extraction time can be changed correspondingly. This represents another advantage of using the rod as the extraction phase, since the length of the rod can be adjusted very easily by making the rod longer or shorter, depending on the experimental requirements. Once the length of the PDMS rod is selected (1 cm long in this study), the surface area is fixed. A suitable extraction time can be determined after obtaining the extraction profile of the PDMS rod in the standard solution.

To perform the extraction, 25 ppb standard solution was prepared by spiking 25 µL of 10 ppm deuterated pyrene into 10 mL of deionized water in a 10 mL vial. The rod was introduced into the vial with a stir bar, stirring at the speed of 1000 rpm. After a specified extraction time, the rod was removed from the solution with tweezers, dried with a lint-free tissue and then immediately

transferred to the GC injector for analysis. As the extraction time increased from 15 min to 800 min, the absorption profile of the standard to the rod was determined and is presented in Figure 3-4. The extraction was repeated for three times with each specified extraction time. Figure 3-4 illustrates that the extracted mass of deuterated pyrene initially increases linearly then becomes stable after more than 2 h extraction. Three rods were involved in the loading method study, and the loading reproducibility was studied with an extraction time of 30 min. The results of the standard loading for all three rods are listed in Table 3-2, and suggest that their loading performances are quite similar with the RSD lower than 7% and nearly one quarter of the total mass in the solution had been extracted by that point. Although the reproducibility would have improved if the extraction time had been longer than 2 h, 30 min standard loading extraction was used in the current study in order to reduce the experimental time and ensure that the reproducibility of the rods was not compromised.

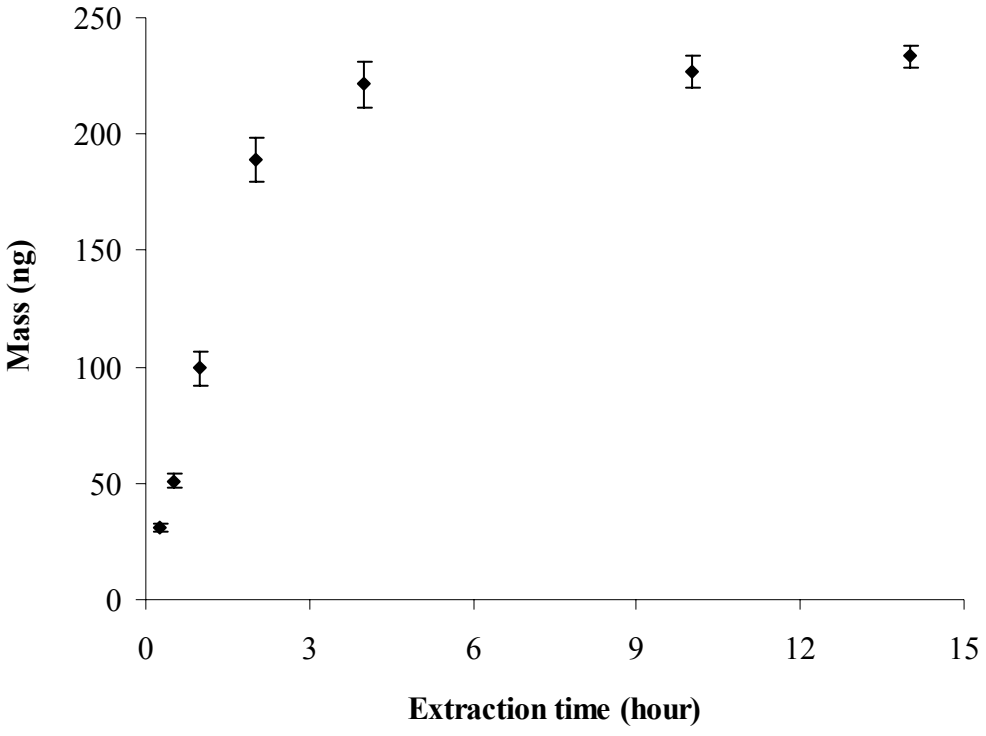

Figure 3-4 Extraction profile of deuterated pyrene (n = 3).

Table 3-2 Results of standard loading with three PDMS rods (n = 3)

	Rod1	Rod2	Rod3
Amount of d_{10}-pyrene extracted by the PDMS rod (ng)*	48.6	45.8	47.7
RSD (%)	6.2	4.4	7.0

* Extraction of a 25 ppb aqueous standard for 30 min at an agitation speed of1000 rpm with stir-bar.

3.4.2 Flow-through System Test

The on-rod standardization technique was first validated with a flow-through system built in the laboratory to measure the TWA concentrations of PAHs in an aqueous system. During the extraction, the PDMS rod was put in a copper mesh cage and hung in the mixing and sampling chamber from the sampling port. After a specified extraction time, the cage was removed from the solution and the rod was picked up with tweezers, dried with a lint-free tissue very quickly and then immediately transferred to the GC injector for desorption.

Experiments were designed to validate the existence of the mirror reflection characteristic of absorption of the analytes and the desorption of the standard first. The PDMS rod was pre-loaded using the aforementioned standard loading method, and then exposed to the flow-through system for different exposure periods. The experiment involved the simultaneous determination of the desorption time profile of deuterated pyrene and the absorption time profile of pyrene. Figure 3-5 presents the value of $\frac{Q}{q_0}$ calculated from the resulting desorption time profile of deuterated pyrene, and the value of $\frac{n}{n_e}$ calculated from the resulting absorption time profile of pyrene. The sum of $\frac{Q}{q_0}$ and $\frac{n}{n_e}$ at any

time is close to 1, which demonstrates the isotropy of the absorption and desorption processes. It also implies that by knowing the behaviour of the desorption of the standard, the absorption of the analytes can be understood.

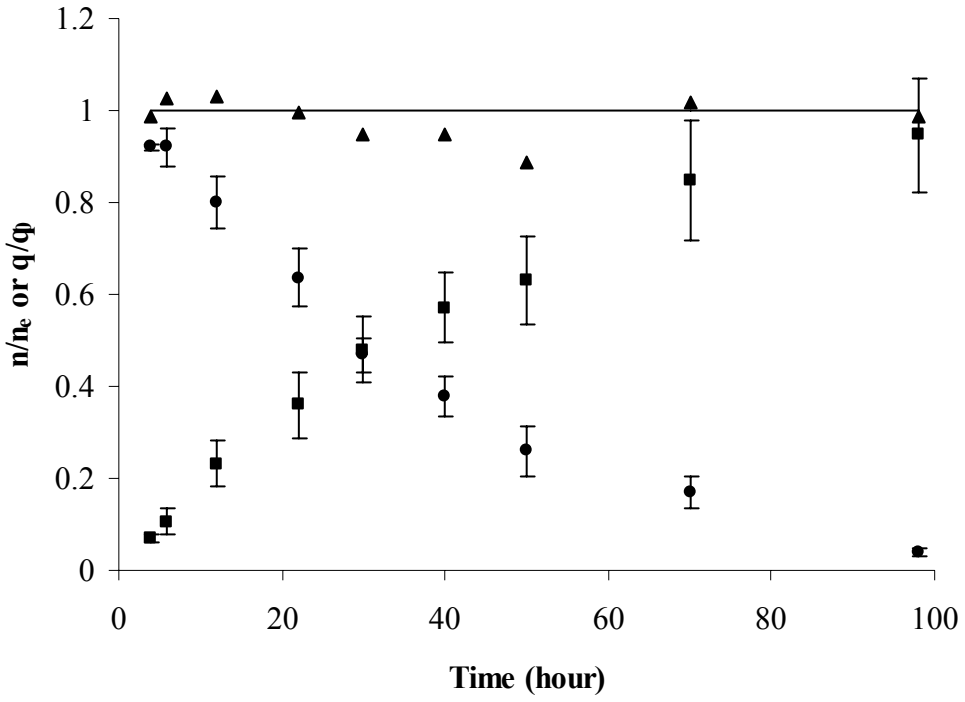

Figure 3-5 Absorption and desorption profiles in PDMS rod. Simultaneous absorption of pyrene (■) onto the PDMS rod from the flow through system and desorption of deuterated pyrene (●) from the PDMS rod into the flow-through system. (▲) represents of the sum of Q/q_0 and n/n_e

Figure 3-5 not only demonstrates the isotropy of the desorption of deuterated pyrene and absorption of pyrene, but also provides the opportunity to calculate the concentration of pyrene in the flow-through system using each pair of the results at different extraction times. By knowing the distribution coefficient K_{fs}, the extracted amount of pyrene, and the ratio of the standard that

remains, $\frac{Q}{q_0}$, the concentration of pyrene in the flow-through system can be obtained by Equation 3.28. The distribution coefficient between PDMS and water for pyrene used in the calculation was obtained in a previous study. [53] It was determined in a flow-through system, which is more reliable since the bias of some published $K_{PDMS/W}$ data caused by the system adsorption effects is minimized. [34] It should be emphasized that Figure 3-4 shows the equilibration process for the very high convection conditions. In that case the boundary layer is very thin and therefore the equilibration time takes only 5 hours in such high convection conditions (the agitation speed of 1000 rpm with stir-bar in the 10 mL vial). However, the time to reach equilibrium for the extraction of pyrene in the flow-through system is about 100 hours because the agitation rates are slower (the agitation speed of 250 rpm with stir-bar in the mixing and sampling chamber). Figure 3-5 shows that good TWA sampling can be obtained within the first 30 hours, when the slope (extraction rate) remains approximately constant. The results from three different extraction times (4, 6 and 12 h) were used to determine the concentration of pyrene in the flow-through system. In the mean time, the concentration of fluoranthene was also estimated using deuterated pyrene as the standard by assuming that the time constants *a* for these two compounds are approximately the same. Since the diffusion through the boundary layer controls the rate of extraction – the small differences in diffusion coefficient between the analyte and the standard could result in some difference, but this difference is within the experimental error. If this difference would be larger then the ratio between the corresponding diffusion coefficients can be used as a correction factor. The concentrations of fluoranthene and pyrene calculated based on the different sampling times in the flow through system are compared in Figure 3-6. The results indicate that the concentrations obtained from the three sampling times are quite similar. The concentrations in the flow through system estimated by the on-rod standardization

method and SPME direct extraction are compared in Table 3-3. The differences between the two sets of experimental results are 18 % and 9 % for fluoranthene and pyrene, respectively.

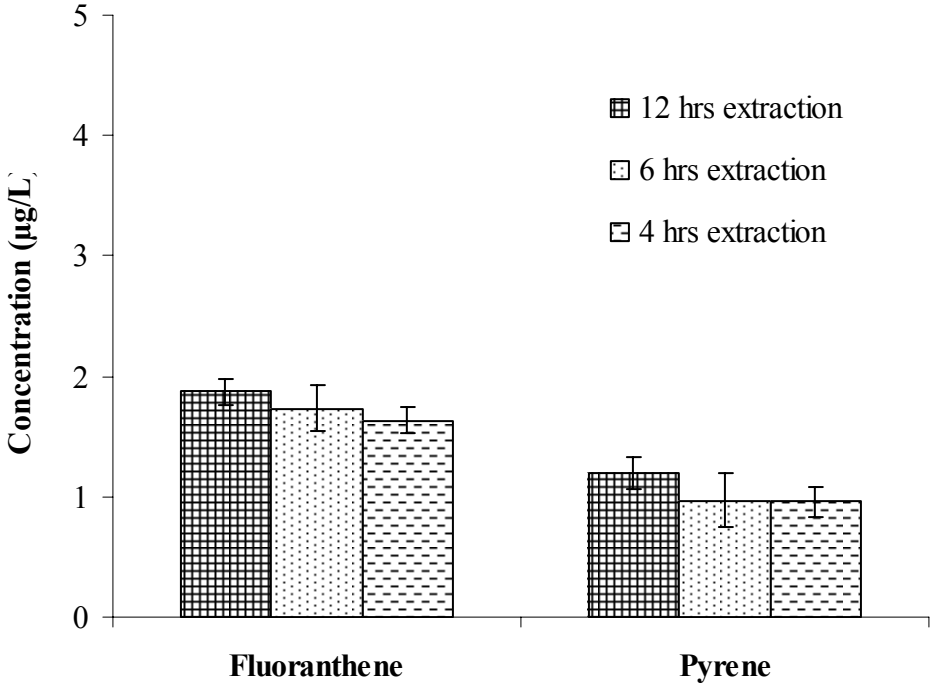

Figure 3-6 Comparison of the estimated concentrations of fluoranthene and pyrene in the flow-through system with different sampling times.

Table 3-3 Estimated concentrations of fluoranthene and pyrene in the flow-through system by SPME calibration and on-rod internal standardizatio method (n=3)

	Concentration (µg/L)	
Compound	Direct SPME	On-rod standardization method
Fluoranthene	1.4 ± 0.1	1.7 ± 0.2
Pyrene	1.0 ± 0.1	1.1 ± 0.2

3.4.3 Field Sampling Trial

The feasibility of the use of a PDMS rod as a passive TWA sampler was successfully demonstrated in a flow-through system in the laboratory, and this technique was then applied to a field sampling trial. In the laboratory, a PDMS rod loaded with a standard or following sample extraction can be immediately placed into the GC injector. However, for field sampling, the transportation time between the sampling site and the laboratory might affect the efficiency of this method and needed to be investigated.

To evaluate the effect of standard loss during storage or transportation, an experiment was pursued in the laboratory prior to field trials. A rod was loaded with the standard as described previously and then sealed in an empty 20 mL vial and kept in a refrigerator for 2 days (generally the longest potential storage time of the standard loaded rod prior to field sampling). The results illustrated that the loss of standard after a 2-day storage period in the refrigerator was less than 5 %. It was suggested that for all future trials, the PDMS rods should be kept at lower temperature to minimize the loss of standard or analyte during transportation.

Hamilton Harbour (Hamilton, ON, Canada) was designated as one of the 43 Areas of Concern (AOCs) around the Great Lakes by the International Joint Commission in 1987. It is surrounded by several steel manufacturers, and the effluent from these factories contributes to high levels of PAHs in the water. The water quality in Hamiton Harbour is continually monitored by conventional analytical techniques by scientists from Environment Canada. The sampling location (Latitude N. 43° 17’ 14”, longitude W. 79° 52’ 19”) was selected to deploy the PDMS rod passive samplers based on Environment Canada data, which identified it as one of the most polluted spots in the harbour. In Hamilton Harbour the convection conditions are substantially smaller than the flow-through system, allowing us to use this approach for extended period of time at TWA sampler. The duration of the sampling was one month in the field trials.

Both deuterated fluoranthene and deuterated pyrene were loaded onto the 1 cm PDMS rods in the laboratory and maintained at low temperature during storage and transportation. The PDMS rods were wrapped with two layers of copper metal meshes to avoid biofouling from sampling in the harbour. When the samplers were collected after one-month duration, it was observed that the PDMS rods that were placed at the middle and bottom depths were quite clean, but the surface ones were dirty likely due to algal growth in the upper layers of the harbour. The extracted amounts of fluoranthene and pyrene, n, as well as the remaining deuterated compounds, Q, at three different depths are listed in Table 3-4. The results from this field trial indicate that the higher flow velocity of the surface water contributed to a loss of the preloaded standard of more than 80%. In comparison, the loss of standard at the bottom depth was between 30-40 %. On the contrary, the amount of the target analytes extracted on the PDMS rod at the surface water depth was greater than the amount extracted from the bottom depth sampling location. The decrease of $\frac{n}{n_e}$ corresponded to an increase in $\frac{Q}{q_0}$. These observations confirm that the on-rod standardization approach can effectively compensate for the turbulence factor that can be encountered in field experiments.

Table 3-4 n and Q for the target analytes and standards on the PDMS rods collected from Hamilton Harbour at different depths after one month duration (n=3)

	mass (ng)			
Depth	Fluoranthene	Fluoranthene-d_{10}	Pyrene	Pyrene-d_{10}
1 m	5.8 ± 0.3	0.7 ± 0.2	5.9 ± 0.3	0.5 ± 0.1
11 m	0.7 ± 0.2	8.9 ± 2.4	1.3 ± 0.2	9.5 ± 1.6
21 m	0.8 ± 0.1	20.4 ± 5.3	0.7 ± 0.1	16.0 ± 4.9

When the PDMS rods were removed from the harbour, spot water samples were also collected from the three sampling depths. The water samples were analyzed by SPME direct extraction in a 10 mL vial using 100 μm PDMS fiber with an agitation speed of 500 rpm. The TWA concentrations of fluoranthene and pyrene detected in the field experiments in September with the on–rod standardization method are shown in Table 3-5. These results are also compared to the concentrations obtained from the water samples using SPME direct extraction. This comparison indicated a strong agreement between the two methods at the 1 m depth, and the concentrations of fluoranthene and pyrene detected by both methods were in the lower ppt range. However, fluoranthene and pyrene could not be detected by SPME direct extraction from the water samples collected at the 11 m and 21 m depths because the small sample volume was analyzed (10 mL) and the extraction amount by SPME fiber was below the detection limit of the instrument although about 70% of the analytes in the 10 mL sample have been extracted. These results illustrate that direct SPME only provides the concentration of one grab sample, while PDMS passive sampler offers the integrative sampling during the sampling period, thereby achieving a lower detection limit.

Table 3-5 Comparison of concentrations of fluoranthene and pyrene in Hamilton Harbour by on-rod standardization method and direct SPME method (n=3)

	Concentration (ng/L)			
	On-rod standardization		Direct SPME	
Depth	Fluoranthene	Pyrene	Fluoranthene	Pyrene
1m	82.8 ± 3.9	70.7 ± 3.9	68.3 ± 5.0	55.7 ± 1.1
11m	17.3 ± 3.9	20.2 ± 2.8	ND*	ND*
21m	17.5 ± 5.8	13.0 ± 3.1	ND*	ND*

* ND – not detected

To monitor the change in PAH concentrations during different time periods, the same experiment was repeated in October and November. The results in the three months are compared in Table 3-6. A similar trend is observed for the three sampling months, illustrating that the PAH concentrations are the highest at the 1 m sampling depth (the surface water). The experimental results obtained by the on-rod standardization method are quite comparable to the Environment Canada data, which are routinely collected by traditional analytical methods like liquid-liquid extraction and have the concentrations of fluoranthene and pyrene in the range of 10-200 ng/L at different spots in Hamilton Harbour.

Table 3-6 Comparison of TWA concentrations of fluoranthene and pyrene in Hamilton Harbour in September, October and November (n=3)

	Concentration (ng/L)					
	Fluoranthene			Pyrene		
Depth	Sept.	Oct.	Nov.	Sept.	Oct.	Nov.
1 m	82.8 ± 3.9	59.9 ± 11.1	73.6 ± 8.9	70.7 ± 3.9	95.2 ± 22.1	106.2 ± 11.0
11 m	17.3 ± 3.9	58.5 ± 8.0	23.9 ± 2.2	20.2 ± 2.8	46.0 ± 3.6	17.7 ± 2.3
21 m	17.5 ± 5.8	30.2 ± 8.8	6.0 ± 1.9	13.0 ± 3.1	43.3 ± 12.7	14.9 ± 3.0

3.5 Conclusion

The preliminary results of the PDMS rod sampler trials are very promising. There are several advantages to use PDMS rod passive sampler for field analysis. It not only combines sampling, isolation and enrichment into one step, but is also relatively inexpensive and easy to use, possesses an integrative capacity over a long sampling period, and does not require any maintenance. Moreover, the PDMS rods have much larger capacity comparing to the commercial SPME fiber coating, which

enables this sampler to detect analytes in the low to sub ng/L levels in the field. The ananlyte concentration was determined by measuring the desorption of standard from the sampler rather than uptake rate of pollutants in other passive sampling techniques, which makes this technique simpler and more practical in field sample analysis.

References

(1) Namiesnik, J.; Zabiegala, B.; Kot-Wasik, A.; Partyka, M.; Wasik, A. *Anal. Bioanal. Chem.* **2005**, *381*, 279.

(2) Wilson, N. *Soil Water and Ground Water Sampling*; Lewis Publishers/CRC Press: St. Paul, 1995.

(3) Huckins, J. N.; Tubergen, M. W.; Manuweera, G. K. *Chemosphere* **1990**, *20*, 533.

(4) Vrana, B.; Allan, I. J.; Greenwood, R.; Mills, G. A.; Dominiak, E.; Svensson, K.; Knutsson, J.; Morrison, G. *Trends Anal. Chem.* **2005**, *24*, 845.

(5) Gorecki, T.; Pawliszyn, J. *Anal. Chem.* **1995**, *67*, 3265.

(6) Gorecki, T.; Namiesnik, J. *Trends Anal. Chem.* **2002**, *21*, 276.

(7) Palmes, E. D.; Gunnison, A. F. *Am. Ind. Hyg. Assoc. J.* **1973**, *34*, 78.

(8) Reiszner, K. D.; West, P. W. *Environ. Sci. Technol.* **1973**, *7*, 526.

(9) Bopp, S., University of Rostock, Leipzig, 2004.

(10) Kot-Wasik, A.; Zabiegala, B.; Namiesnik, J. *Trends Anal. Chem.* **2000**, *19*, 446.

(11) Kot-Wasik, A. *Chem. Anal. (Warsaw)* **2004**, *49*, 691.

(12) Sodergren, A. *Environ. Sci. Technol.* **1987**, *21*, 855.

(13) Peterson, S. M. A., S. C.; Batley, G. E.; Coade, G.. *Chem. Spec. Bioavailab.* **1995**, *7*, 83.

(14) Litten, S.; Mead, B.; Hassett, J. *Environ. Toxicol. Chem.* **1993**, *12*, 639.

(15) DiGlano, F. A.; Elliot, D.; Leith, D. *Environ. Sci. Technol.* **1988**, *22*, 1365.

(16) Lebo, J. A.; Zajicek, J. L.; Huckins, J. N.; Petty, J. D.; Peterman, P. H. *Chemosphere* **1992**, *25*, 697.

(17) Johnson, B. T.; Huckins, J. N.; Petty, J. D.; Clark, R. C. *Environ. Toxicol.* **2000**, *15*, 248.

(18) Granmo, A.; Ekelund, R.; Berggren, M.; Brorstrom-Lunden, E.; Bergqvist, P. A. *Environ. Sci. Technol.* **2000**, *34*, 3323.

(19) Huckins, J. N.; Tubergen, M. W.; Lebo, J. A.; Gale, W.; Schwartz, T. R. *J. Assoc. Off. Anal. Chem.* **1990**, *73*, 290.

(20) Arthur, C. L.; Pawliszyn, J. *Anal Chem* **1990**, *62*, 2145.

(21) Pawliszyn, J., Ed. *Sampling and sample preparation for field and laboratory*; Elsevier: Amsterdam, 2002.

(22) Pawliszyn, J. *Applications of Solid Phase Microextraction*; Royal Society of Chemistry: Cambridge, 1999.

(23) Chai, M.; Pawliszyn, J. *Environ. Sci. Technol.* **1995**, *29*, 693.

(24) Shirey, R.; Mani, V.; Mindrup, R. *Am. Environ. Lab.* **1998**, *10*, 21.

(25) Nilsson, T.; Montanarella, L.; Baglio, D.; Tilio, R.; Bidoglio, G.; Facchetti, S. *Int J Environ Anal Chem* **1998**, *69*, 217.

(26) Martos, P. A.; Pawliszyn, J. *Anal. Chem.* **1999**, *71*, 1513.

(27) Koziel, J.; Jia, M.; Khaled, A.; Noah, J.; Pawliszyn, J. *Analytica Chimica Acta* **1999**, *400*, 153.

(28) Chen, Y.; Pawliszyn, J. *Anal. Chem.* **2003**, *75*, 2004.

(29) Ouyang, G.; Chen, Y.; Pawliszyn, J. *Anal. Chem.* **2005**, *77*, 7319.

(30) Baltussen, E.; Cramers, C. A.; Sandra, P. *Anal. Bioanal. Chem.* **2002**, *373*, 3.

(31) Nickerson, M. A.; Patent, U. S., Ed.

(32) Blomberg, S.; Roeraade, J. *J. Chromato.* **1987**, *394*, 443.

(33) Baltussen, E.; Sandra, P.; David, F.; Cramers, C. A. *J. Microcolumn Sep.* **1999**, *11*, 737.

(34) E. Baltussen, P. S., F. David, H-G. Janssen, and C. Cramers *Anal. Chem.* **1999**, *71*, 5213.

(35) Baltussen, E.; Janssen, H. G.; Sandra, P.; Cramers, C. A. *J. High Resolut. Chromatogr.* **1997**, *20*, 385.

(36) Pettersson, J.; Kloskowski, A.; Zaniol, C.; Roeraade, J. *J. Chromato. A* **2004**, *1033*, 339.

(37) Vrana, B.; Popp, P.; Paschke, A.; Schuurmann, G. *Anal. Chem.* **2001**, *73*, 5191.

(38) Vrana, B.; Paschke, A.; Popp, P. *Environ. Pollut.* **2006**, *144*, 296.

(39) Ai, J. *Anal. Chem.* **1997**, *69*, 1230.

(40) Chen, Y.; Pawliszyn, J. *Anal. Chem.* **2004**, *76*, 5807.

(41) Wang, Y.; O'Reilly, J.; Chen, Y.; Pawliszyn, J. *J. Chromatogr. A.* **2005**, *1072*, 13.

(42) Ouyang, G.; Zhao, W.; Pawliszyn, J. *Anal. Chem.* **2005**, *77*, 8122.

(43) Scheller, D.; Kolb, J. *J. Neurosci. Methods* **1991**, *40*, 31.

(44) Larsson, C. I. *Life Sci.* **1991**, *49*, PL73.

(45) Wang, Y.; Wong, S. L.; Sawchuk, R. J. *Pharm. Res.* **1993**, *10*, 1411.

(46) Wong, S. L.; Wang, Y.; Sawchuk, R. J. *Pharm. Res.* **1992**, *9*, 332.

(47) Rene Bouw, M.; Hammarlund-Udenaes, M. *Pharm. Res.* **1998**, *15*, 1673.

(48) Prest, H. F.; Jarman, W. M.; Burns, S. A.; Weismuller, T.; Martin, M.; Huckins, J. N. *Chemosphere* **1992**, *25*, 1811.

(49) Booij, K.; Sleiderink, H. M.; Smedes, F. *Environ. Toxicol. Chem.* **1998**, *17*, 1236.

(50) Huckins, J. N.; Petty, J. D.; Lebo, J. A.; Almeida, F. V.; Booij, K.; Alvarez, D. A.; Cranor, W. L.; Clark, R. C.; Mogensen, B. B. *Environ. Sci. Technol.* **2002**, *36*, 85.

(51) Vrana, B.; Schuurmann, G. *Environ. Sci. Technol.* **2002**, *36*, 290.

(52) Ouyang, G.; Chen, Y.; Pawliszyn, J. *J. Chromatogr. A* **2006**, *1105*, 176.

(53) Shurmer, B. P., J. *Anal. Chem.* **2000**, *72*, 3660.

Chapter 4
Sorption Characteristics Study of Hydrophobic Chemicals in Complex Aqueous Matrices by Solid Phase Microextraction

4.1 Introduction

The concentration of pollutants in aqueous system is not always well defined due to their interaction with humic organic matter (HOM) in the system. HOM comprise extraordinarily complex, amorphous mixtures of highly heterogeneous, chemically reactive yet refractory molecules. They are produced during early diagenesis in the decay of biomatter, and formed ubiquitously in the environment via processes involving chemical reaction of species randomly chosen from a pool of diverse molecules and through random chemical alternation of precursor molecules. [1-3] HOM are generally classified into humic acid (HA), fulvic acid (FA), and humin based on their solubility in water as a function of pH. HA is the HOM fraction insoluble in water at pH < 2 and soluble at higher pH; FA is very hydrophilic in nature and soluble in water at all pH; whereas humin is insoluble in water at all pH values.

Numerous studies have been conducted to investigate HOM due to their environmental importance.[4-12] The investigation of sorption of organic chemicals to HOM is important in the determination of the fate of these compounds in the environment, i.e., their transport and availability for chemical degradation.[13] Furthermore, the sorption also affects the biological availability, thereby influencing bioaccumulation, biodegradation and potential toxic effects in organisms.[14, 15]

To determine the sorption of organic chemicals on HOM, various techniques have been developed for measuring sorption coefficient, including the fluorescence quenching technique,[9, 16] flocculating method, [17, 18]dialysis membrane method,[8, 19] fast solid phase extraction (SPE) or reversed

phase (RP) method,[20, 21] solubility enhancement method,[5, 22, 23] and gas purging or headspace partitioning method.[24, 25] These methods more or less fail to meet the requirements of multi-component analysis without disturbing the existing sorption equilibrium.

Recently, several studies on the application of SPME for investigating the sorption characteristic have been published.[26-28] SPME combines sampling and sample preparation into one step, which is simple, less time-consuming, solvent free, and applicable for multi-component analysis. Another advantage of SPME technique in sorption studies is that sorption equilibrium between the target analytes and HOM is not significantly affected by the extraction because the SPME fiber only removes small amounts of analyte due to its extremely small volume (e.g., 0.026 μL for a fiber with 7 μm film thick). Therefore, only the freely dissolved portion of the target analyte is extracted by the fiber coating, rather than the proportion bound to HOM. The application of SPME for determining the freely dissolved concentrations of organic pollutants in aqueous matrices can be measured by external calibration.[27]

In this study, a group of PAHs, including naphthalene, acenaphthylene, fluorene, anthracene, and pyrene, was chosen as target analytes to demonstrate the ability of SPME technique to monitor the organic pollutants in complex aqueous samples. For risk assessment purposes, factors that would affect the sorption of target analytes to HOM were studied. These include the concentration of HOM present in samples, pH value, ionic strength, and different types of organic matter. Freely dissolved concentrations and sorption coefficients of the organic pollutants were determined using SPME technique.

4.2 Theory

4.2.1 Determination of K_D

The sorption coefficient (K_D) is commonly used to quantify sorption of organic pollutants onto HOM in water systems. The K_D value is simply a ratio of the sorbed phase concentration to the solution phase concentration at equilibrium. [29]

$$K_D = \frac{C_b^\infty}{C_s^\infty} \qquad \text{Equation 4.1}$$

where C_s^∞ is the equilibrium concentration of the analyte in the sample solution, and C_b^∞ is the equilibrium concentration of analyte bound onto HOM (mg/kg).

For direct SPME in the presence of HOM, the mass balance of the fiber-water-HOM system at equilibrium is given by:

$$C_f^\infty V_f + C_s^\infty V_s + C_b^\infty C_{HOM} V_s = C_s^0 V_s \qquad \text{Equation 4.2}$$

where C_s^0 is the initial analyte concentration in the matrix; C_f^∞ is the equilibrium concentration of the analyte in the fiber coating, and C_{HOM} is the concentration of HOM in sample matrix (mg/L). V_f and V_s are the volumes of the fiber coating and sample matrix, respectively.

By defining the sorption coefficient as $K_D = \frac{C_b^\infty}{C_s^\infty}$ (mL g^{-1}) and substituting $C_s^\infty = C_f^\infty / K_{fs}$ into equation 4.2, the following equation is obtained:

$$C_f^\infty V_f + C_f^\infty V_s / K_{fs} + K_D C_f^\infty C_{HOM} V_s / K_{fs} = C_s^0 V_s \qquad \text{Equation 4.3}$$

By rearranging equation 4.3, K_D can be expressed as:

$$K_D = \frac{C_s^0 V_s - C_f^\infty V_f - C_f^\infty V_s / K_{fs}}{C_f^\infty C_{HOM} V_s / K_{fs}} \qquad \text{Equation 4.4}$$

By spiking certain amount of analyte to the sample matrix and using SPME equilibrium calibration, the sorption coefficient can be calculated using the above equation. When the capacity of fiber coating is small relative to that of the sample matrix, equation 4.4 can be rewritten and K_D can be expressed as:

$$K_D = \frac{K_{fs} C_s^0 V_f - n}{n C_{HOM}} \qquad \text{Equation 4.5}$$

where *n* is the amount of analyte extracted by the fiber coating at equilibrium.

For the same system in the absence of HOM, the amount of analyte extracted by the fiber coating at equilibrium can be expressed as:

$$n_0 = K_{fs} C_s^0 V_f \qquad \text{Equation 4.6}$$

Substituting equation 4.6 into equation 4.5, equation 4.7 is given:

$$K_D = \frac{n_0 - n}{n C_{HOM}} = \left(\frac{n_0}{n} - 1 \right) \frac{1}{C_{HOM}} \qquad \text{Equation 4.7}$$

Comparing equation 4.4 to equation 4.7, equilibrium extraction needs to be achieved at both conditions. The distribution coefficient is not required to determine K_D using equation 4.7. However, the requirement of large sample volume needs to be satisfied. Equation 4.4 can be applied to calculate K_D when the sample volume is small, providing the distribution coefficient is known.

4.2.2 Determination of K_{fs}

The SPME fiber coating/water distribution coefficient K_{fs} can be estimated from physicochemical data and chromatographic parameters.[13, 30] Some correlations can also be used to anticipate trends in K_{fs} for analytes, such as the correlation between octanol/water distribution coefficients K_{ow} and K_{fs}.[31, 32]

In the current study, K_{fs} was determined using SPME technique in the flow-through system described in the previous chapter.[33] The equation for calculating the mass of analyte extracted by the fiber at equilibrium is:

$$n = \frac{K_{fs} C_s^0 V_s V_f}{V_s + K_{fs} V_f} \qquad \text{Equation 4.8}$$

Assuming that the term $K_{fs} V_f$ in the denominator is negligibly small, the amount of analyte extracted by the fiber at equilibrium is independent of the sample volume, and equation 4.8 simplifies to:

$$n = K_{fs} C_s^0 V_f \qquad \text{Equation 4.9}$$

In the flow-through system used in this study, the sample volume (500 mL in sampling chamber) is much larger than $K_{fs} V_f$ (less than 2 mL). Therefore, the distribution coefficient K_{fs} can be determined by:

$$K_{fs} = \frac{n}{C_s^0 V_f} \qquad \text{Equation 4.10}$$

4.2.3 Correlations between log K_D and log K_{ow}

Due to the large number of chemical substances, the experimental effort to determine the sorption coefficients is extensive. Therefore, the development of predictive models for an estimation

of sorption coefficients, such as the quantitative structure activity relationship model (QSAR-model), is attractive. The most common QSAR-model for describing sorption of hydrophobic organic compounds is the relation of the octanol-water distribution coefficient (K_{ow}) and the sorption coefficient (K_D):

$$\log K_D = a * \log K_{ow} + b \qquad \text{Equation 4.11}$$

This is a one-parameter linear free-energy relationship (LFER), which correlates two partitioning processes: one between water and HOM and the other between water and *n*-octanol. Several studies have shown that log K_D to log K_{ow} correlations for describing sorption onto organic matters are class specific. In this study, the empirical correlations between K_{ow} and K_D for PAHs' sorption onto three different HOMs were obtained using the sorption coefficients determined by the SPME technique.

4.3 Experimental Section

4.3.1 Chemicals and Supplies

HPLC grade methanol, hydrochloric acid, sodium azide and sodium hydroxide were obtained from BDH (Toronto, Canada). Naphthalene, acenaphthylene, fluorene, anthracene and pyrene were purchased from Supelco (Bellefonte, PA, USA). [$^2H_{10}$]Pyrene (pyrene-d_{10}) was purchased from Sigma-Aldrich (Mississauga, Canada). Deionized water was obtained using a Barnstead/Thermodyne NANO-pure ultrapure water system (Dubuque, IA, USA). The SPME holder and 7 μm PDMS fibers were obtained from Supelco (Oakville, Canada).

Humic acid was purchased from Sigma-Aldrich (Milwaukee, WI, USA) and used in the majority of the experiments. Two well-characterized matrices obtained from International Humic Substances Society (IHSS) were also investigated to compare their sorption characteristics: 1) IHSS

Suwannee River fulvic acid standard, and 2) IHSS Suwannee River NOM (RO isolation). Suwannee River fulvic acid contains only hydrophobic organic acids. However, the reference NOM sample contains not only the hydrophobic and hydrophilic acids but also other soluble organic solutes present in natural waters.

4.3.2 Sorption Experiments

Dissolved humic substance solutions were prepared by dissolving the solid HOM in diluted NaOH. The solution was further diluted and anti-microbial agent NaN_3 (200 mg/L) was added to inhibit microbial activity. The final concentrations of HOM ranged between 25 – 200 mg/L. The HOM solution was agitated and allowed to come to equilibrium for at least 1 day. The stock methanolic solution of the target analytes were spiked into the HOM solution to obtain specified analyte concentrations in the complex matrix. SPME was applied using the direct immersed extraction mode due to the low volatility of the target analytes. The pH value was adjusted by adding hydrochloric acid as needed. The pH value was measured using a pH meter from METTLER TOLEDO GmbH (Schwerzenbach, Switzerland). The ionic strength in the system was adjusted by adding sodium chloride and was measured using a conductivity meter from Wissenschaftlich-Technische Werkstatten Gmbh & Co KG (Weilheim, Germany).

4.3.3 Instrument

A Saturn 3800GC/2000 ITMS system (Varian Associate, Sunnyvale, CA, USA) was used for the PAHs analyses. The GC-MS was equipped with a 1079 Programmable Temperature Vaporizing Injector and coupled to a SPB-5 column (30 m, 0.25 mm I.D., 0.25 μm film thickness) (Supelco, Mississauga, Canada) with a SPI liner (2.4 mm I.D. × 4.6 mm O.D. × 54 mm). Helium was used as the carrier gas at a flow rate of 1 mL/min. The injector was set at 270 °C for SPME injection, and set at 40 °C and then increased to 250 °C at a rate of 100 °C/min, for liquid injection. Desorption time of

the fiber in the injector was 10 min. The column temperature was maintained at 40 °C for 1 min and then programmed to increase at a rate of 25 °C /min to 270 °C, at which it was held for 5 min. The MS system was operated in the electron ionization (EI) mode, and tuned to perfluorotributylamine (PFTBA).

4.4 Results and Discussion

4.4.1 Sorption Kinetics Study

The sorption kinetics was studied by spiking standard pyrene into the sample matrix with the presence of humic acid (100 mg/L), and then waiting for more than 24 hrs to confirm the system reached equilibrium. After equilibrium was reached, the same amount of pyrene-d_{10} was added to the solution, which was set as the zero point on the time scale shown in Figure 4-1. After a series of different incubation times with constant agitation, the samples were extracted using 7 μm PDMS fiber for 1 min followed by direct desorption of the fiber in the GC injection port for analysis. The ratio of extracted amount of pyrene to deuterated pyrene was plotted against the different incubation times (Figure 4-1).

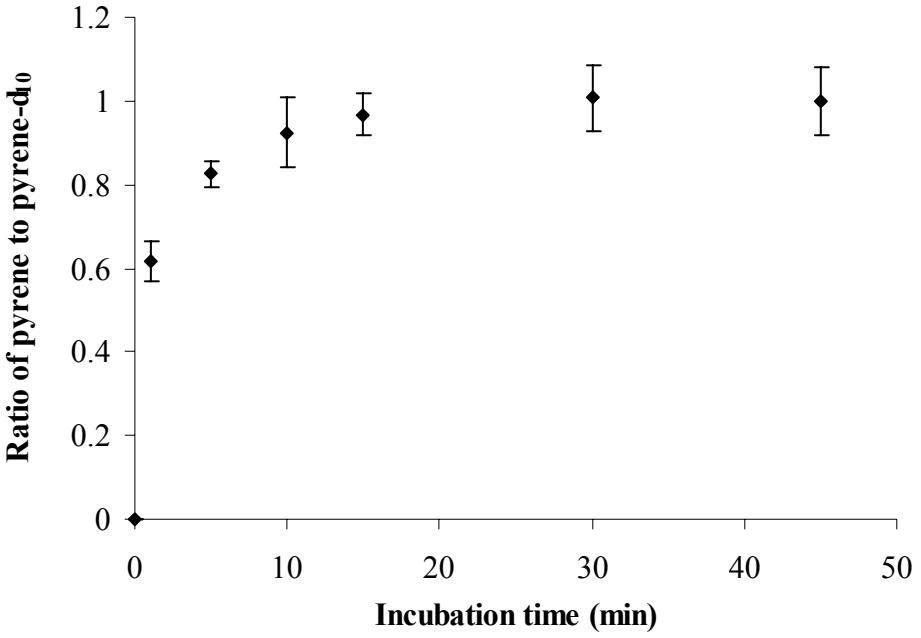

Figure 4-1 Sorption kinetics of pyrene onto humic acid (Sigma-Aldrich) (n=2).

The result indicated that sorption equilibrium between pyrene and humic acid can be reached in about 15 mins at the current agitation condition. In this study, the spiked solution was normally stored for more than 12 hrs to ensure that sorption equilibrium between the analyte and HOM in the system had been reached.

4.4.2 Competition Test for Displacement Effect

Experiments were performed to study whether a displacement effect occurs between the analytes during their sorption by HOM in the sample system: (1) conducting SPME direct extraction with a single PAH compound in the aqueous solution in the presence of HOM; and (2) conducting SPME direct extraction with the aqueous solution in the presence of HOM, and spiked with 5 PAHs together (naphthalene, acenaphthylene, fluorene, anthracene and pyrene). The extracted amounts of each compound in these two scenarios were compared in order to determine whether the existence of

other compounds in the same system would cause displacement of compounds with a poor affinity toward the HOM in the system by analytes with stronger binding. Concentrations of HOM were kept constant at 50 mg/L, and the concentration of each PAH was 30 ppb in these two samples. The extraction time lasted 4 hrs with the 7 μm PDMS fiber.

Figure 4-2 presents the extracted amounts at these two conditions. The difference on the extracted amount between the multi-components extraction and single compound extraction remained within 10% for the five compounds. This indicates that within our experimental error, no significant displacement effect occurred in the presence of HOM in the sample solution under the current experimental conditions.

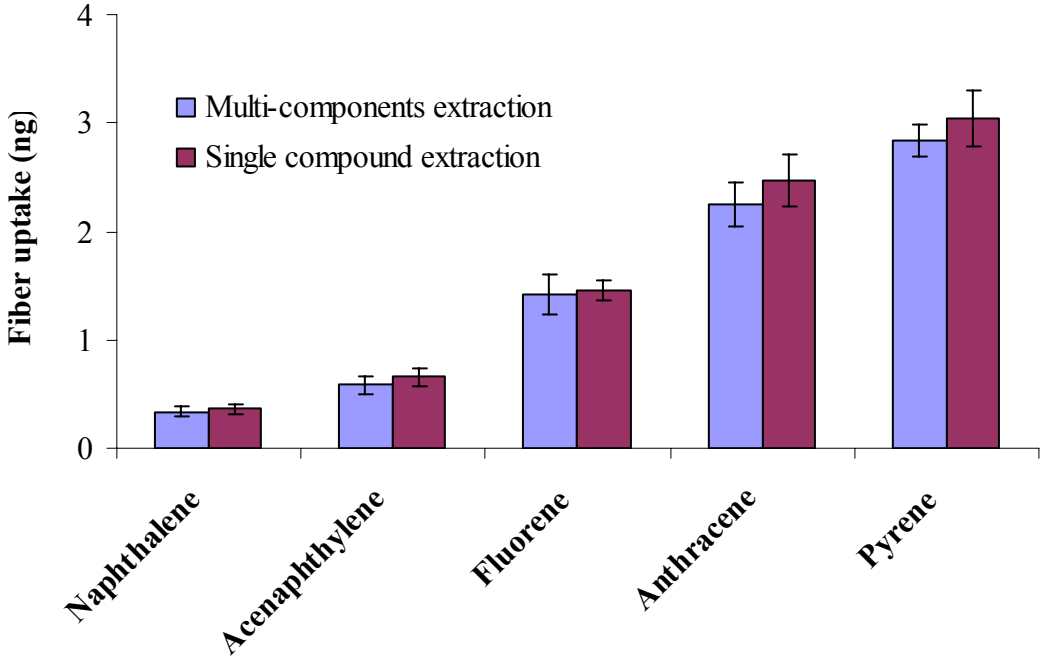

Figure 4-2 SPME uptakes from solutions containing one component and multi-components in the presence of humic acid (Sigma – Aldrich) (n=3)

4.4.3 Comparison of Fiber Uptake in the Presence and Absence of HOM

The sorption of organic chemicals to HOM is important for determining the fate of these compounds because the bioavailability of these organic pollutants is greatly affected by the presence of HOM in the environmental aqueous samples. [13] Figure 4-3 compares fiber uptakes from the SPME extractions in aqueous solutions with or without humic acid, using a 7 μm PDMS fiber. The spiked PAH concentrations in both systems were 30 ppb. The humic acid concentration in the sample matrix was 50 mg/L.

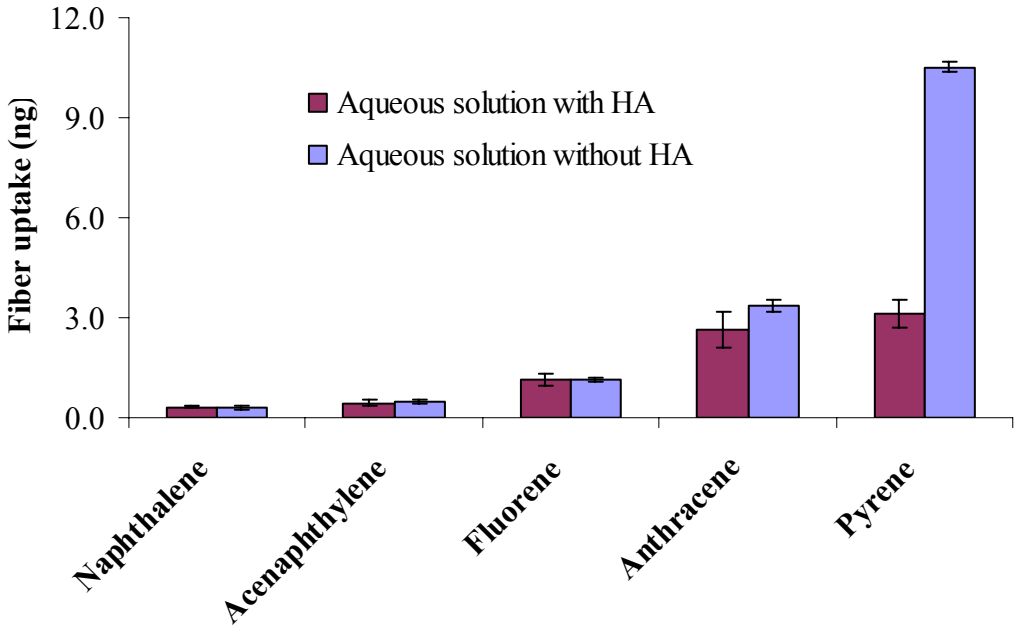

Figure 4-3 Fiber uptakes of PAHs by SPME in aqueous samples with or without humic acid (n=3).

Figure 4-3 demonstrates that no significant variation in extracted amount for the less hydrophobic compounds (naphthalene, acenaphthylene and fluorene) with or without the presence of HA. However, the binding effect between the analyte and HOM becomes stronger with more hydrophobic analyte. The experimental data give ample evidence that the sorption of the target analyte to HA is significant for the more hydrophobic compounds like pyrene. The extracted amount by the SPME fiber is dramatically lower in the presence of HOM in the sample matrix comparing to

the pure aqueous solution for pyrene. The results also demonstrate that the bound analyte is not extractable, which serves as the basis for the equilibrium extraction method for determining the concentration of freely dissolved analyte in the sample.

4.4.4 Effect of pH Value

Changes in aqueous samples can affect PAH compounds and HOM present in the system, as well as their interactions. One such change is the coagulation of HOM with decreases in pH. Effect of pH value was investigated and the pH value was adjusted by adding 0.1 M HCl in the current study while keeping the ionic strength constant. The three different pH values studied were 6.9, 6.2, and 5.7. The extracted amount by the SPME fiber at different sample-matrix pHs are compared in Figure 4-4 with humic acid at 200 mg/L. No significant change of the extracted amount was observed within the range of pH values studied.

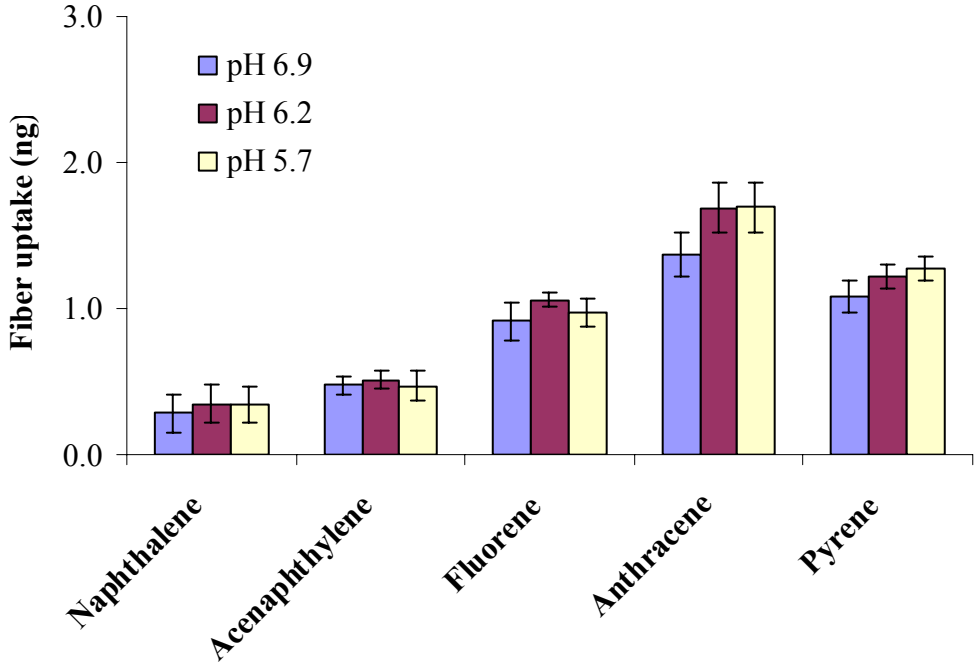

Figure 4-4 Fiber uptakes at different pHs of sample-matrix with humic acid (Sigma-Aldrich) (n=3).

4.4.5 Effect of Ionic Strength

Another change that would affect the interaction between PAHs and HOM is the salting-out effect of PAHs with increasing salinity. PAH sorption onto HOM generally decreases with increasing salinity due to complex competition phenomena. [34, 35]

The effect of ionic strength in the system was investigated using SPME technique. The three different ionic strengths studied were: 0.023 M, 0.035 M and 0.050 M. The ionic strength was adjusted by adding NaCl into the system. The amounts extracted by the SPME fiber at different ionic strengths are compared in Figure 4-5 with humic acid at 200 mg/L. In the range investigated in this study, the ionic strength effect on the sorption of PAHs onto HOM is not very remarkable.

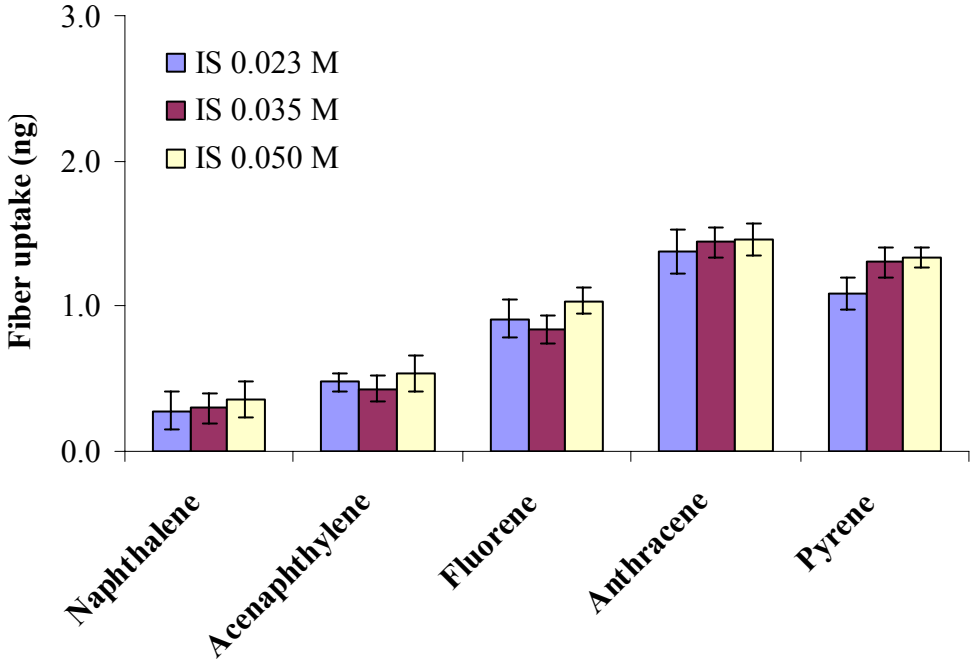

Figure 4-5 Fiber uptakes at different ionic strengths of sample matrix with humic acid (Sigma – Aldrich) (n=3).

4.4.6 Extraction Profile with Different HOMs

Extraction profiles of the five PAHs with and without HOMs are presented in Appendices 1–3. The three HOMs studied are: humic acid from Sigma-Aldrich, fulvic acid standard from IHSS Suwannee River fulvic acid standard, and NOM (RO isolation) from IHSS Suwannee River. The nominal concentrations of each analyte in the sample matrices are kept constant at 30 ppb with and without the presence of HOM.

Mathcad genfit functions were used to fit the data to an Expotential curve model and the fitted extraction profiles are presented as the curves in the figures. The comparison of the extraction profiles of PAHs in the aqueous solutions and matrices with HOMs demonstrated that the absorption kinetics of the fiber coating is not significantly affected by the presence of HOM in the sample matrix under the current experimental conditions, which means that there is no net contribution of the desorption of analyte from the HOM-analyte complexes in the diffusion layer to the mass transfer rate. This observation can be ascribed to the slow desorption kinetics between analytes and HOM comparing with the diffusion rate of the free analyte from the bulk solution to the static boundary layer.

4.4.7 Effect of HOM Concentrations

Four different HOM concentrations (25 mg/L, 50 mg/L, 75 mg/L and 100 mg/L) were tested to study its effect on analyte uptake by a 7 μm PDMS fiber. Figure 4-6 through Figure 4-8 show fiber uptakes at different HOM concentrations with humic acid, fulvic acid and NOM, respectively. Spiked analyte concentrations in the systems were 30 ppb and the extraction time was set as 4 hrs. The results indicate that the fiber uptake decreased dramatically for the more hydrophobic compounds by increasing humic acid concentrations. The fiber uptake for pyrene with humic acid at 25 mg/L was more than twice as it was at 100 mg/L. However, for the less hydrophobic compounds like

naphthalene, there is not much difference between the fiber uptakes at different humic acid concentrations. For the sample matrix containing fulvic acid and NOM, a similar trend was found although the concentration effect was not as significant as that of humic acid. The results further demonstrate that the fiber uptakes of all target compounds are quite comparable in the presence of fulvic acid and NOM, which indicates their similar sorption characteristics. However, the fiber uptake of pyrene drops dramatically in the presence of humic acid comparing to those two HOMs from nature sources. These observations are consistent with the understanding that commercial humic acids are not completely representative of natural humic substances. Commercial HA are known to be less polar and to possess a higher sorption potential for organic pollutants than HOMs from natural sources.

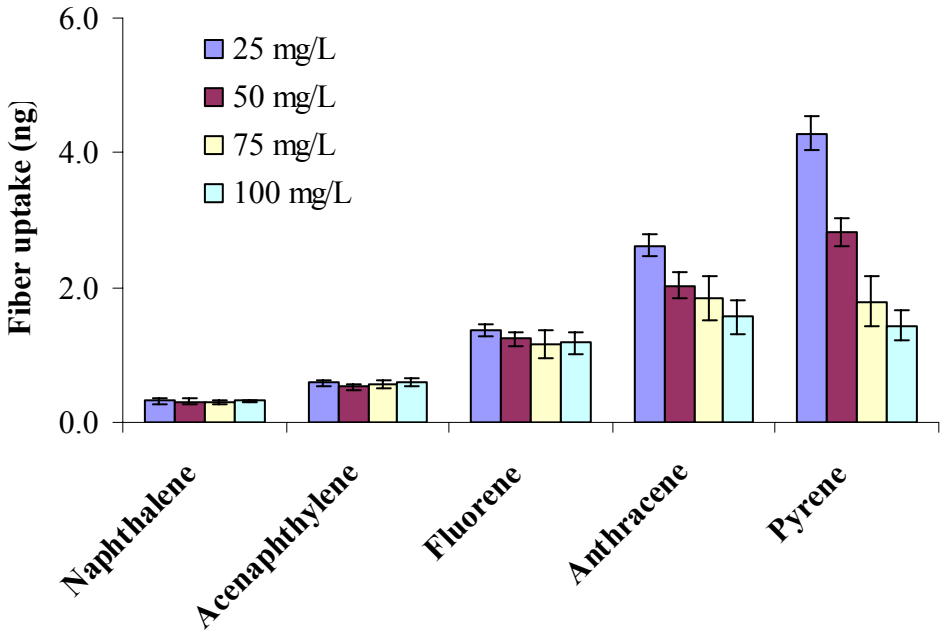

Figure 4-6 Comparison of fiber uptake at different concentrations of humic acid (n=3).

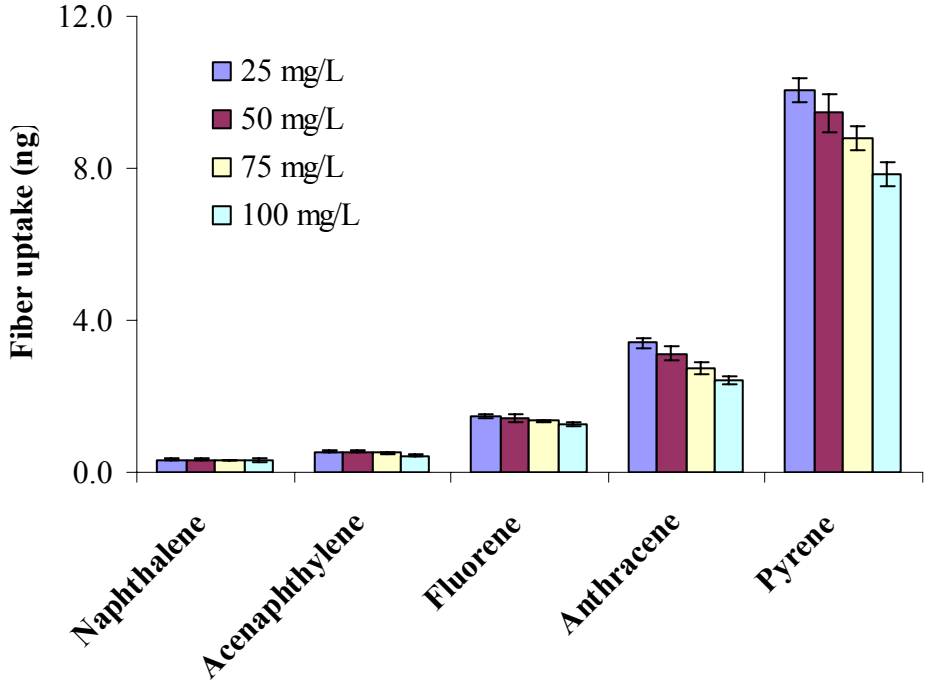

Figure 4-7 Comparison of fiber uptake at different concentrations of fulvic acid (n=3).

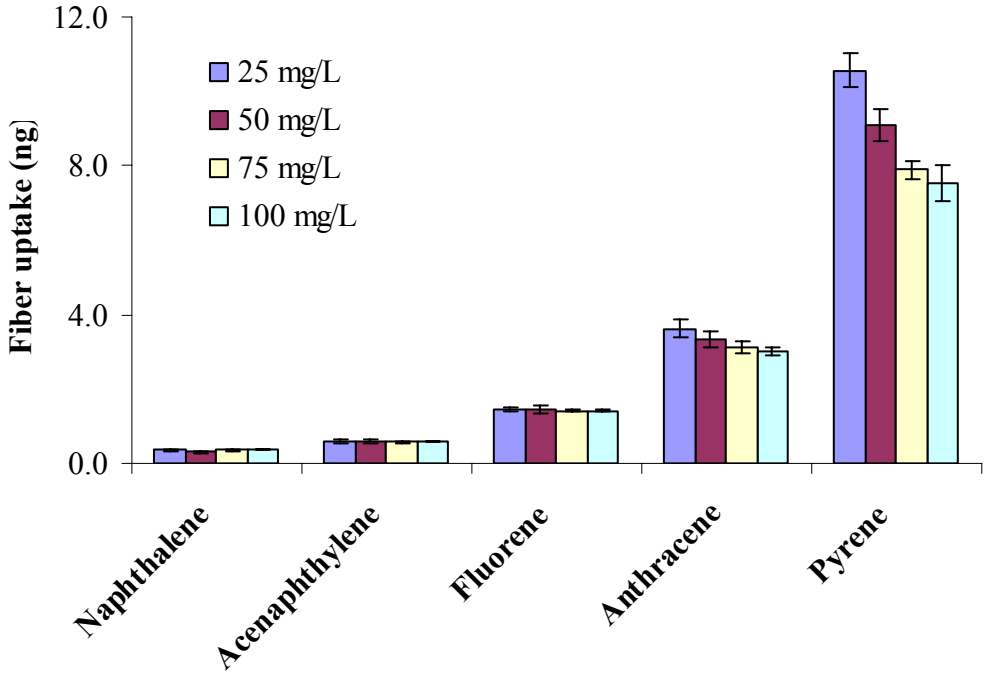

Figure 4-8 Comparison of fiber uptake at different concentrations of NOM (n=3).

4.4.8 Calibration of Freely Dissolved Concentration

The freely dissolved analyte concentration can be determined by external calibration because the amount extracted by the SPME fiber is limited, which does not affect the sorption equilibrium in the system. To change the free concentration of the target analytes in aqueous solution by less than 10%, the criterion is:[27]

$$V_s > 10K_{fs}V_f \qquad \text{Equation 4.12}$$

where K_{fs} is the distribution coefficient between the fiber coating and the sample; V_s, V_f represent the volume of sample matrix and fiber coating, respectively.

According to the fiber manufacturer, the volume of 7 μm PDMS fiber coating is 0.026 μL. Therefore, the criterion as shown in equation 4.12 is satisfied for all the analytes studied while using the sample volume as 20 mL by using 7 μm PDMS fiber.

With a spiking PAH concentration of 30 ppb, the freely dissolved concentration in the presence of humic acid, fulvic acid, and NOM were calculated based on the external calibration method and listed in Table 4-1.

The results compared in Table 4-1 demonstrate that humic acid has a much stronger binding effect on the analyte in the sample matrix compared to the other two matrices. Fulvic acid and NOM exhibited very limited sorption to the target pollutants, especially to less hydrophobic compounds like naphthalene, acenaphthylene and fluorene.

Table 4-1 Freely dissolved concentration of PAHs in the sample matrix containing humic acid, fulvic acid, and NOM

Compound name	Free concentration of PAHs (ng/mL) (%RSD) (n=3)		
	Humic acid	Fulvic acid	NOM
Naphthalene	27.4 (11.5)	29.5 (8.6)	29.2 (8.4)
Acenaphthylene	25.2 (9.0)	28.5 (6.5)	28.3 (9.7)
Fluorene	23.8 (8.8)	28.1 (7.5)	27.2 (6.0)
Anthracene	14.4 (9.3)	25.9 (7.1)	25.8 (6.8)
Pyrene	6.8 (7.2)	24.1 (5.7)	23.4 (4.3)

4.4.9 Determination of K_{fs}

In the current study, K_{fs} value was determined using the SPME equilibrium calibration without HOM and headspace presented. The extractions were performed in the flow-through system with a 7 μm PDMS fiber. The fiber was allowed to reach equilibrium in the flow-through system before separation and analysis by GC-MS. Table 4-2 compares the log K_{fs} values determined in this study to the reference data.[34]

Table 4-2 Comparison of log K_{fs} values determined from the SPME method and reference data

Compound	log K_{fs} *(Exptl.)*	log K_{fs} *(reference)*
Naphthalene	3.29	3.26
Acenaphthylene	3.49	NA
Fluorene	3.69	NA
Anthracene	4.32	4.29
Pyrene	4.65	4.61

4.4.10 Determination of Sorption Coefficient K_D

The sorption coefficients of PAHs to humic acid were determined using SPME technique with sample volume of 10 mL and 500 mL by using equation 4.4 and 4.7, respectively. The concentration of HA in the sample matrix was 50 mg/L. To minimize the loss of analytes to sampling system (e. g. stir-bar, wall of sampling vial) when the limited sample volume applied, silanized vials were used by applying shaking in the agitator of CombiPAL autosampler instead of stir-bar agitation during extraction. The experimentally determined sorption coefficients of 5 PAHs to HA are shown in Table 4-3, which indicate comparable results by these two approaches.

However commercial humic acid are not completely representative of natural humic substances. The commercial HA are known to be less polar and possess a higher sorption potential for organic pollutants than HOM from natural sources. Therefore, sorption coefficients of PAHs have also been determined on HOMs from IHSS using a large sample volume of 500 mL. HOM concentrations in the sample matrix were 50 mg/L. The calculated K_D values for these three HOMs are listed in Table 4-4. The results in Table 4-4 demonstrate that the K_D values for HA is much higher than those for fulvic acid and NOM, which indicates that HA has the highest sorption potential toward PAHs while FA and NOM from IHSS have similar sorption characteristics. This is consistent

with earlier observations and results from other researchers, and reflects the compositional differences among organic matters of different origins. [35]

Table 4-3 Experimentally determined sorption coefficients of 5 PAHs to HA using 10 mL and 500 mL sample volume

Compound	log K_D	
	10 mL	500 mL
Naphthalene	3.36	3.28
Acenaphthylene	3.67	3.58
Fluorene	3.83	3.72
Anthracene	4.54	4.33
Pyrene	5.07	4.83

Table 4-4 Comparison of experimentally determined sorption coefficients of 5 PAHs with HA, fulvic acid and NOM

Compound	log K_D		
	fulvic acid	NOM	HA
Naphthalene	2.63	2.73	3.28
Acenaphthylene	3.02	3.08	3.58
Fluorene	3.11	3.23	3.72
Anthracene	3.48	3.51	4.33
Pyrene	3.69	3.75	4.83

Based on the K_D values determined above using the SPME technique, sorption on these three HOMs can be described well by linear log K_D to log K_{ow} correlations within the class of PAHs (Figure 4-10).

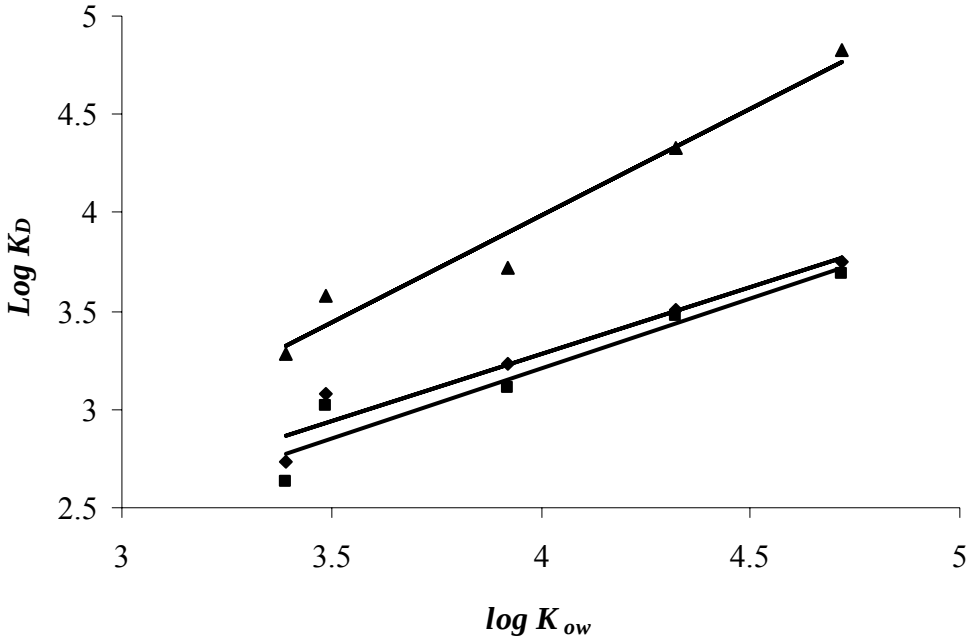

Figure 4-9 log K_D to log K_{ow} correlations for PAHs binding to HOMs. Humic acid (▲), Fulvic acid (■), and NOM (♦).

Humic acid (Sigma-Aldrich):

$$\log K_D = (1.09 \pm 0.13) \log K_{ow} - (0.39 \pm 0.51) \quad (r^2 = 0.9608) \qquad \text{Equation 4.12}$$

NOM:

$$\log K_D = (0.68 \pm 0.10) \log K_{ow} + (0.57 \pm 0.42) \quad (r^2 = 0.9334) \qquad \text{Equation 4.13}$$

Fulvic acid:

$$\log K_D = (0.71 \pm 0.12) \log K_{ow} + (0.38 \pm 0.50) \quad (r^2 = 0.9172) \qquad \text{Equation 4.14}$$

These results indicate that differences in sorption among PAHs are correlated with their polarity. The LFER model allows for the estimation of sorption constants of PAHs without performing extensive experimental tests. However, the models are specifically relevant to the property of the sorption matrix. Developing the modeling approaches which can handle the wide variety of chemical properties of the target analytes and binding matrix continues to be a challenge.

4.5 Conclusion

The SPME technique was applied to monitor the selected organic pollutants (PAHs) in aqueous solutions in the presence of humic substances of different origins in order to assess their partition and sorption onto these materials. The freely dissolved concentrations of analytes and their sorption coefficients were determined. Within the ranges investigated in this study, pH value and ionic strength of the sample matrix seem to have no significant effect on fiber extraction. The empirical correlation between log K_D and log K_{ow} generalized allows for the prediction of different affinities in the class of PAHs.

References

(1) Jones, M. N.; Bryan, N. D. *Adv. Coll. Int. Sci.* **1998**, *78*, 1.

(2) Carter, C. W.; Suffet, I. H. *Environ. Sci. Technol.* **1982**, *16*, 735.

(3) Chiou, C. T.; Malcom, R. C.; Brinton, T. I.; Kile, D. E. *Environ. Sci. Technol.* **1986**, *20*, 502.

(4) Chin, Y.; Weber, J. *Environ. Sci. Technol.* **1989**, *27*, 976.

(5) Schlautman, M. A.; Morgan, J. J. *Environ. Sci. Technol.* **1993**, *27*, 961.

(6) McCarthy, J. F.; Jimenez, B. D. *Environ. Sci. Technol.* **1985**, *19*, 1072.

(7) Gauthier, T. D. ; Shane, E. C.; Guerin, W. F.; Seitz, W. R. ; Grant, C. L. *Environ. Sci. Technol.* **1986**, *20*, 1162.

(8) Hasset, P. J.; Millicic, E. *Environ. Sci. Technol.* **1985**, *19*, 628.

(9) Sita, A. D. *J. Phys. Chem. Ref. Data* **2001**, *30*, 187.

(10) Poerschmann, J.; Kopinke, F. E. *Environ. Sci. Technol.* **2001**, *35*, 1142.

(11) Schwarzenbach, R. P.; Gschwend, P. M.; Imboden, D. M. *Environmental organic chemistry*, 2 ed.; John Wiley & Sons: Hoboken: New Jersey, 2003.

(12) Semple, K. T.; Morriss, W. J.; Paton, G. I. *Eur. J. Soil Sci.* **2003**, *54*, 809.

(13) Alexander, M. *How toxic are toxic chemicals in soils* Oxford University Press: New York, 1994.

(14) Kumke, M. U.; Loehmannsroeben, H.-G.; Roch, T. *Analyst* **1994**, *119*, 997.

(15) Laor, Y. R., M. *Environ. Sci. Technol.* **1997**, *31*, 3558.

(16) GieBl, H. *Environ. Sci. Pollut. Res.* **1999**, *6*, 77.

(17) De Paolis, F.; Kukkonen, J. *Chemosphere* **1997**, *34*, 1693.

(18) Landrum, P. F.; Nihart, S. R.; Eadie, B. J.; Gardner, W. S. *Environ. Sci. Technol.* **1984**, *18*, 187.

(19) Maxin, C. R.; Koegel-Knabner, I. *Europ. J. Soil Sci.* **1995**, *46*, 193.

(20) Kopinke, F.-D.; Georgi, A.; Mackenzie, K. *Anal.Chim. Acta.* **1997**, *355*, 101.

(21) Tanaka, S.; Oba, K.; Fukushima, M.; Nakayasu, K.; Hasebe, K. *Anal. Chim. Acta.* **1997**, *337*, 351.

(22) Lueers, F.; Ten Hulscher, T. E. M. *Chemosphere* **1996**, *33*, 643.

(23) Hassett, J. P.; Milicic, E. *Environ. Sci. Technol.* **1985**, *19*, 638.

(24) Kopinke, F.-D.; Porschmann, J.; Remmler, M. *Naturwissenschaften* **1995**, *82*, 28.

(25) Poerschmann, J.; Zhang, Z.; Kopinke, F.-D.; Pawliszyn, J. *Anal. Chem.* **1997**, *69*, 597.

(26) Poerschmann, J.; Kopinke, F.-D.; Pawliszyn, J. *Environ. Sci. Technol.* **1997**, *31*, 3629.

(27) Alley, W. *Regional groundwater quality*; Van Nostrand Reinhold: New York, 1994.

(28) Zhang, Z.; Pawliszyn, J. *J. Phys. Chem.* **1996**, *100*, 17648.

(29) Arthur, C. L.; Killam, L.; Motlagh, S.; Lim, M.; Potter, D.; Pawliszyn, J. *Environ. Sci. Technol.* **1992**, *26*, 979.

(30) Dean, J.; Tomllnson, W.; Makovskaya, V.; Cumming, R.; Hetheridge, M.; Comber, M. *Anal. Chem.* **1996**, *68*, 130.

(31) Ouyang, G.; Chen, Y.; Pawliszyn, J. *J. Chromatogr. A.* **2006**, *1105*, 176.

(32) Randall, L.; Weber, J. H. *Sci. Total Environ.* **1986**, *57*, 191.

(33) Dai, S. Q.; Huang, G. L.; Cai, Y. *Environ. Pollut.* **1993**, *82*, 217.

(34) Shurmer, B.; Pawliszyn, J. *Anal. Chem.* **2000**, *72*, 3660.

(35) Carter, C. W.; Suffet, I. H. *Environ. Sci. Technol.* **1982**, *25*, 1103.

(36) Georgi, A.; Kopinke, F. *Environ. Toxicol. Chem.* **2002**, *21*, 1766.

Chapter 5
Kinetics Study of Solid Phase Microextraction in Complex Aqueous Sample Matrix

5.1 Introduction

SPME has found extensive applications in environmental aqueous sample analysis, where it has been applied for the analysis of hydrophobic, semivolatile, and volatile organics in surface water, wastewater, and sediment porewater since its inception in 1996. [1-11] A specific application of SPME is to measure the sorption of hydrophobic organic pollutants to binding matrix like humic organic matter (HOM). By studying the effect of binding matrix on the extraction of analytes in aqueous solutions using SPME, it is possible to assess their impact on the risk of chemicals in the environment. Due to the presence of binding matrix, the measurement of organic pollutants concentration in solution containing HOM using SPME is complex, which has been recognized by several researchers. [12-15]

Up to now, several different approaches have been proposed to mathematically model the extraction kinetics of SPME fiber. Vaes et al. [16] and Heringa et al. [17] model the fiber as a classical one compartment, first-order kinetic model with absorption and desorption rate constants as parameters. The model is simple but it is not explicitly based on processes like diffusion and partitioning of the analyte and the experimental conditions, like medium volume and fiber geometry, are not considered in their model. A mechanistically based modelling approach has been employed by Pawliszyn. [3] In this approach, the mass transfer of the target analyte from the bulk to the fiber coating is considered to be controlled by the molecular diffusion in the stagnant boundary layer around the fiber coating. The influence of the agitation condition on the uptake kinetics can be explained by this model and it can also be applied in predicting kinetics based on parameters such as distribution coefficient, diffusion

coefficients and diffusion boundary layer thickness. However, additional parameters, such as the fluid linear speed at the fiber surface, the fluid's kinematic viscosity and the diffusion coefficient of the analyte in the medium, are required to determine the boundary layer thickness. In 1997, a kinetic model of pre-equilibrium extraction method for quantification with SPME was proposed by Ai. [18] Based on this method, the kinetics of the absorption of analyte from sample matrix and desorption of analyte from the fiber coating in an aqueous solution was studied simultaneously and a new calibration method was developed by Chen and Pawliszyn. [19] The method used the desorption of the standard, which was pre-loaded in the fiber coating to calibrate the extraction of the analytes, and was called as in-fiber standardization method.

With the presence of a binding matrix, the extraction kinetics of SPME can be affected. [20] In the current work, a theoretical model was built to investigate the kinetics of SPME extraction of the target analyte in a sample matrix containing dissolved organic matter. Realistic parameter values are used to theoretically evaluate the efficiency of SPME for analyzing the complex system, predictions from the derived equations are compared to previous experimental results in the literature. [17] The analytical performance of SPME is predicted as a function of physicochemical properties of analyte and fiber coating. Furthermore, the effects of the agitation speed, the concentration of binding matrix and analyte are also investigated. With the presence of binding matrix, the mirror reflection characteristic of absorption of analyte from the sample matrix and desorption of analyte from the fiber coating was demonstrated in this work and it was further applied to calculate the total concentration of analyte in the system.

5.2 Theory

In the aqueous system containing dissolved organic matter, equilibrium can be reached very fast for the association and dissociation reaction between the analyte and binding matrix:

$$free\ dissolved\ analyte + binding\ matrix \quad \Leftrightarrow \quad bound\ analyte$$

$$K_a = \frac{C_{bs}}{C_s \times C_b} \qquad \text{Equation 5.1}$$

where K_a is the equilibrium binding constant; C_s, C_b, and C_{bs} are the analyte concentration, the binding matrix concentration and the bounded analyte concentration in bulk solution, respectively.

In the most common situation, the concentration of the binding matrix is much larger than the concentration of analytes due to the trace concentration of target compounds in the environmental aqueous samples. Under this circumstance, the concentration of binding matrix can be considered as constant, equation 5.2 can be rewritten as:

$$K_a = \frac{C_{bs}}{C_s \times C_b^0} \qquad \text{Equation 5.2}$$

Rearranging equation 5.2, the following equation is obtained:

$$C_{bs} = K_a C_s C_b^0 \qquad \text{Equation 5.3}$$

The mass balance for the analyte in the system can be expressed as:

$$C_s + C_{bs} + \frac{n}{V_s} = C_s^0 \qquad \text{Equation 5.4}$$

where C_s^0 is the total concentration of analyte in the system and *n* is the amount of anayte being extracted by the fiber coating.

Substituting equation 5.3 into equation 5.4,

$$C_s + K_a C_s C_b^0 + \frac{n}{V_s} = C_s^0 \qquad \text{Equation 5.5}$$

The rearrangement of equation 5.5 results in:

$$C_s = \frac{C_s^0 - \frac{n}{V_s}}{1 + K_a C_b^0}$$ Equation 5.6

The equilibrium binding constant K_a can be calculated using equation 5.6 with the equilibrium SPME extraction.

5.2.1 Kinetic Considerations of Extraction

The extraction process follows Fick's first law of diffusion. Therefore a linear concentration gradient in the boundary layer and fiber is assumed. Following the same deduction procedures as described in Chapter 3, equation 5.7 can be expressed as:

$$\frac{1}{A}\frac{dn}{dt} = h_s(C_s - \frac{C_f}{K_{fs}}) = h_f(C_f - C_f^{'})$$ Equation 5.7

where K_{fs} is the distribution coefficient of the analyte between the fiber coating and the sample matrix. h_s and h_f are mass transfer coefficients in the boundary layer and the fiber coating, respectively. C_s is the concentration of the analyte in the sample matrix, C_f is the concentration of the analyte in the fiber coating at the interface of the fiber coating and boundary layer, $C_f^{'}$ is the concentration of the analyte at the axis of the fiber coating.

A linear concentration gradient is assumed in the fiber coating,

$$n = V_f \frac{(C_f + C_f^{'})}{2}$$ Equation 5.8

Combining equation 5.7 and 5.8

$$C_f = \frac{K_{fs}(2nh_f + h_s V_f C_s)}{V_f(2K_{fs}h_f + h_s)}$$ Equation 5.9

Substitution of equation 5.9 into equation 5.7 gives

$$C_f - C_f^{'} = \frac{2K_{fs}h_s C_s}{2K_{fs}h_f + h_s} - \frac{2h_s n}{V_f(2K_{fs}h_f + h_s)}$$ Equation 5.10

Substitution of equation 5.10 into equation 5.7 gives

$$\frac{1}{A}\frac{dn}{dt} = h_f(C_f - C_f^{'}) = h_f[\frac{2K_{fs}h_s C_s}{2K_{fs}h_f + h_s} - \frac{2h_s n}{V_f(2K_{fs}h_f + h_s)}]$$ Equation 5.11

Equation 5.12 is obtained by substituting equation 5.6 into equation 5.11:

$$\frac{dn}{dt} + A\frac{2K_{fs}h_s V_f + 2h_s V_s\left(1 + K_a C_b^0\right)}{\left(2K_{fs}h_f + h_s\right)\left(1 + K_a C_b^0\right)V_s V_f}n = A\frac{K_{fs}h_s C_s^0}{\left(2K_{fs}h_f + h_s\right)\left(1 + K_a C_b^0\right)}$$

Equation 5.12

Let

$$a = A\frac{2K_{fs}h_s V_f + 2h_s V_s\left(1 + K_a C_b^0\right)}{\left(2K_{fs}h_f + h_s\right)\left(1 + K_a C_b^0\right)V_s V_f}$$ Equation 5.13

$$b = A\frac{K_{fs}h_s C_s^0}{\left(2K_{fs}h_f + h_s\right)\left(1 + K_a C_b^0\right)}$$ Equation 5.14

Equation 5.12 is simplified as

$$\frac{dn}{dt} = b - an$$ Equation 5.15

The solution to equation 5.15 is

$$n = \frac{b}{a}[1 - \exp(-at)] \qquad \text{Equation 5.16}$$

and

$$\frac{b}{a} = \frac{K_{fs} C_s^0 V_s V_f}{K_{fs} V_f + K_a C_b^0 V_s + V_s} = n_e \qquad \text{Equation 5.17}$$

where n_e is the amount of the analyte extracted in the fiber coating when the system reaches equilibrium.

Substituting equation 5.17 and equation 5.13 into equation 5.16:

$$n = \frac{K_{fs} C_s^0 V_s V_f}{K_{fs} V_f + K_a C_b^0 V_s + V_s} \left[1 - \exp\left(- A \frac{2K_{fs} h_s V_f + 2h_s V_s \left(1 + K_a C_b^0\right)}{\left(2K_{fs} h_f + h_s\right)\left(1 + K_a C_b^0\right) V_s V_f} t \right) \right]$$

Equation 5.18

which can be simplified as

$$\frac{n}{n_e} = 1 - \exp(-at) \qquad \text{Equation 5.19}$$

The parameter a defined in equation 5.19 is a measure of how fast the equilibrium can be reached in the system. It is determined by mass transfer coefficients, distribution coefficient, binding constant and physical dimensions of the sample matrix and the SPME fiber coating. For a constantly agitated system, a is a constant. The binding constant can be determined from equation 5.17 by using SPME equilibrium extraction.

The extraction profile with the presence of binding matrix in the sample can be predicted using equation 5.18. The mass transfer coefficient can be determined by knowing the thickness of the fiber coating and boundary layer, and the diffusion coefficient of analyte in sample matrix and fiber

coating. The thickness of the boundary layer can be estimated by the semi-empirical relationship when the direction of the sample flow is axis-symmetrical around the circumference of the fiber (as when a fiber is placed in the central position of a vial containing a magnetically stirred sample) [3]:

$$\delta_s = 2.64\left(b / Re^{0.50} Sc^{0.43}\right) \qquad \text{Equation 5.20}$$

where b is the radius of the fiber, Re is the Reynolds number ($Re = \frac{2ub}{v}$), and Sc is the Schmidt number ($Sc = \frac{v}{D_s}$), u is the linear velocity of the sample, and v is the kinematic viscosity of the matrix medium.

The flow velocity u around the fiber can be calculated according to the following equation [3]:

$$u = 1.05\pi N r\left[2 - \left(r / 0.74R_s\right)^2\right] \qquad \text{Equation 5.21}$$

where N is the magnetic stirrer speed in revolutions per second, r is the distance between the fiber and the centre of the vial, and R_s is the radius of the stirring bar.

5.2.2 Kinetic Considerations of Desorption

The desorption of the standard that is preloaded onto the fiber coating also follows Fick's first law of diffusion, which can be rewritten as:

$$\frac{1}{A}\frac{dq}{dt} = -h_{ss}\left(C_{ss} - \frac{C_{fs}}{K'_{fs}}\right) = -h_{fs}\left(C_{fs} - C'_{fs}\right) \qquad \text{Equation 5.22}$$

where q is the amount of the standard desorbed from the fiber coating during sampling time t, K'_{fs} is the distribution coefficient of the standard between the coating and the sample matrix, C_{ss} is the concentration of the standard in the sample matrix, C_{fs} is the concentration of the standard in the

fiber coating at the interface of the coating and boundary layer, and C'_{fs} is the concentration of the standard at the axis of the fiber coating. h_{ss} and h_{fs} are mass transfer coefficients of the standard in the boundary layer and the fiber coating, respectively.

Assuming there is a linear concentration gradient in the fiber coating,

$$Q = q_0 - q = V_f \frac{C_{fs} + C'_{fs}}{2} \qquad \text{Equation 5.23}$$

where Q is the amount of the standard left on the fiber after sampling time t and q_0 is the amount of the standard initially loaded onto the fiber before exposure of the fiber to the sample matrix.

Combining equation 5.23 and equation 5.22:

$$C_{fs} = \frac{2K'_{fs}h_{fs}Q + K'_{fs}h_{ss}V_f C_{ss}}{V_f(2K'_{fs}h_{fs} + h_{ss})} \qquad \text{Equation 5.24}$$

Substitution of equation 5.24 into equation 5.22:

$$-\frac{1}{A}\frac{dQ}{dt} = -h_{ss}\left(C_{ss} - C'_{ss}\right) = -h_{ss}\left(C_{ss} - \frac{2h_{fs}Q + h_{ss}V_f C_{ss}}{V_f\left(2K'_{fs}h_{fs} + h_{ss}\right)}\right) \qquad \text{Equation 5.25}$$

Similar to equation 5.6,

$$C_{ss} = \frac{q_0 - Q}{V_s\left(1 + K_a C_b^0\right)} \qquad \text{Equation 5.26}$$

Substituting equation 5.26 into equation 5.25 and rearranging as:

$$\frac{dQ}{dt} + A\frac{2K'_{fs}h_{fs}V_f + 2h_{fs}V_s\left(1 + K_a C_b^0\right)}{\left(2K'_{fs}h_{fs} + h_{ss}\right)\left(1 + K_a C_b^0\right)V_s V_f}n = A\frac{2K'_{fs}h_{fs}q^0}{V_s\left(2K'_{fs}h_{fs} + h_{ss}\right)\left(1 + K_a C_b^0\right)}$$

Equation 5.27

Let

$$a' = A\frac{2K'_{fs}h_{fs}V_f + 2h_{fs}V_s\left(1+K_aC_b^0\right)}{\left(2K'_{fs}h_{fs}+h_{ss}\right)\left(1+K_aC_b^0\right)V_sV_f} \qquad \text{Equation 5.28}$$

$$b' = A\frac{2K'_{fs}h_{fs}q^0}{V_s\left(2K'_{fs}h_{fs}+h_{ss}\right)\left(1+K_aC_b^0\right)} \qquad \text{Equation 5.29}$$

Then equation 5.27 is simplified as:

$$Q' + a'Q = b' \qquad \text{Equation 5.30}$$

The general solution to equation 5.30 is:

$$Q\exp\int a'\,dt = \int b'\left(\exp a'\,dt\right)dt + Z \qquad \text{Equation 5.31}$$

$$Q\exp a't = \frac{b'}{a'}\left(\exp a't - 1\right) + Z \qquad \text{Equation 5.32}$$

The boundary condition to equation 5.32 is: $t = 0$, $Q = q_0$

Therefore, $Z = q_0$. Equation 5.32 becomes

$$Q = \frac{b''}{a}\left(1-\exp(-at)\right) + q_0\exp(-at) \qquad \text{Equation 5.33}$$

$$\frac{b'}{a'} = \frac{K'_{fs}q_0V_f}{K'_{fs}V_f + K_aC_b^0V_s + V_s} = q_e \qquad \text{Equation 5.34}$$

where q_e is the amount of the preloaded analyte left in the fiber coating when the system reaches equilibrium.

Rearranging equation 5.34,

$$\frac{Q-q_e}{q_0-q_e} = \exp(-a't) \qquad \text{Equation 5.35}$$

As discussed before, time constant a' in equation 5.35 has the same definition as in equation 5.19, which means the value of constant a and a' should be the same for both absorption and

desorption under the same experimental conditions when the analyte and standard have the same distribution coefficient and mass transfer coefficient. Combining equations 5.19 and 5.35,

$$\frac{n}{n_e} + \frac{Q - q_e}{q_0 - q_e} = 1 \qquad \text{Equation 5.36}$$

Substituting equation 5.34 into equation 5.36 results in equation 5.37:

$$n_e = \frac{q_0 n\left(K_a C_b^0 V_s + V_s\right)}{(K_{fs}^{'} V_f + K_a C_b^0 V_s + V_s)(q_0 - Q)} \qquad \text{Equation 5.37}$$

Equation 5.17 and equation 5.37 can be combined to

$$C_s^0 = \frac{q_0 n\left(K_a C_b^0 + 1\right)}{K_{fs} V_f (q_0 - Q)} \qquad \text{Equation 5.38}$$

The above equation indicates that by pre-loading a certain amount of standard, q_0, onto the PDMS fiber coating, and exposing the fiber into a sample matrix for a definite time, then, *n*, the amount of analyte extracted by the sampler and *Q*, the amount of standard remaining in the sampler, can be determined. Consequently, the total concentration of the target analyte in the sample matrix, C_s^0, can be calculated by equation 5.38 by knowing the distribution coefficient K_{fs} and binding constant K_a.

5.3 Experimental Section

5.3.1 Chemical and Supplies

HPLC grade methanol, hydrochloric acid, sodium azide and sodium hydroxide were obtained from BDH (Toronto, Canada). Fluorene and pyrene were purchased from Supelco (Bellefonte, PA, USA). Deionized water was obtained using a Barnstead/Thermodyne NANO-pure ultrapure water system (Dubuque, IA, USA). The SPME holder and 7 μm PDMS fibers were obtained from Supelco (Oakville, Canada). Humic acid (HA) was purchased from Sigma-Aldrich (Milwaukee, WI, USA).

5.3.2 Sorption Experiments

Dissolved humic substance solution was prepared by dissolving the solid HA in diluted NaOH. The solution was further diluted and anti-microbial agent NaN_3 (200 mg/L) was added to inhibit the microbial activity. The HA solution was agitated and allowed to come to equilibrium for at least two days. The stock methanolic solution of the target analytes were spiked into the HA solution. Direct SPME was applied in the current study.

5.3.3 Instrument

A Saturn 3800GC/2000 ITMS system (Varian Associate, Sunnyvale, CA, USA) was used for the analyses. The GC-MS was equipped with a 1079 Programmable Temperature Vaporizing Injector and coupled to a SPB-5 column (30 m, 0.25 mm I.D., 0.25 μm film thickness) (Supelco, Mississauga, Canada) with a SPI liner (2.4 mm I.D. × 4.6 mm O.D. × 54 mm). Helium was used as the carrier gas at a flow rate of 1 mL/min. The injector was set at 270 $^{\circ}$C when the PDMS fiber was used. The desorption time of the fiber in the injector is 10 min. The column temperature was maintained at 40 $^{\circ}$C for 1 min and then programmed to increase at a rate of 25 $^{\circ}$C /min to 270 $^{\circ}$C, held for 5 min.

5.4 Result and Discussion

5.4.1 Kinetic Model of Extraction

The kinetic model derived in the current study as equation 5.18 was first validated using the experimental results of Heringa et al. [17, 28] The parameters used in the kinetic model are listed in Table 5-1.

Table 5-1 The parameters used in the kinetic model

Parameters	Value
Concentration of analyte (M)	7.1×10^{-9}
Concentration of binding matrix (M)	1.6×10^{-5}
Thickness of fiber coating (μm)	7
Distribution coefficient	5.04×10^{3}
Binding constant (M^{-1})	8.9×10^{4}
Sample volume (mL)	1.6
Diffusion coefficient in sample matrix (m^2/s)	7.96×10^{-10}
Diffusion coefficient in fiber coating (m^2/s)	3.33×10^{-15}

Figure 5-1 shows the extraction profiles of [^{3}H]estradiol at different BSA concentrations. The points are experimental results from Heringa et. al. [17] The curves are drawn based on the calculation results from the kinetic model as equation 5.18. It can be seen that the calculated results are in good agreement with the experimental data, which demonstrate the model can accurately describe the extraction process in the complex sample system.

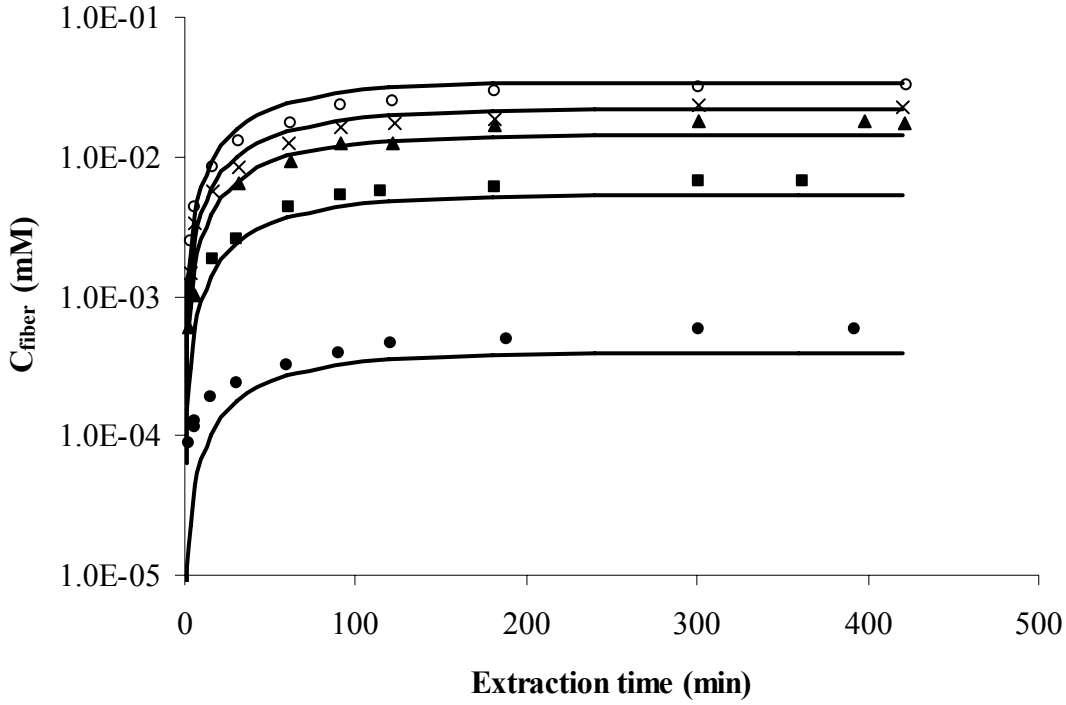

Figure 5-1 Extraction profiles of [^{3}H]estradiol at different BSA concentrations: 0 M (○), 6.5×10^{-6} M (×), 1.6×10^{-5} M (▲), 6.4×10^{-5} M (■) and 1.0×10^{-3} M (●). The curves are drawn based on the calculation results from the kinetic model.

Based on the kinetic model of equation 5.18, the factors that would affect the sorption characteristics and kinetics of SPME are investigated, which include the concentration of HA and target analytes in the sample matrix system, agitation condition, physicochemical properties of the target analytes such as binding constant and distribution coefficient.

5.4.1.1 Effect of Concentration of Binding Matrix

Figure 5-1 illustrates the predicted dependence of the extracted amount of analyte by fiber coating *vs.* the initial concentration of binding matrix in the sample. The results indicate that the higher concentration of the binding matrix do not change the shape of the extraction profile, but only

affect the maximum concentration of the analyte in the fiber. This maximum is related to the free concentration in the solution, which is, of course, lower at the higher concentration of binding matrix. The presence of binding matrix does not seem to have an effect on the uptake kinetics of the analyte to the fiber coating under the current experimental conditions.

5.4.1.2 Effect of Total Concentration of Target Analyte

Figure 5-2 presents the theoretical relationship between the extracted amount of analyte by the fiber *vs*. the total concentration of target analyte [^{3}H]estradiol, for five different values with the range of a few orders.

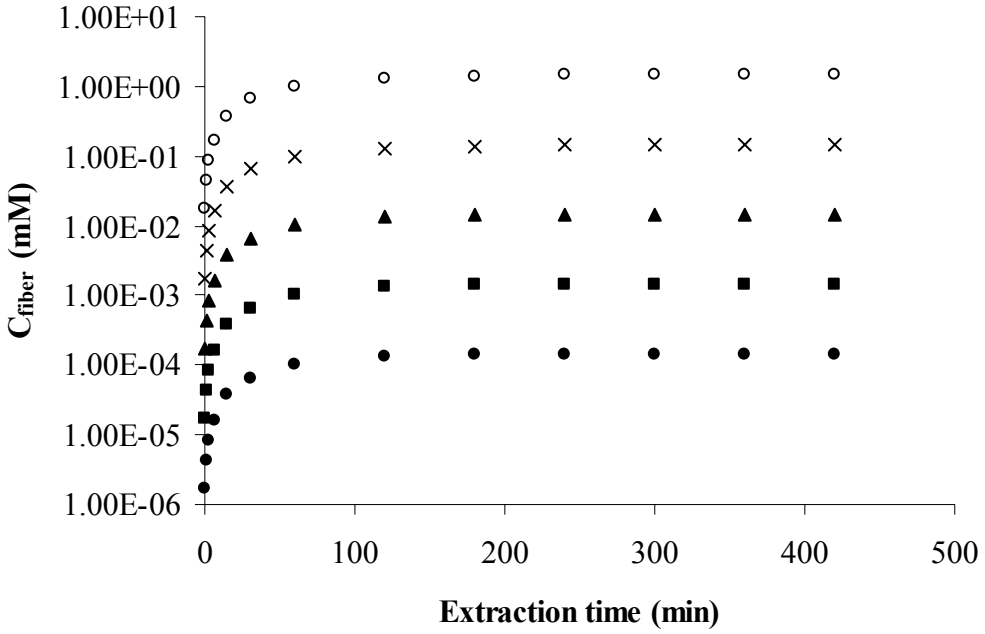

Figure 5-2 Extraction profiles at different total analyte concentrations: 7.11×10^{-7} M (○), 7.11×10^{-8} M (×), 7.11×10^{-9} M (▲), 7.11×10^{-10} M (■) and 7.11×10^{-11} M (●).

It is clear that with the increase of the total concentration of the analyte, the fiber uptake increases proportionally. This is obvious when looking at equation 5.18, the extraction amount of analyte is proportional to the total concentration of target analyte, providing the sample, fiber and the concentration of binding matrix are held constant. The figure also demonstrates that the equilibrium time is independent of the concentration of analyte in the system.

5.4.1.3 Effect of Agitation Condition

For a constantly agitated system, *a* is a constant. By increasing agitation speed, the thickness of the boundary layer will decrease and in turn will cause the increase of constant *a*. With the decrease of the boundary layer, the mass transfer rate will become much faster. Therefore, the time to reach equilibrium becomes much shorter. As demonstrated in Figure 5-3, the equilibrium is reached at around 300 min with the agitation speed of 100 rpm comparing to 60 min when the agitation speed increased to 1200 rpm.

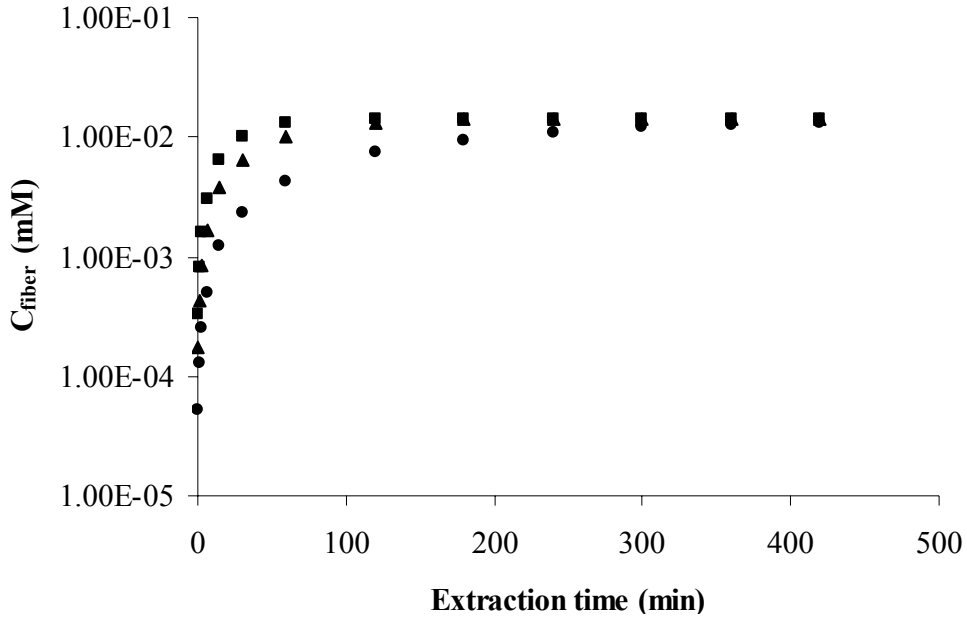

Figure 5-3 Extraction profiles at different agitation condition: 1200 rpm (■), 600 rpm (▲) and 100 rpm (●).

5.4.1.4 Effect of Binding Constant K_a

Figure 5-4 presents the theoretical relationship between the extracted amount of analyte by fiber coating and the binding constant K_a of the analyte to the binding matrix. It is intuitively obvious that when the analyte has a higher affinity to the binding matrix, more analyte will be bound by the binding matrix and less free analyte will be present in the sample solution. Therefore, the fiber uptake will decrease correspondingly because it is directly related to the free concentration of target analyte in the sample matrix.

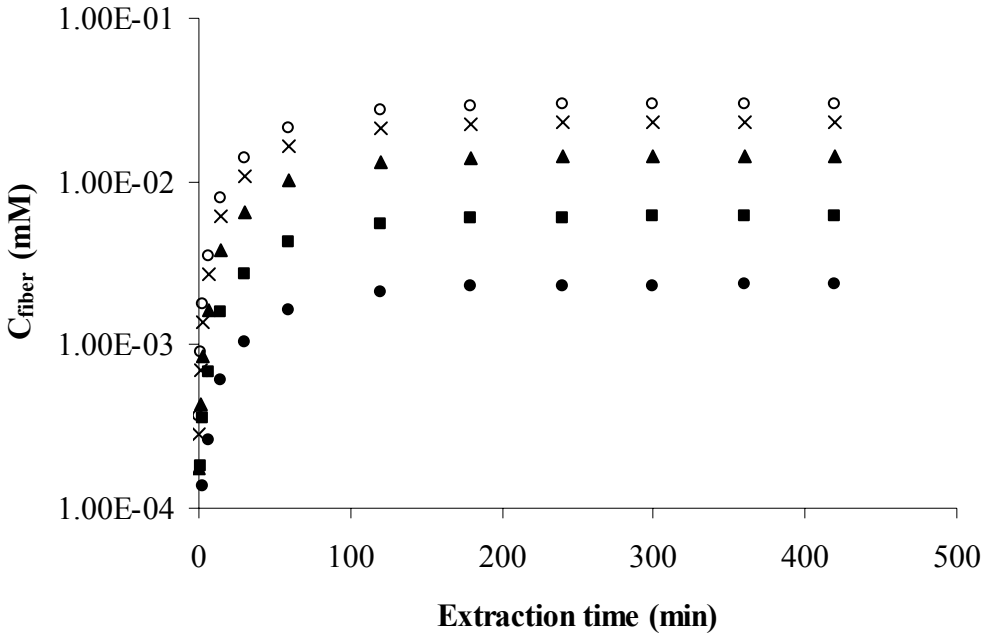

Figure 5-4 Extraction profiles with different binding constants: 8.9×10^3 (○), 3.0×10^4 (×), 8.9×10^4 (▲), 3.0×10^5 (■) and 8.9×10^5 (●).

5.4.1.5 Effect of Distribution Coefficient K_{fs}

The effect of distribution coefficient K_{fs} on the fiber uptake of target analyte was investigated with the range of log K_{fs} value from 3 to 5 as shown in Figure 5-5. The figure demonstrates that the higher distribution coefficient, the more analyte extracted by fiber coating at equilibrium condition. The equilibrium time is affected by the distribution coefficient, which is also indicated in the definition of time constant *a*. The extraction process has not reached equilibrium with seven hours extraction when the distribution coefficient is as high as 100000, instead of about 30 minutes with distribution coefficient of 1000.

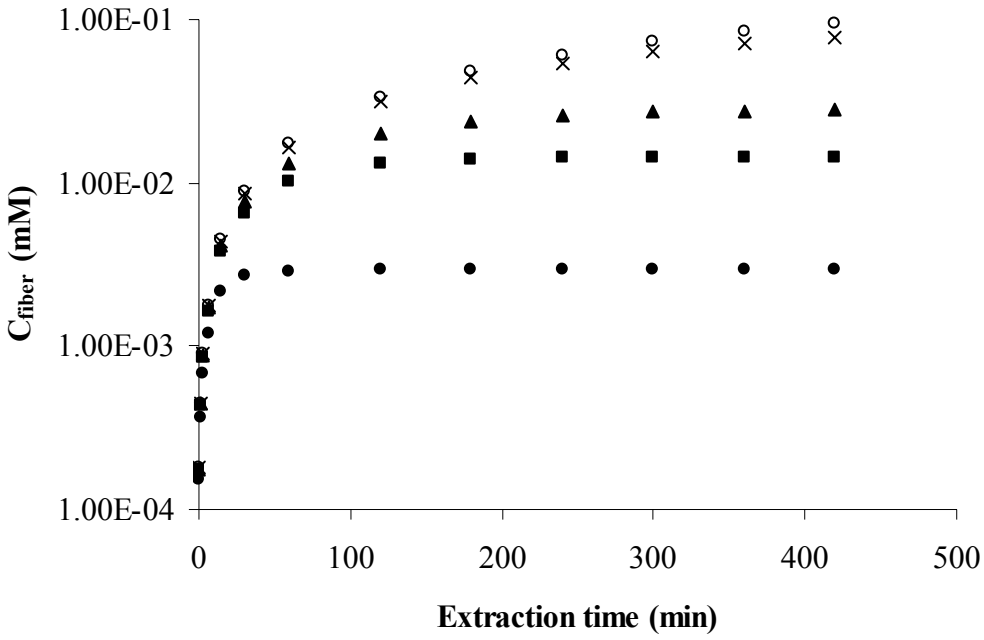

Figure 5-5 Extraction profiles with different distribution coefficients: log K_{fs} = 5.00 (○), log K_{fs} = 4.70 (×), log K_{fs} = 4.00 (▲), log K_{fs} = 3.70 (■) and log K_{fs} = 3.00 (●).

5.4.2 Determination of Time Constant *a*

In equation 5.13, the parameter *a*, is a constant that measures how quick an extraction equilibrium can be reached. It is determined by the mass-transfer coefficients, the distribution coefficient and the physical dimensions of the sample matrix and fiber coating. Analysis of how these factors affect parameter *a* would be helpful for a better understanding of the mass transfer process associated with the extraction of analyte onto a SPME fiber. The experiments in the current study were performed using fluorene and pyrene as the target analytes and HA as the binding matrix. Duplicate extractions were conducted at each sampling time. The extraction profiles of fluorene and pyrene with the presence of HA at the static and agitation conditions are compared in Figure 5-6. The sample volume is 20 mL with the HA at a concentration of 100 mg/L. The results indicates that the equilibrium will be reached faster at the agitation condition, which is caused by the acceleration of mass transfer due to the decrease of the stagnant boundary layer around the fiber coating. The time constant *a* of absorption calculated based on equation 5.19 is presented in Table 5-2 at the case of static extraction and extraction with the agitation speed of 500 rpm. The results showed that the time constant for static extraction is much smaller than those obtained with dynamic agitation, which demonstrates that higher agitation will result in a shorter equilibrium time. The results also show that the time constant *a* will increase with the decrease of the hydrophobicity of the target analyte. In other word, the extraction of fluorene will reach equilibrium much faster than the extraction of pyrene.

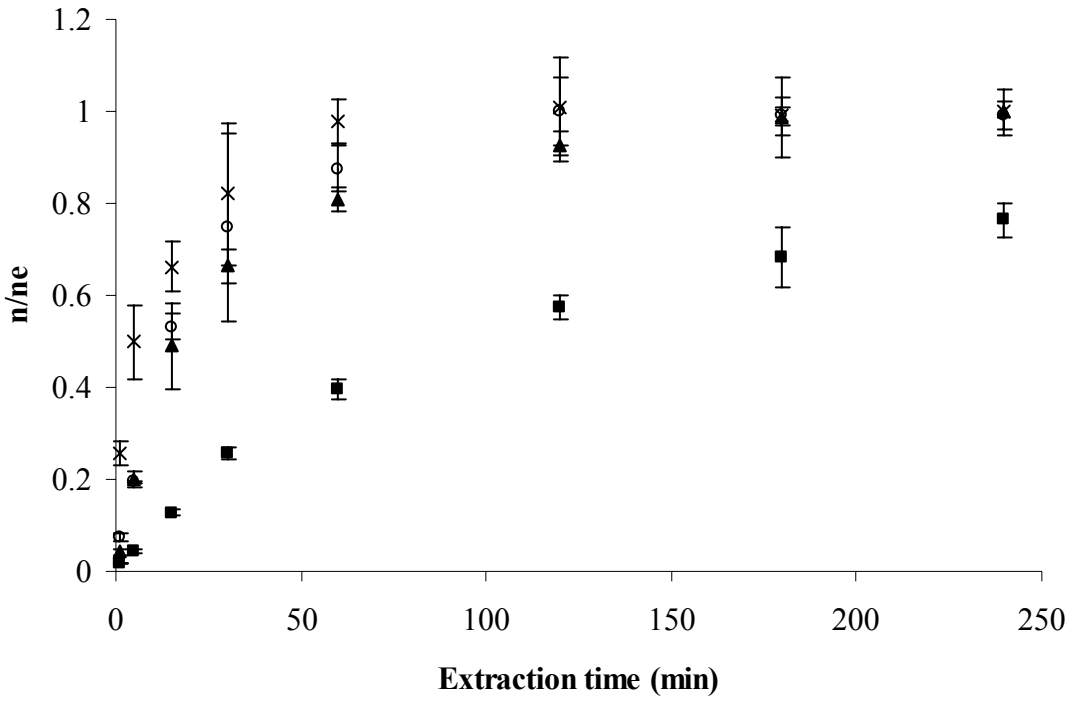

Figure 5-6 Extraction profiles at the static and agitation condition. Fluorene: static condition (○), 500 rpm (×); Pyrene: static condition (■), 500 rpm (▲).

Table 5-2 Time constant *a* for the absorption of fluorene and pyrene by SPME from the sample matrix with the presence of HA (n=2)

Compound	Time constant *a* (min^{-1})	
	static	agitation
Fluorene	0.038 ±0.003	0.064 ±0.004
Pyrene	0.008 ±0.001	0.027 ±0.002

5.4.3 Determination of Total Concentration Using Desorption Based Calibration

Experiments were carried out to validate the mirror reflection characteristic of absorption and desorption as presented in equation 5.36, which involved the simultaneous determination of the desorption time profile of deuterated pyrene (*d*-10) and the absorption time of pyrene. A 7 μm PDMS fiber was preloaded with deuterated pyrene, and the fiber was then exposed to a sample solution contained in a vial with the presence of HA for different extraction times. Figure 5-7 presents the values of $\frac{Q-q_e}{q_0-q_e}$ calculated from the resulting desorption time profile, the values of $\frac{n}{n_e}$ calculated from the resulting absorption time profile, and the sum of $\frac{n}{n_e}$ and $\frac{Q-q_e}{q_0-q_e}$. Although the sum of $\frac{n}{n_e}$ and $\frac{Q-q_e}{q_0-q_e}$ are close to 1 at different extraction times, larger deviation of the sum from 1 can be found comparing to the pure aqueous solution. This can be ascribed to not only the difference of physicochemical properties between deuterated pyrene and pyrene, but also the experimental errors introduced by the complex sample matrix.

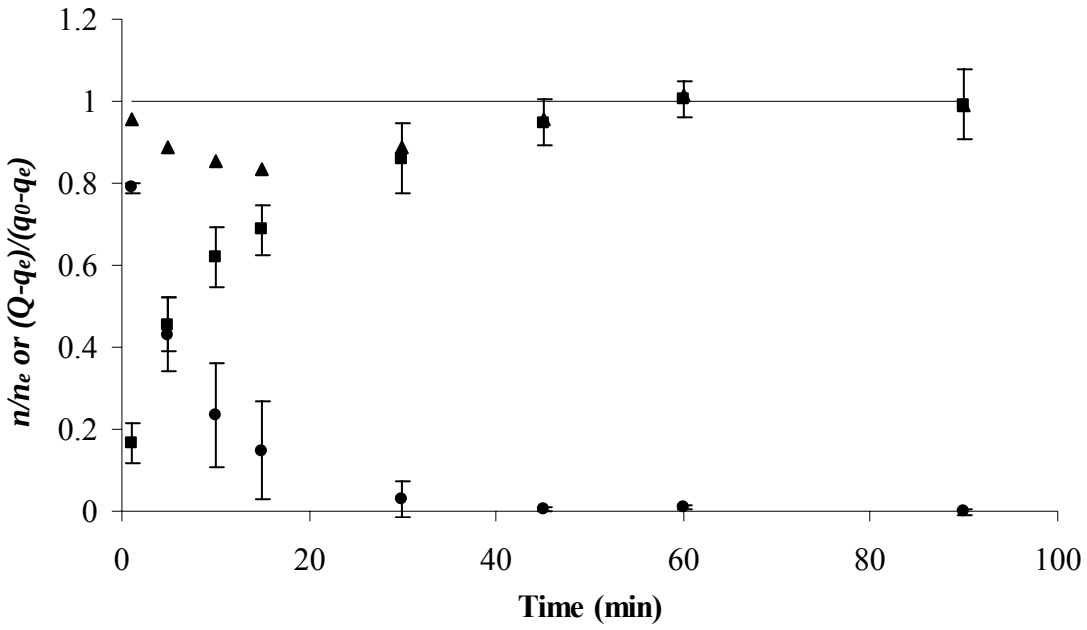

Figure 5-7 Absorption and desorption profiles in SPME fiber in the complex sample matrix with humic acid. Simultaneous absorption of pyrene (■) onto the PDMS fiber and desorption of deuterated pyrene (●) from the PDMS fiber. (▲) represents of the sum of $\frac{Q-q_e}{q_0-q_e}$ and $\frac{n}{n_e}$.

The total concentration of pyrene in a complex sample matrix containing HA was determined by using equation 5.38. The experiment was completed by exposing a PDMS fiber loaded with deuterated pyrene to a pyrene sample solution with the presence of HA for 1 min. The nominal pyrene concentration in the sample solution is 30 ppb. The predicted total concentration of pyrene in the sample matrix using equation 5.38 was 26.8 ppb. It is quite comparable to the experimental spiked concentration considering the complexity of the sample matrix, which demonstrated the feasibility of the proposed calibration method.

5.5 Conclusion

A mathematical model has been proposed to investigate the kinetics of the absorption of SPME fiber in the sample matrices with HOM. The important influence of organic matter on SPME procedure was confirmed by this model. The analytical performance of SPME is predicted as a function of physicochemical properties of analyte and fiber coating, agitation conditions as well as sample parameters. The new model demonstrates how the factors would affect the kinetics and SPME performance in the sample matrix containing HOM. However, the agitation condition and physicochemical properties of the analyte need to be known in advance.

Furthermore, the mirror reflection characteristic of absorption and desorption in SPME has been demonstrated in the complex sample matrix, which allows for the calibration of absorption using desorption. This is especially important for the on-site calibration since the agitation condition of the matrix is difficult to control and internal standard calibration is not possible by direct spiking of standard into the matrix. In this study, successful calibration of total concentration of analytes in complex sample matrix was accomplished by introducing standard together with the extraction phase, while investigating kinetics of the absorption and desorption process.

References

(1) Liu, Y.; Lee, M. L.; Hageman, K. J.; Yang, Y.; Hawthorne, S. B. *Anal. Chem.* **1997**, *69*, 5001.

(2) Ulrich, S. *J. Chromatogr. A* **2000**, *902*, 167.

(3) Pawliszyn, J. *Solid Phase Microextraction: Theory and Practice*; Wiley-VCH: New York, 1997.

(4) Scheppers Wercinski, S. S.; Dekker, M., Eds. *Solid phase microextraction: a practical guide*: New York, 1999.

(5) Louch, D.; Motlagh, S.; Pawliszyn, J. *Anal. Chem.* **1992**, *64*, 1187.

(6) Potter, D. W.; Pawliszyn, J. *Environ. Sci. Technol.* **1994**, *28*, 298.

(7) Stahl, D. C.; Tilotta, D. C. *Environ. Sci. Technol.*, **1999**, *33*, 814.

(8) Bernhard, M. J.; Simonich, S. L. *Environ. Sci. Technol.* **2000**, *19*, 1705.

(9) Achten, C.; Puttmann, W. *Environ. Sci. Technol.* **2000**, *34*, 1359.

(10) Magbanua, B. S.; Mitchell, D. R.; Fehniger, S. M.; Bowyer, R. L.; Grady, C. P. L. *Water Environ. Res.* **2000**, *72*, 98.

(11) Mayer, P.; Vaes, W. H. J.; Wijnker, F.; Legierse, K. C. H. M.; Kraaij, R.; Tolls, J.; Hermens, J. L. M. *Environ. Sci. Technol.* **2000**, *34*, 5177.

(12) Poerschmann, J. *J. Microcolumn Sep.* **2000**, *12*, 603.

(13) Zeng, E. Y.; Noblet, J. A. *Environ. Sci. Technol.* **2002**, *36*, 3385.

(14) Yuan, H.; Ranatunga, R.; Carr, P. W.; Pawliszyn, J. *Analyst* **1999**, *124*, 1443.

(15) Mayer, P.; Vaes, W. H. J.; Schwarzenbach, R. P. *Analyst* **2002**, *127*, 42.

(16) Vaes, W. H. J.; Urrestarazu Ramos, E.; Verhaar, H. J. M.; Seinen, W.; Hermens, J. L. M. *Anal. Chem.* **1996**, *68*, 4463.

(17) Heringa, M. B.; Pastor, D.; Algra, J.; Vaes, W. H. J.; Hermens, J. L. M. *Anal. Chem.* **2002**, *74*, 5993.

(18) Ai, J. *Anal. Chem.* **1997**, *69*, 1230.

(19) Chen, Y.; Pawliszyn, J. *Anal. Chem.* **2004**, *76*, 5807.

(20) Poerschmann, J.; Kopinke, F.-D.; Pawliszyn, J. *Environ. Sci. Technol.* **1997**, *31*, 3629.

(21) Hanna, G. J.; Noble, R. D. *Chem. Rev.* **1985**, *85*, 583.

(22) Danesi, P. R.; Chiarizia, R. *CRC Crit. Rev. Anal. Chem.* **1980**, *10*, 1.

(23) Laddha, G. S.; Degaleesan, T. E. *Transport phenomena in liquid extraction*; Tata McGraw-Hill: New Delhi, 1976.

(24) Tarasov, V. V.; Yogodin, G. A. *Ion exchange and solvent extraction*; Marcel Dekker: New York, 1988.

(25) Davies, J. T.; Rideal, E. K. *Interfacial phenomena*; Academic press: New York, 1961.

(26) Pratt, H. R. *Handbook of solvent extraction*; Wiley: New York, 1983.

(27) Cussler, E. L. *Diffusion: Mass transfer in fluid systems*; Cambridge University Press: Cambridge, 1984.

(28) vanEijkeren, J. C. H.; Heringa, M. B.; Hermens, J. L. M. *Analyst* **2004**, *129*, 1137.

Chapter 6
Numerical Simulation of Solid Phase Microextraction in Aqueous Sample Analysis Using COMSOL Multiphysics

6.1 Introduction

Solid phase microextraction (SPME), a novel sample preparation and sampling technique, has been widely used in water sample analysis. [1-8] SPME can be performed in three basic modes: headspace extraction, direct extraction and membrane-protected extraction. For the target analytes with low Henry coefficients and low diffusion coefficients in the membrane, like polycyclic aromatic hydrocarbons (PAHs), it is suggested to use a direct extraction mode to achieve good sensitivity in a reasonable extraction period. In the direct extraction mode, the coated fiber is inserted into the sample and the analytes are transported directly from the sample matrix into the extracting phase. To facilitate rapid extraction, some level of agitation is required to transport analyte from the bulk of the solution to the vicinity of the fiber. To evaluate the performance of SPME direct extraction of organic pollutants in environmental aqueous samples, it is necessary to have a thorough understanding of the flow pattern and kinetics of SPME under different conditions.

Until now, the kinetics of SPME has been studied based both on costly laboratory experimentation [9, 10] and simplified mathematical models. [9, 11-15] In kinetic modelling, the models are often over-simplified by ignoring mass and heat transfer complexities. However, increased computation capabilities and advances in the application of numerical techniques have opened up possibilities to include all transport steps in kinetic modelling. The availability of *a priori* numerical prediction can make the complex fluid and thermodynamic processes transparent to the researchers. An understanding of the fundamentals of thermodynamics and mass transfer will provide insight and direction when developing methods and identifying parameters for rigorous control and optimization.

Effective use of the theory minimizes the number of experiments that need to be performed. As an alternative to the expensive and time-consuming experimental approach, numerical simulation is being widely used to provide fast and economical solutions to flow and mass transfer problems.

The aim of the current study is to investigate mass transfer characteristics as well as flow patterns in the extraction process of SPME using COMSOL Multiphysics, and to determine the influence of the important variables on the kinetics of SPME direct extraction, which includes physicochemical properties of the analyte, physical dimensions of the fiber, the presence of binding matrix in the sample and flow velocity. Numerical simulations were performed in two-dimensional steady state and time-dependent configurations. The mass and momentum balance equations were solved with the finite volume method using commercial software COMSOL Multiphysics 3.3.

6.2 Introduction to COMSOL

COMSOL Multiphysics is a state-of-the-art software package, which offers a powerful interactive environment for modelling and solving different types of scientific and engineering problems such as fluid flow, heat transfer and chemical reactions, based on partial differential equations (PDEs) in one or more physical domains simultaneously. These functions are accessible through an interactive graphical user interface for problem definition, computation and graphical post-processing.

6.2.1 Solution Technique

COMSOL Multiphysics models a wide range of phenomena by solving the conservation equations for mass, momentum, energy and chemical species. A finite volume scheme is used to solve the equations for interpolation between grid points and to calculate the derivatives of the flow variables. The set of discretised algebraic equations is solved by semi-implicit iterative scheme.

6.2.2 Program Structure

Figure 6-1 shows the organizational structure of COMSOL Multiphysics.

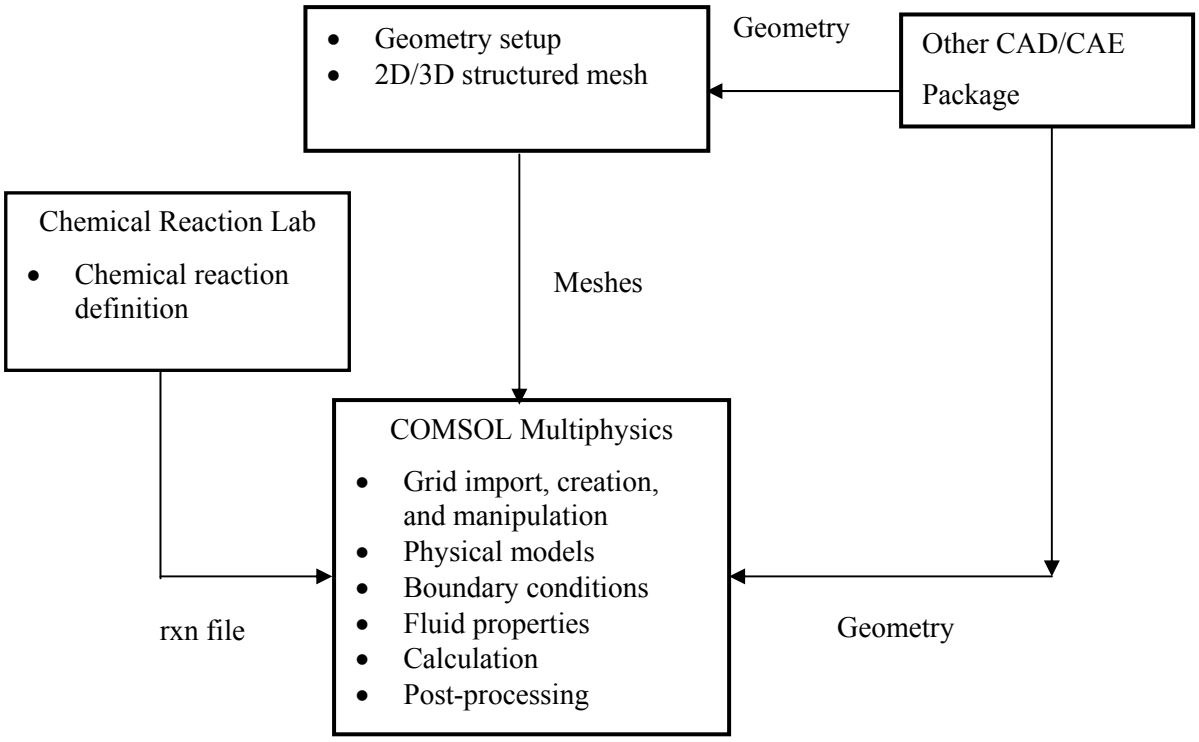

Figure 6-1 Structure of COMSOL Multiphysics.

In the present study, the geometry with meshes was built in COMSOL Multiphysics directly. In the case of binding matrix study, the association and dissociation reaction between the analyte and binding matrix was input in Chemical Reaction Lab and transported to the COMSOL Multiphysics thereafter.

6.2.3 Outline of Procedures in COMSOL Multiphysics

Generally, the steps followed to solve a problem in COMSOL Multiphysics are:

- Definition of the geometry
- Definition of the physics in the volume and at the boundaries

- Meshing
- Solving
- Postprocessing
- Parametric studies

According to these procedures described above, the numerical simulation of SPME direct extraction was achieved by using COMSOL Multiphysics in the current study.

6.3 Model Definition

6.3.1 Geometry and Mesh

Two different geometries were built to simulate the scenarios: (1) fiber extraction in a static sample solution; and (2) fiber extraction in a flow-through system. In static sample solution, it is assumed that there are no angular gradients present in SPME direct extraction, a two-dimensional axisymmetric structure was built to save the computational time.

To establish an optimum simulation scheme, it is necessary to confirm that the calculation was independent of the grid size. When too fine a mesh was used, it may take too long to obtain a converged result or sometime the solution did not converge after a particular level and the residuals kept fluctuating. On the other hand, very coarse mesh did not capture the flow field accurately due to the lack of resolution. For simplicity, quadrilateral grids and triangular grids were built for the static sample system and flow-through system, respectively. The final mesh was confirmed by doubling the total number of cells without notifying the change of the simulation results. The schematic diagrams of meshes generated were displayed in Figure 6-2 and 6-3, respectively.

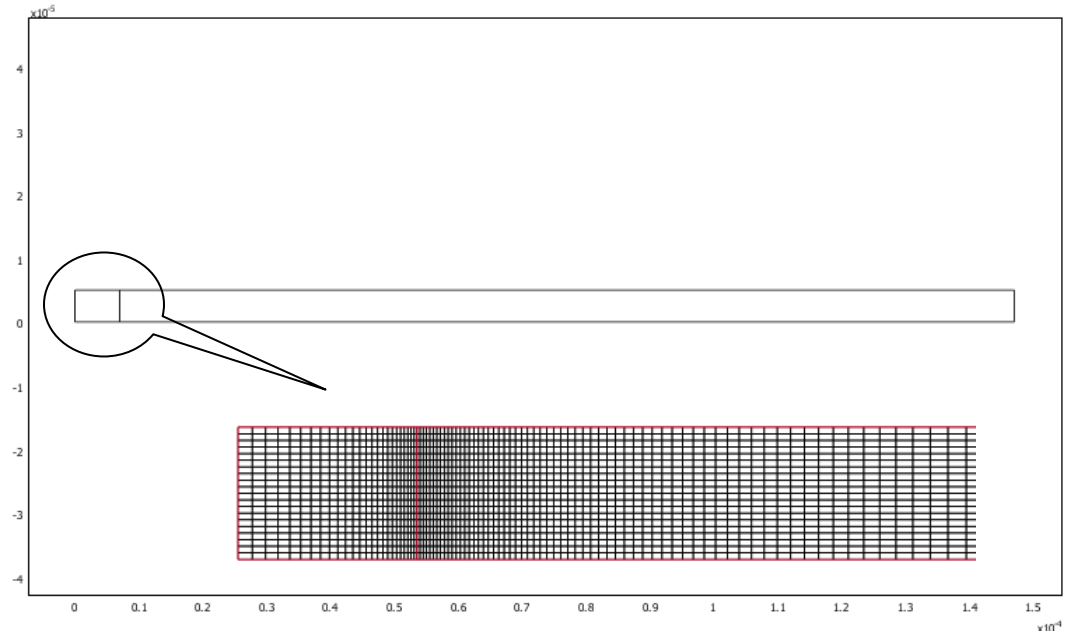

Figure 6-2 Schematic diagram of model domain and mesh generated for static sample.

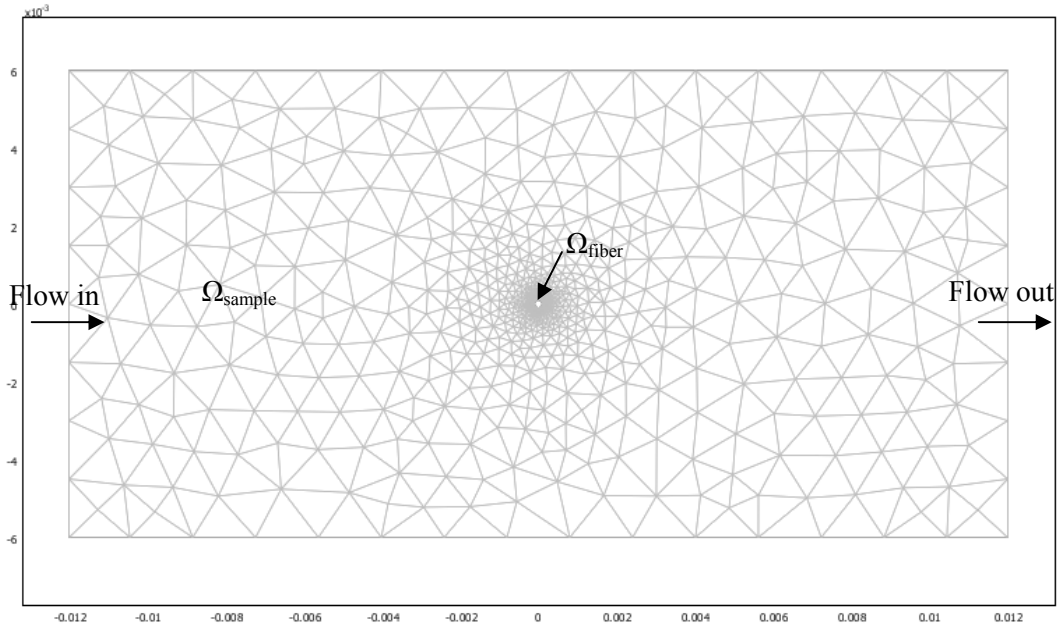

Figure 6-3 Schematic diagram of model domain and mesh generated for flow-through system.

6.3.2 Domain Equations

The physics models used to describe SPME extraction are:

- Convection and diffusion in sample matrix
- Diffusion of analytes in SPME fiber coating
- Incompressible Navier-Stokes equation: normal flow to the fiber
- Reaction association and dissociation between the analyte and binding matrix when a binding matrix is present

6.3.2.1 Convection and Diffusion

The analyte is transported by diffusion and convection in the aqueous phase, whereas diffusion is the only transport mechanism in the fiber coating. The following mass balances can be formulated to describe the time-dependant system:

$$\frac{\partial C_s}{\partial t} + \nabla \cdot \left(- D_s \nabla C_s + C_s \mathbf{u} \right) = 0 \qquad \text{in } \Omega_{\text{sample}} \qquad \text{Equation 6.1}$$

$$\frac{\partial C_f}{\partial t} + \nabla \cdot \left(- D_f \nabla C_f \right) = 0 \qquad \text{in } \Omega_{\text{fiber}} \qquad \text{Equation 6.2}$$

where C_s and C_f denote the concentrations of the analyte (mol m^{-3}) in the aqueous phase and fiber coating, respectively. D_s is the diffusion coefficient (m^2 s^{-1}) in the aqueous phase, and D_f is the diffusion coefficient in the fiber coating, while **u** denotes the velocity vector in the aqueous phase.

The analyte will dissolve from the sample matrix into the fiber coating to be extracted. The concentration distribution between the liquid and extraction phases is described by the distribution coefficient, K_{fs} :

$$K_{fs} = \frac{C_f}{C_s'} \qquad \text{Equation 6.3}$$

A schematic concentration profile is shown in Figure 6-4. As there will be discontinuities in the concentration profile at the boundaries between liquid and extraction phases, the stiff-spring method is applied to set a special type of boundary condition to obtain continuous flux over the phase boundaries. Instead of defining Dirichlet concentration conditions according to the distribution coefficient, K_{fs}, which would destroy the continuity of the flux – the continuous flux conditions are defined, at the same time, to force the concentrations to the desired values:

$$\left(D_f \nabla C_f\right) \cdot \mathbf{n} = M' \left(K_{fs} C_s - C_f\right) \qquad \text{at } \Omega^{f/s} \qquad \text{Equation 6.4}$$

$$\left(-D_s \nabla C_s + C_s \mathbf{u}\right) \cdot \mathbf{n} = M' \left(C_f - K_{fs} C_s\right) \qquad \text{at } \Omega^{s/f} \qquad \text{Equation 6.5}$$

where M' is a large enough number to let the concentration differences in the brackets approach zero. Equation 6.3 will thereby be satisfied. In this specific case, M' is set as 10000, which is sufficiently large to give continuity in flux.

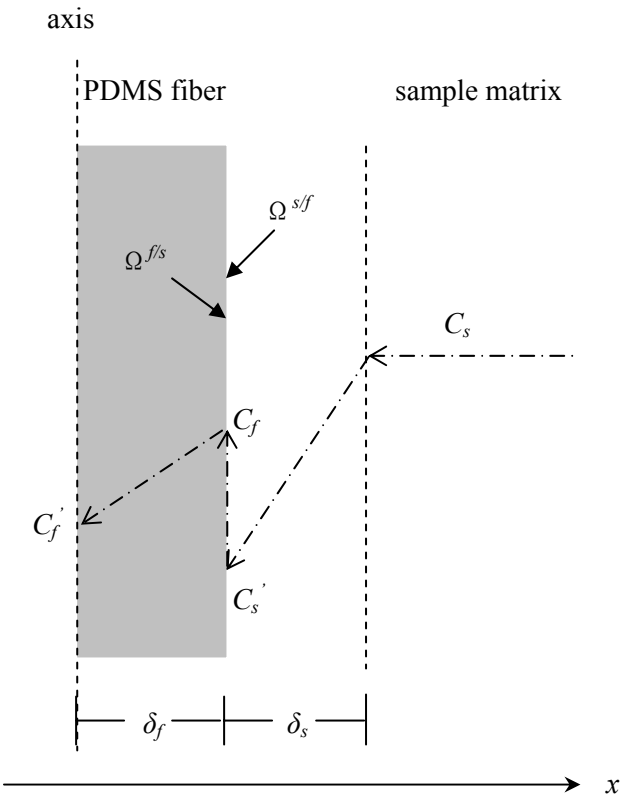

Figure 6-4 Schematic representation of the concentration profile at the phase boundary due to the partition. C_s is the concentration of the analyte in the sample matrix and $C_s^{'}$ is the concentration of the analyte in the boundary layer at the interface of the boundary layer and fiber coating ($\Omega^{s/f}$). C_f is the concentration of the analyte in the fiber coating at the interface of the fiber coating and boundary layer ($\Omega^{f/s}$), $C_f^{'}$ is the concentration of the analyte at the axis of the fiber.

The concentration boundary condition was defined for the outer cylinder boundary in the domain of sample matrix according to:

$$C = C_s^0 \qquad \text{Equation 6.6}$$

where C_s^0 is the initial concentration of the target analyte in sample matrix.

In the domain of sample matrix, it is assumed that there is no transport at the horizontal insulation/symmetry boundaries:

$$\left(-D_s \nabla C_s + C_s \mathbf{u}\right) \cdot \mathbf{n} = 0 \qquad \text{Equation 6.7}$$

It also assumes symmetry at the horizontal boundaries of the fiber coating in the domain of fiber coating:

$$\left(D_f \nabla C_f\right) \cdot \mathbf{n} = 0 \qquad \text{Equation 6.8}$$

6.3.2.2 Navier-Stokes Equations

The Navier-Stokes equations are the fundamental partial differential equations that describe the motion of incompressible fluids. They can be expressed as:

$$\rho \frac{\partial \mathbf{u}}{\partial \mathbf{t}} - \nabla \cdot \eta\left(\nabla \mathbf{u} + \left(\nabla \mathbf{u}\right)^T\right) + \rho \mathbf{u} \cdot \nabla \mathbf{u} + \nabla p = \mathbf{F} \qquad \text{Equation 6.9}$$

$$\nabla \cdot \mathbf{u} = \mathbf{0} \qquad \text{Equation 6.10}$$

where η denotes the dynamic viscosity (M L^{-1} T^{-1}), $\mathbf{u}$ is the velocity vector (L T^{-1}), ρ is the density of the fluid (M L^{-3}), p is the pressure (M L^{-1} T^{-2}) and $\mathbf{F}$ is a body force term (M L^{-2} T^{-2}).

6.3.2.3 Reaction Association and Dissociation between the Target Analyte and Binding Matrix

When there is a binding matrix like humic organic matter present in the sample matrix, the association and dissociation between the freely dissolved analyte and the binding matrix in the sample matrix domain is given as:

$$S + B \underset{k_{dis}}{\overset{k_{as}}{\rightleftharpoons}} BS$$

where S is freely dissolved analyte, B represents the binding matrix, BS is the bound species, k_{as} is the rate constant for the association reaction and k_{dis} is the rate constant for the dissociation reaction.

The material balance for the domain of sample matrix, including convection, diffusion and the reaction rate expression for the bound species, C_{bs}, is:

$$\frac{\partial C_{bs}}{\partial t} + \nabla \cdot \left(- D_{bs} \nabla C_{bs} + C_{bs} \mathbf{u} \right) = k_{as} C_s C_b - k_{dis} C_{bs} \qquad \text{Equation 6.11}$$

where D_{bs} represents diffusion coefficient of the bound species in the sample matrix.

The equation for the reaction expression includes the concentration of the bulk species, c_s. Thus, the equation for the reaction in combination with the mass balance in the bulk must be solved.

6.3.3 Set-up of Problem

After generating the geometry and mesh as well as defining the physics models for the simulation, the properties of the sample matrix and fiber coating need be input before starting solving the problem. Table 6-1 lists the properties of sample matrix and fiber coating, as well as the physicochemical properties of pyrene, which is used as the target compound in the simulation.

Table 6-1 Input data used in the model

Property	Static sample	Flow-through system
δ_{fiber} (μm)	7	100
Concentration of analyte (mM)	1.485×10^{-4}	9.96×10^{-6}
log K_{fs}	4.65	4.65
D_s (m^2/s)	6.59×10^{-10}	6.59×10^{-10}
D_f (m^2/s)	1.51×10^{-11}	1.51×10^{-11}

6.4 Results and Discussion

6.4.1 Static Pure Aqueous Solution

6.4.1.1 Steady State Analysis

The SPME direct extraction in a pure static aqueous solution was first studied and the initial analysis was conducted using the stationary solver. The grid size of quadratic grids of 150 x 20 = 3000 cells was applied in the simulation. The solution time was within 40 seconds. Figure 6-5 represents the concentration distribution of the analyte in the fiber coating. The analyte concentration is constant in the whole domain of fiber coating, which indicates that the equilibrium has been reached. The concentration of analyte in the fiber coating at the steady state is 6.633 mol/m^3.

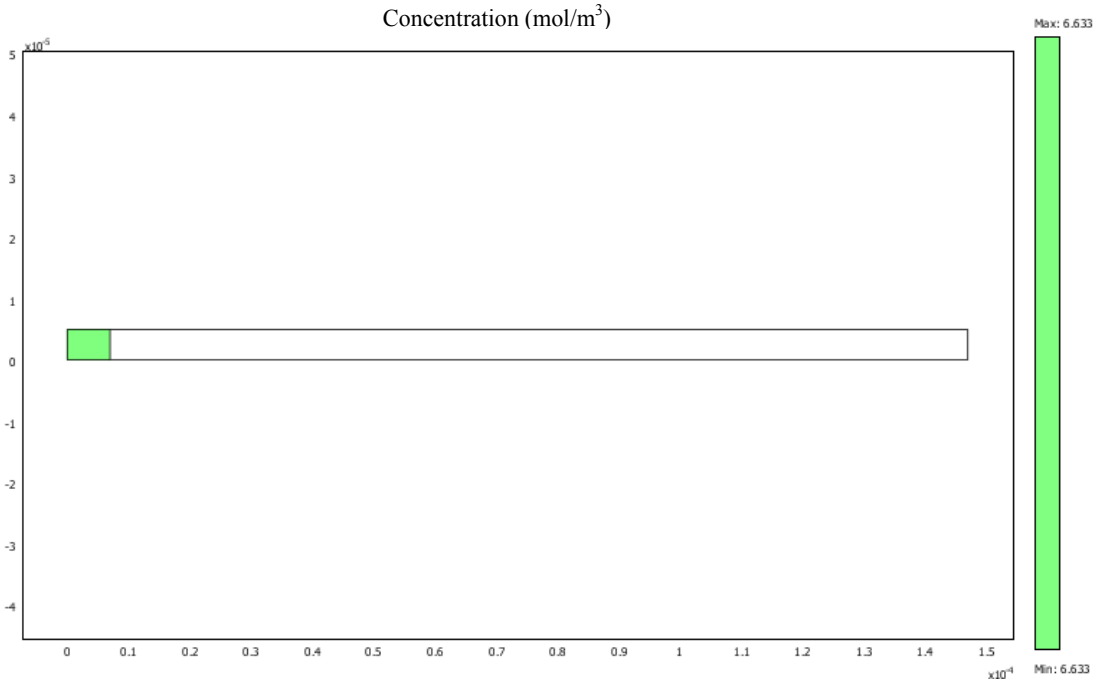

Figure 6-5 Surface concentration profile in the fiber coating at steady state.

6.4.1.2 Time-dependant Analysis

Time-dependant analysis was also conducted on the same case in order to investigate the kinetics of SPME direct extraction. Figures 6-6 – 6-9 display the surface concentration profile in the fiber coating at different extraction time points: 0.01 s, 1 s, 60 min and 14 hr. The figures clearly indicate the process of diffusion of the analyte to the fiber coating along with the time. It is observed that the longer extraction time, the deeper the analyte diffused into the fiber coating. At the extraction time of 5 hrs, equilibrium is already reached in the system with a fiber coating concentration at 6.485 mol/m^3.

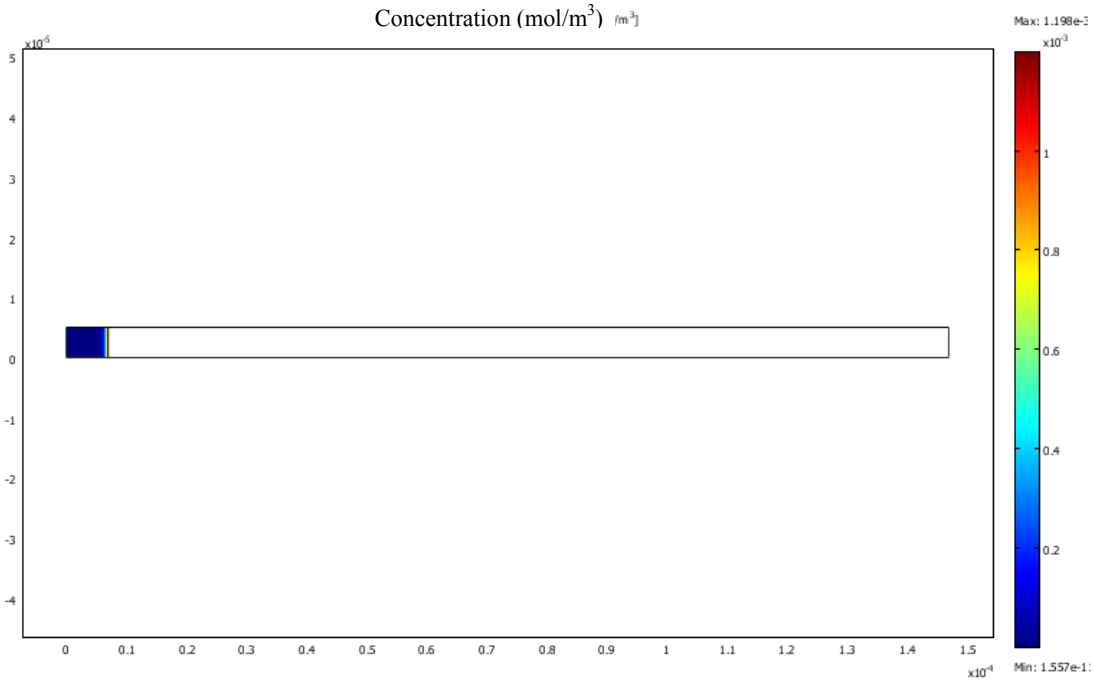

Figure 6-6 Surface concentration profile on the fiber coating at t = 0.01 s.

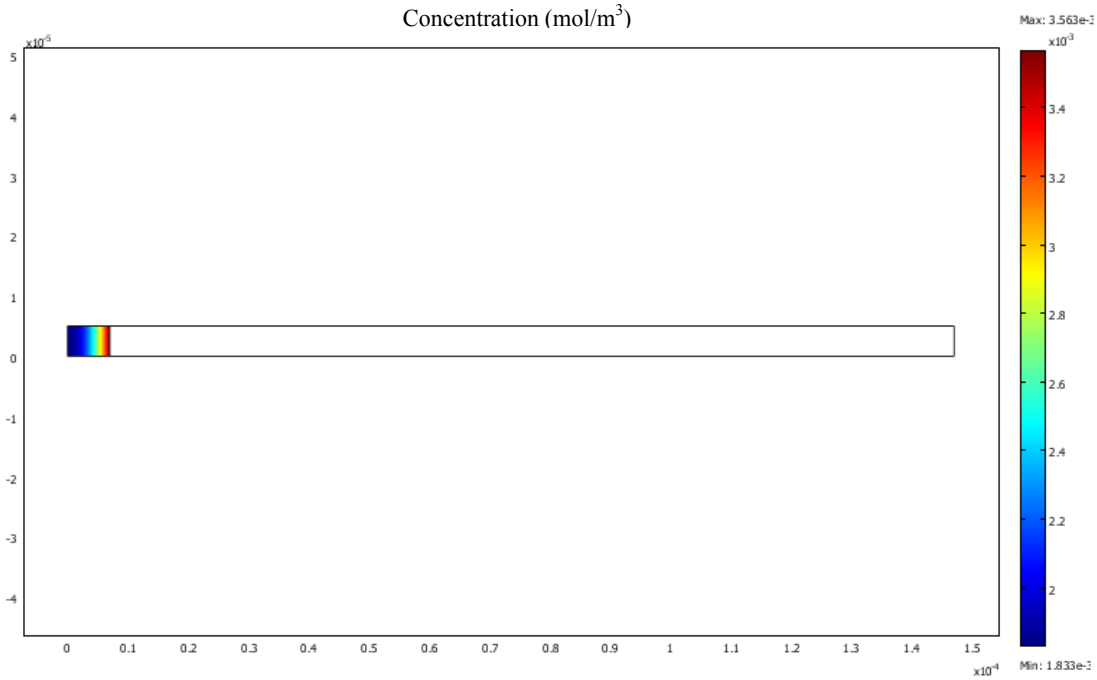

Figure 6-7 Surface concentration profile on the fiber coating at t = 1 s.

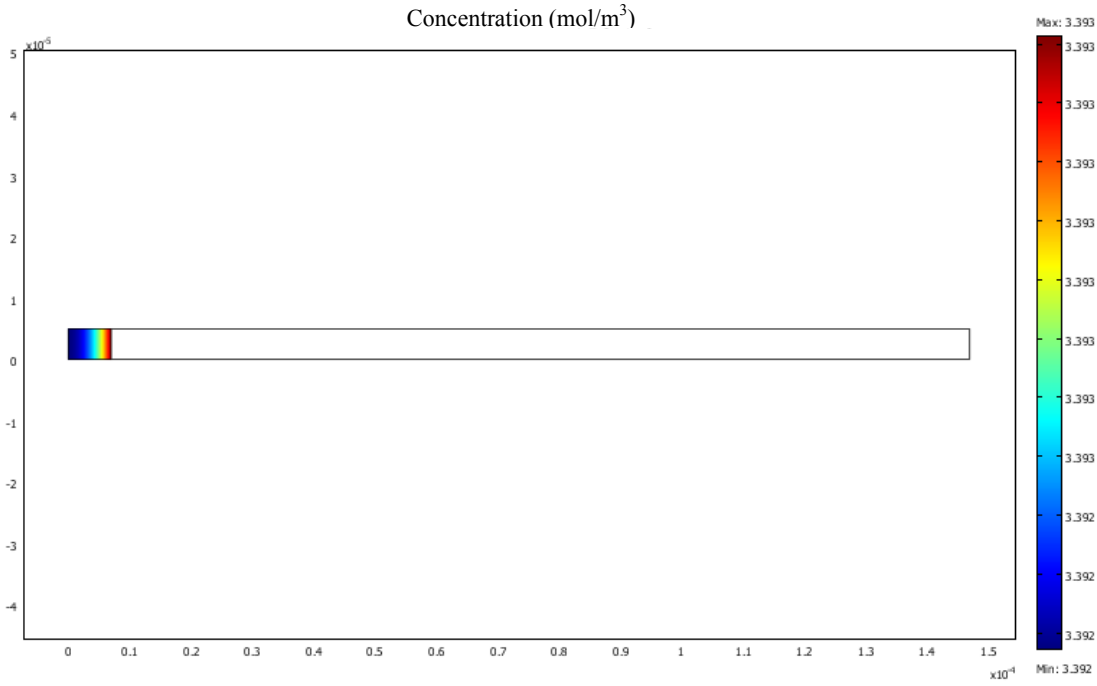

Figure 6-8 Surface concentration profile on the fiber coating at t = 60 min.

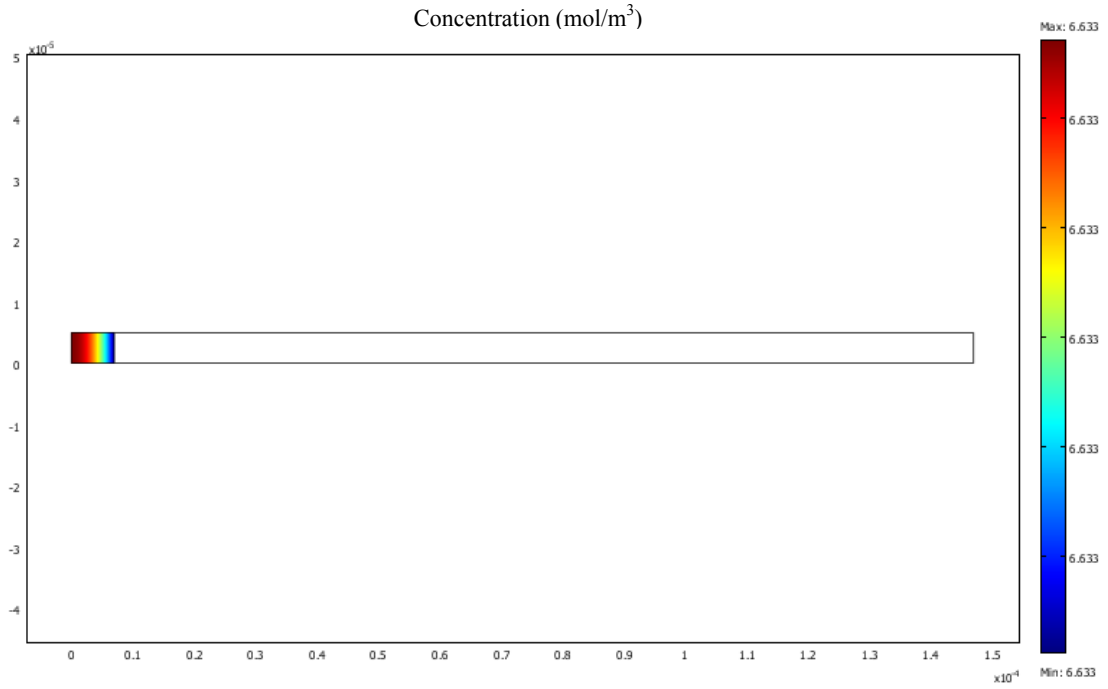

Figure 6-9 Surface concentration profile on the fiber coating at t = 14 hr.

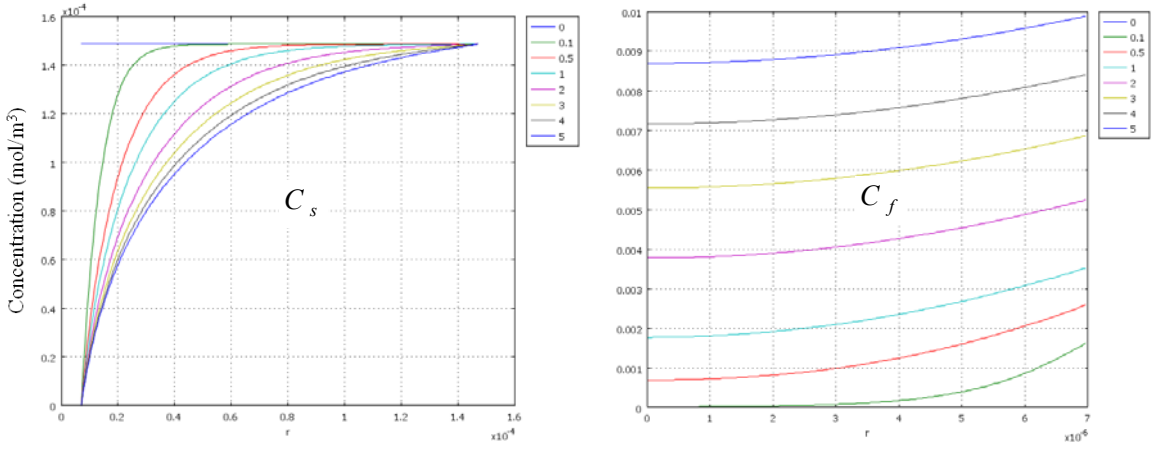

Figure 6-10 Concentration distribution profile in sample (C_s) and in fiber coating (C_f) at different extraction times from 0 to 5 s.

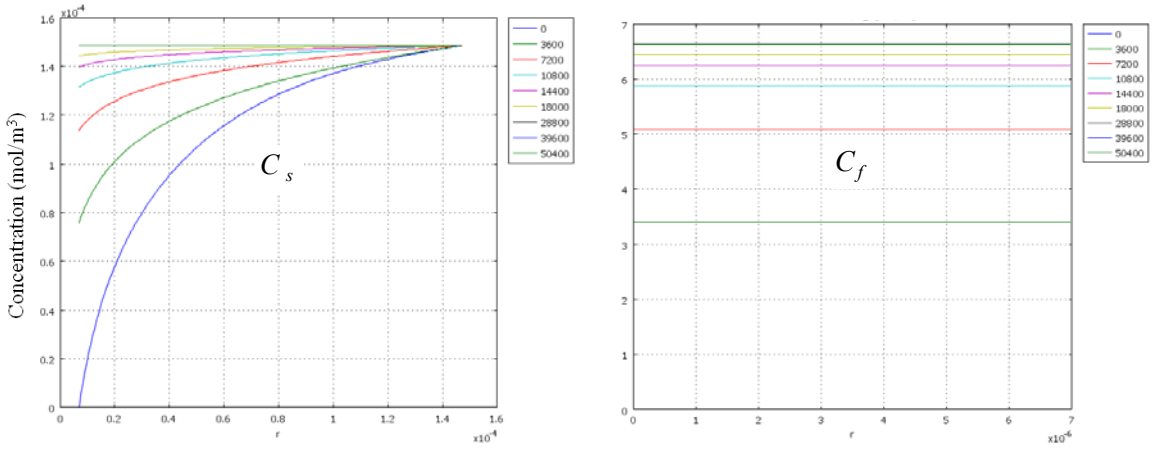

Figure 6-11 Concentration distribution profile in sample (C_s) and in fiber coating (C_f) at different extraction times from 0 to 15 hrs.

The analyte concentration profile along the x direction in the sample and fiber coating at different extraction times are displayed in Figures 6-10 and 6-11. At the beginning of the extraction, the analyte concentration in the sample at the interface of the fiber coating and sample matrix drops dramatically due to the fast extraction and slow diffusion of the analyte from the bulk. With the increase of the extraction time, the equilibrium will finally be reached and there is no gradient of concentration in both the sample matrix and the fiber coating. The above two figures also indicate that there is no significant concentration gradient in the fiber coating even at the very beginning of the extraction (few seconds after extraction starts). On the other hand, the concentration gradient in the sample matrix keeps changing and gets to be stabilized after several hours. The results indicate that the extraction is controlled by the diffusion in the boundary layer at the current condition. The diffusion of the analyte in the fiber coating is not the controlling step to determine the kinetics of SPME direct extraction in static aqueous samples.

6.4.1.3 Effect of Extraction Parameters and Conditions

The effects of certain extraction conditions and parameters on partitioning can be predicted by COMSOL easily without performing the experimental trial. The result can be used to optimize the extraction conditions with a minimum number of experiments. Extraction conditions that affect SPME performance studied here include distribution coefficient K_{fs}, thickness of fiber coating and the presence of binding matrix.

6.4.1.3.1 Distribution Coefficient K_{fs}

The effect of distribution coefficient K_{fs} on the extraction performance was simulated using COMSOL. Figure 6-12 presents the simulated extraction profiles of the compounds characterized by log K_{fs} as 2.65, 3.65 and 4.65 from a static aqueous solution. During the extraction, the concentration of analyte in the thin layer of sample close to the water/coating interface is lower compared to the bulk concentration due to the depletion of analyte by the fiber coating. The transport of analyte from the progressively thicker depleted layer to the fiber coating determines the overall extraction speed. The higher distribution coefficient, the greater the amount of analyte that will be extracted by the fiber coating, resulting in substantially slower equilibrium because the analytes need more time to be transported to the vicinity of the fiber. The equilibrium time for log K_{fs} = 4.65 is about 24000 s, while for log K_{fs} = 2.65 it corresponds to only 240 s, which is 100-times faster, closely matching the ratio of appropriate distribution coefficients.

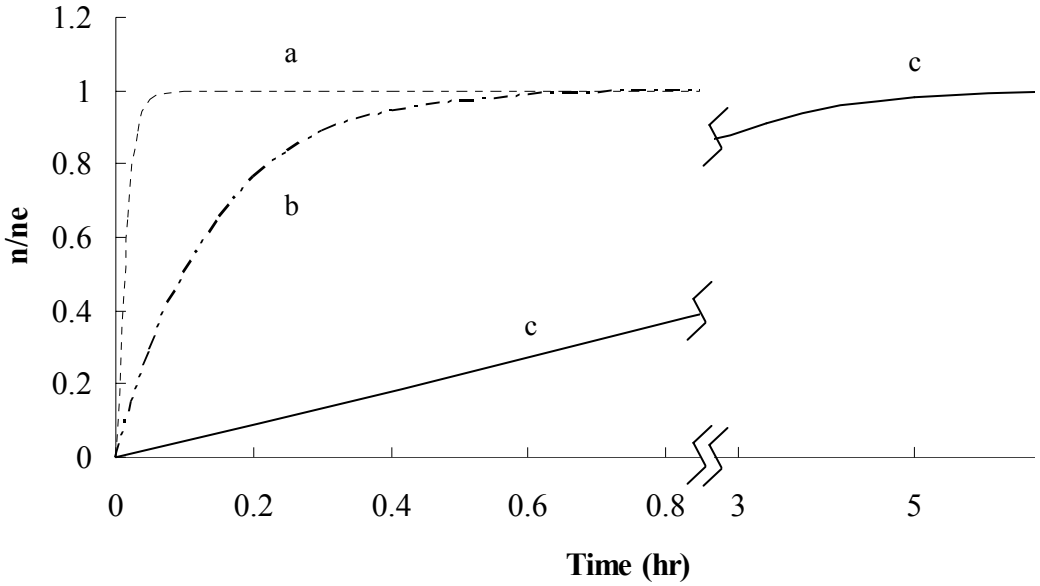

Figure 6-12 Extraction profile with different distribution coefficients. (a) log K_{fs} = 2.65, (b) log K_{fs} = 3.65 and (c) log K_{fs} = 4.65.

6.4.1.3.2 Thickness of Fiber Coating

Three different fiber coating thicknesses were simulated to evaluate the effect of fiber coating thickness using COMSOL Multiphysics: 7 μm, 14 μm and 35 μm. Their extraction profiles are compared in Figure 6-13. As expected, the equilibrium times are affected by the thickness of the fiber coating. The equilibrium time becomes much longer as around 72 hrs for the case with 35 μm coating compared to about 5 hrs and 18 hrs for the coatings of 7 μm and 15 μm, respectively. When the system reached equilibrium, the analyte concentrations in the fiber coating are constant with different fiber coating thickness. However, the sensitivity of thicker fiber coating is higher due to its larger extraction phase volume.

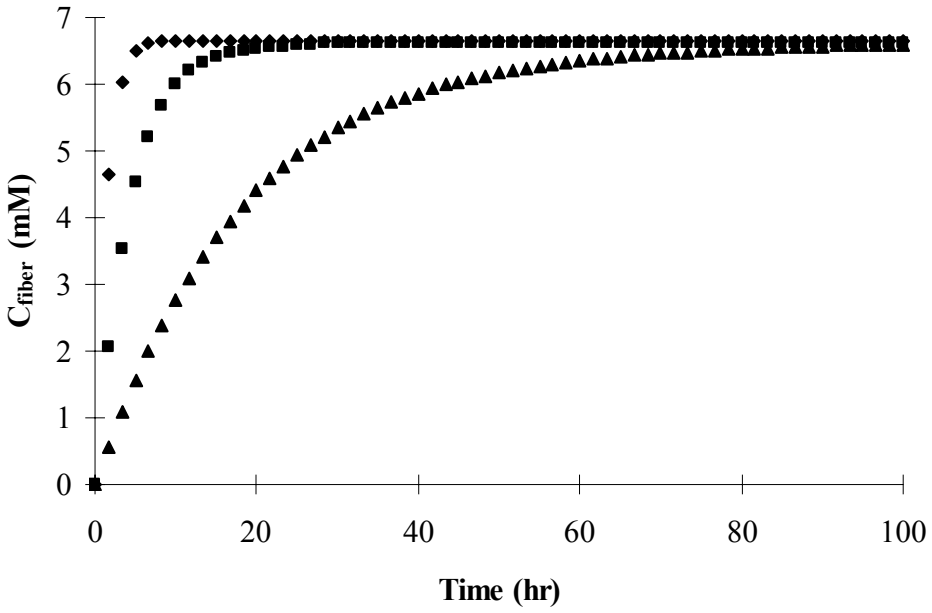

Figure 6-13 Extraction profiles with different thickness of fiber coatings. (◆) 7 μm, (■) 14 μm and (▲) 35 μm.

6.4.1.3.3 Effect of Binding Matrix

The effect of the presence of binding matrix on SPME direct extraction can also be examined using COMSOL by inputting the reaction parameters, such as association and dissociation constant or binding constant between the analyte and binding matrix. The parameters applied in the simulation are the same as listed in Table 6-1, the association constant and dissociation constant applied in the simulation are 3100 and 0.13, respectively.

Different scenarios were simulated: 1) same total concentration of target analyte in the sample systems with and without the presence of binding matrix. 2) same free concentration of target analyte in the sample systems with and without the presence of binding matrix. When the total concentrations are kept the same, the simulated results indicate that the extracted amount with the presence of binding matrix is much lower than the pure aqueous solution due to the sorption of analyte onto the binding matrix which subsequently decreases the free concentration of target analyte

in the aqueous solution. However, the extraction kinetics is not affect by the presence of the binding matrix when the same total concentration of analyte is applied. On the other hand, the presence of the binding matrix will shorten the equilibrium time when the free concentrations of analyte in the systems are kept the same. Figure 6-14 presents the extraction profiles of target compound in the systems with and without the presence of binding matrix with the same free concentration of analyte. The simulated results demonstrate that the kinetics of SPME extraction can be affected by the presence of binding matrix. This effect can be explained by the "boundary layer effect". The free dissolved analyte in the static layer around the fiber is depleted due to the extraction by the fiber coating. With the presence of binding matrix, analyte-binding matrix complexes diffuse from the sample bulk phase into the static layer around the fiber. Due to depletion of the analyte, analyte concentration in the boundary layer is compensated by desorption from the complexes, which will increase the overall extraction speed.

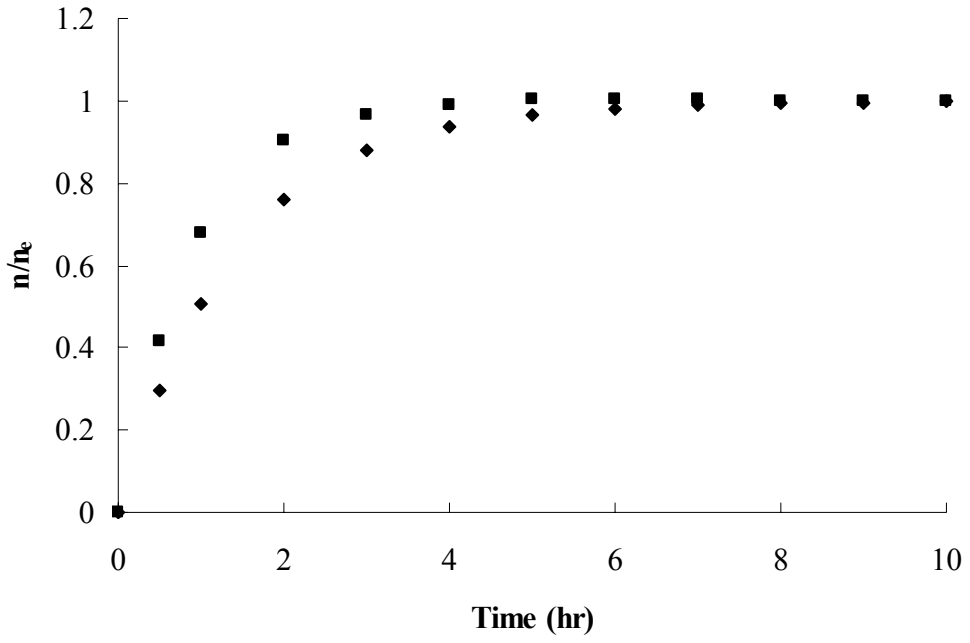

Figure 6-14 Extraction profiles in the sample matrix with the same free concentration of analyte. (■) with the presence of binding matrix; (◆) without the presence of binding matrix.

6.4.2 Flow - through System

In an open system or the laboratory built flow through system, the above simulation using two-dimensional sysmmetric model cannot fully represent the true situation. Therefore, the SPME extraction in a flow through aqueous system was investigated using the second model.

The geometry to simulate and the mesh generated are shown in Figure 6-3. The flow is introduced from the left side and exits from the right side. The extraction phase is a 100 μm thick fiber coating, which is coated onto an inner-fused silica rod. The initial concentration in the sample matrix is 9.9×10^{-6} mol/m^3 with a target compound of log $K_{fs} = 4.65$.

6.4.2.1 Flow Pattern

When a SPME fiber is exposed to a fluid sample whose motion is normal to the axis of the fiber in the bulk fluid surrounding, the diffusion layer around the fiber coating is of nonuniform thickness. The fluid is brought to rest at the forward stagnation point from which the boundary layer develops with increasing x under the influence of a favourable pressure gradient. Due to the nonuniform thickness of the boundary layer, nonsymmetrical concentration distribution along the surface of the fiber coating was expected. Figure 6-15 shows that the maximum velocity occurs in the region between the fiber and the symmetry lines of top and bottom. Meanwhile it can also be noticed that there are two stagnation zones in front of and behind the fiber.

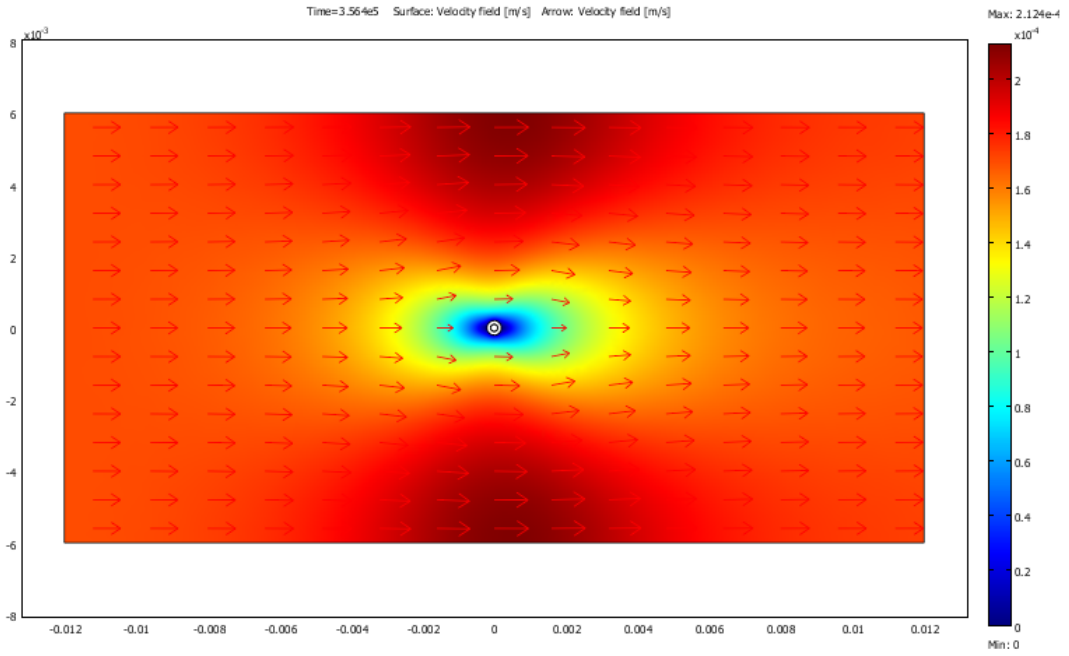

Figure 6-15 The flow pattern around the fiber coating. The colour bar represents the modulus of the velocity vector, while the arrows symbolize the flow velocity vector.

6.4.2.2 Effect of Flow Velocity

The time to reach equilibrium is greatly dependant on the thickness of the stagnant layer near the fiber coating. The thicker the boundary layer, which corresponds to the lower flow velocity passing the fiber or even static flow, the more time needed for the analyte to transport through the boundary layer to be extracted by the fiber coating. In this study, the effect of flow velocity on the kinetics of SPME is studied by applying three different velocities: 8.5×10^{-6} m/s, 8.5×10^{-5} m/s and 1.7×10^{-4} m/s. The extraction profiles at different velocities are compared in Figure 6-16. Figure 6-16 shows that the extraction is still in the linear range after 100 hrs' extraction at velocity of 8.5×10^{-6} m/s, which indicates that the extraction is still far from the equilibrium. The mass transfer rate is significantly increased by increasing the flow velocity from 8.5×10^{-6} m/s to 8.5×10^{-5} m/s. The

equilibrium time with flow velocity of 8.5×10^{-5} m/s is around 100 hrs comparing to about 50 hrs at 1.7×10^{-4} m/s, closely matching the ratio of appropriate flow velocities.

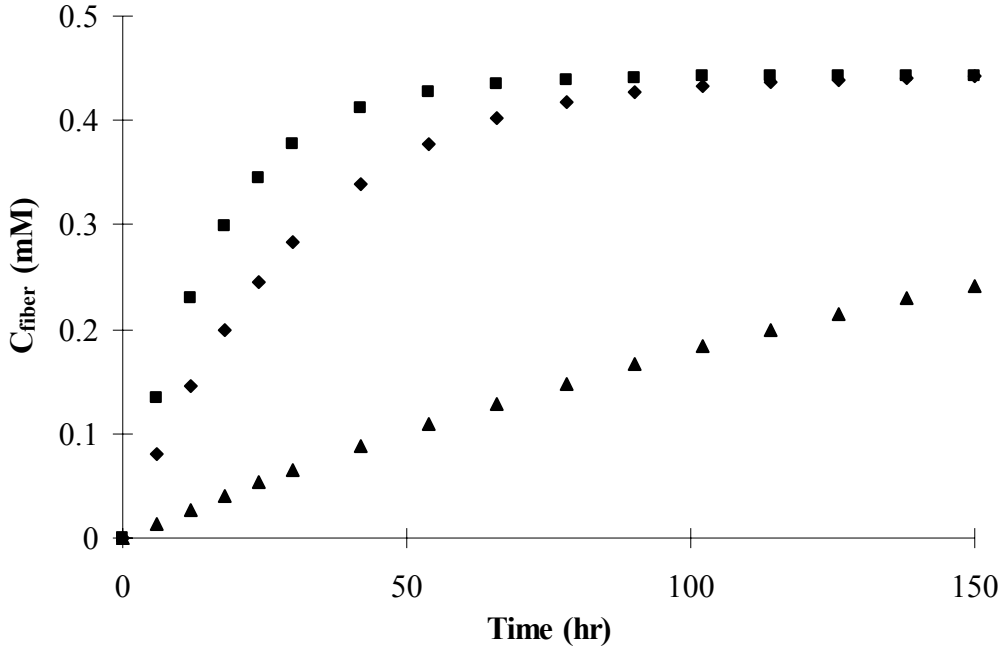

Figure 6-16 Extraction profiles at different flow velocities. (■) 1.7×10^{-4} m/s, (◆) 8.5×10^{-5} m/s and (▲) 8.5×10^{-6} m/s.

6.4.3 Comparison with Experimental Results

The extraction profile of pyrene using a 7 μm PDMS fiber was studied by experiment and COMSOL simulation. The experiment was performed in a static sample. The extraction profile created from the simulated results is compared with the experimental data in Figure 6-17. It can be observed from Figure 6-17 that the calculated results fit experimental data well with similar slope and shape of the curves. The equilibrium time in experiment is slightly longer than the predicted results. The discrepancy between these two sets of results can be attributed to the experimental error and the estimated parameters applied in the model such as distribution coefficient.

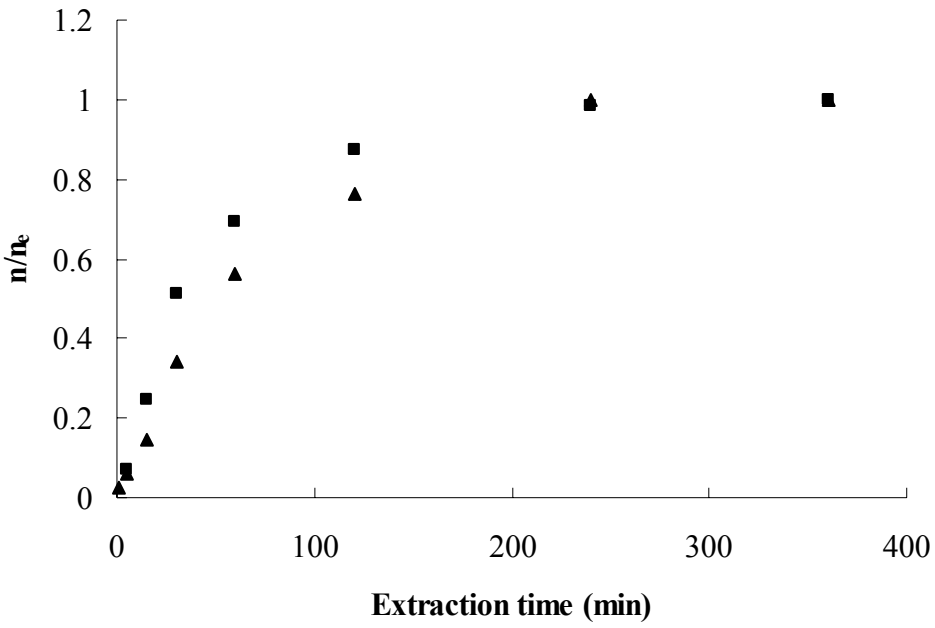

Figure 6-17 Comparison of extraction profiles from simulation results and experimental data. (■) simulation results and (▲) experimental data (Static sample).

Furthermore, the extraction profiles of pyrene by experiment and COMSOL simulation using a 100 μm PDMS fiber were also compared at a flow velocity of 8.5E-5 m/s, which is shown in Figure 6-18. The good agreement between the experimental and simulation results was also noticed. The extraction profiles are still in the linear range up to 3 hrs due to the thick fiber coating used.

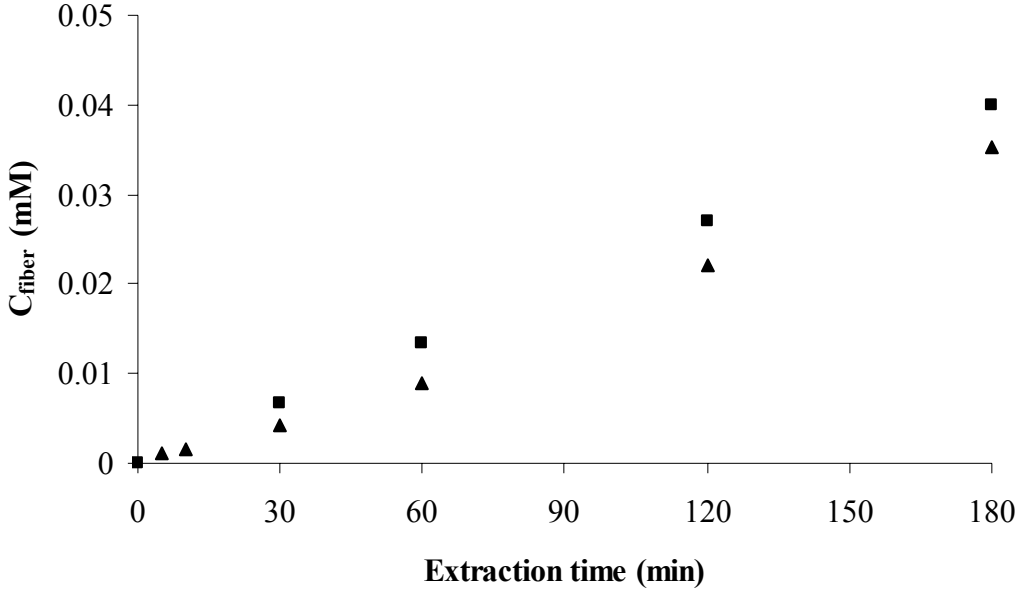

Figure 6-18 Comparison of extraction profiles from simulation results and experimental data. (■) simulation results and (▲) experimental data (Flow velocity = 8.5×10^{-5} m/s).

6.5 Conclusion

In this study, the exercise was successfully conducted in predicting complicated fluid dynamics and kinetics of SPME extraction in aqueous solution with COMSOL. The kinetics of SPME extraction is confirmed to be dependent on physicochemical properties of the target compounds, the fiber coating as well as the flow velocity around the fiber. The simulation results of COMSOL compare well with our experimental data. Overall, the results obtained from the computer modelling exercise have demonstrated that simulation using commercial software is a reliable and relatively inexpensive method of characterizing the performance of SPME. This method of analysis is almost certainly less expensive than experiment, and represents a cost-effective approach for experimental design optimization.

References

(1) Takino, M.; Daishima, S.; Nakahara, T. *Analyst* **2001**, *126*, 602.

(2) Ouyang, G.; Chen, Y.; Pawliszyn, J. *J. Chromatogr. A* **2006**, *1105*.

(3) Hirayama, Y.; Ohmichi, M.; Tatsumoto, H. *J. Health Sci.* **2005**, *126*, 602.

(4) Eisert, R. P., J. *Anal. Chem.* **1997**, *69*, 3140.

(5) Gou, Y.; Eisert, R.; Pawliszyn, J. *J. Chromato. A.* **2000**, *873*, 137.

(6) Gou, Y.; Pawliszyn, J. *Anal. Chem.* **2000**, *72*, 2774.

(7) Gou, Y.; Tragas, C.; Lord, H.; Pawliszyn, J. *J. Microcolumn Separations* **2000**, *12*, 125.

(8) Kataoka, H.; Mitani, K.; Takino, M. *Method Biotechnol* **2006**, *19*, 365.

(9) Pawliszyn, J. *Solid Phase Microextraction: Theory and Practice*; Wiley-VCH: New York, 1997.

(10) Pawliszyn, J. *Applications of Solid Phase Microextraction*; Royal Society of Chemistry: Cambridge, 1999.

(11) Dewulf, J.; VanLangenhove, H.; Everaert, M. *J. Chromato. A.* **1997**, *761*, 205.

(12) Vaes, W. H. J.; Urrestarazu Ramos, E.; Verhaar, H. J. M.; Seinen, W.; Hermens, J. L. M. *Anal Chem* **1996**, *68*, 4463.

(13) vanEijkeren, J. C. H.; Heringa, M. B.; Hermens, J. L. M. *Analyst* **2004**, *129*, 1137.

(14) Ai, J. *Anal. Chem.* **1997**, *69*, 1230.

(15) Sukola, K.; Koziel, J.; Augusto, F.; Pawliszyn, J. *Anal. Chem.* **2001**, *73*, 13.

Chapter 7
Summary

7.1 SPME in Aqueous Sample Analysis

SPME is a simple, solvent-free, and reliable microextraction technique that combines sampling, sample preparation, and preconcentration into a single step requiring no additional cleanup before chromatographic analysis. It is demonstrated in the previous chapters that SPME is a viable tool for sampling organic pollutants in water for both spot and TWA sampling.

The kinetic calibration method is a novel approach that has been developed for field sampling/sample preparation, in which an internal standard is preloaded onto a SPME fiber for calibration of the extraction of target analytes in field samples. The same method can also be used for in-vial sample analysis. In this study, different techniques to load the standard to a non-porous SPME fibre were investigated. It was found that the appropriateness of the technique depends on the physical properties of the standards that are used for the analysis. The main advantage of the different approaches investigated in this study is that the standard generation vials can be reused for hundreds of analyses without exhibiting significant loss. Moreover, the standard loading process can be performed automatically, which is more efficient and precise. The standard loading technique and in-fibre standardization method were applied to a complex matrix (milk) and the results illustrated that the matrix effect can be effectively compensated with this approach.

Spot sampling in water quality monitoring has considerable temporal and spatial limitations when assessing organic pollutants concentrations. A new SPME device, PDMS rod sampler, was developed as a passive sampler to determine the TWA concentrations of pollutants in the aqueous media. The calibration was achieved by using the on-rod standardization technique. The PDMS rod passive sampler benefits from the inherent advantages of the SPME approach: it incorporates

sampling, isolation and enrichment into one step. There are a few additional advantages to use a piece of PDMS rod as the extraction phase for sampling organic compounds like PAH in water: (1) simplicity and ease of deployment; (2) low cost; and (3) higher extraction efficiency or sensitivity due to large capacity. Rather, with this approach, TWA concentrations of target analytes can be obtained by one sampler, and can be analyzed directly, with no further sample preparation treatment required. The combination of SPME technique and kinetic calibration demonstrated that the new device is a successful quantitative technique for on-site sampling and sample preparation, where the composition of the sample matrix is very complicated, and/or the agitation of the sample matrix is variable or unknown.

The sorption of organic compounds to dissolved organic matter in water affects the fate of organic compounds and must be studied and well-understood in risk assessments of chemicals in the environment. The matrix effect caused by the sorption of the analyte to the matrix in the sample solution was investigated using SPME technique. The uptake kinetics was affected by the presence of matrix when the sample solutions with and without the binding matrix have the same free concentration. The effect can be ascribed to the desorption of analyte from the matrix in the stagnant water layer, where the transport of analytes to the fiber coating occurs only by diffusion. In the current study, both experiment and mathematical model has been proposed to investigate the kinetics of the absorption of SPME fiber in the sample matrices with HOM. The important influence of organic matter on SPME procedure was confirmed. Successful calibration of free and total concentration of analytes in complex sample matrix was accomplished by using SPME technique.

A new approach was presented in this study to study the kinetics of SPME direct extraction in aqueous sample analysis using a general-purpose CFD program called COMSOL Multiphysics. The simulation of flow pattern and extraction characteristics in SPME provides a better approach for understanding the complicated flow dynamics of the extraction process. The number of required

experimental trials is therefore reduced, while an economical design practice, greatly facilitated by the availability of *a priori* numerical predictions, clarifies complex fluid and thermo-dynamic processes for the researcher. Simulation results compared reasonably well with the experimental data. The results indicate a promising role of numerical simulation in designing experiments. However, it must be emphasized that, before relying on computed results, it is essential to carry out careful and systematic validation tests comparing the numerical predictions against experimental data.

7.2 Perspective

Future research in aqueous sample analysis using SPME should focus on:

- the sorption study of polar and ionized compounds and various binding matrices
- different coating applications

Far less knowledge is currently available on the sorption of the diverse group of polar and ionized compounds. The polar and ionic characteristics cause these compounds to adsorb to the binding matrix by various interactions, such as hydrogen bonding, electrostatic attraction, and surface reactions. These types of sorption interactions are likely to be more prominent than hydrophobic partitioning. Hence, the use of the SPME technique for those compounds requires further examination. Furthermore, more research must be performed into various binding matrix in order to develop a model that can handle the various chemical properties of the analyte and the binding matrix.

Since fall of 1996, Supelco has provided users with several coatings, which includes: liquid polymer coatings, (e.g., PDMS coatings of variable thicknesses and PA), and new mixed phases based on solid/liquid sorption, (e.g., Carbowax-DVB, PDMS-DVB and Carboxwax /TR). These coatings satisfy the needs of various organic compounds analysis in many applications. The PA phase is suitable for more polar compounds. Mixed phase coatings have complementary properties

compared with PDMS and PA. The majority of interactions are determined by the adsorption process in the porous coatings. For porous coating fibers, the extraction is completely controlled by the diffusion through the boundary layer, which could be used in conjunction with the kinetic calibration in water sampling, even at highly agitated conditions. The application of different coatings in aqueous sample analysis needs further investigation.

Appendix

(a)

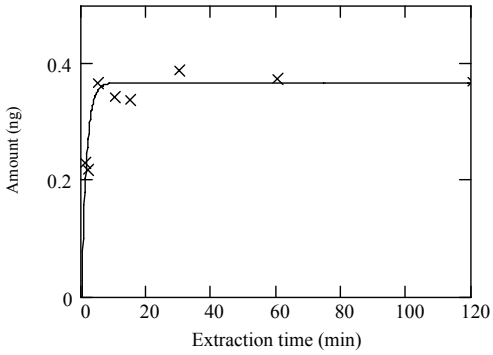

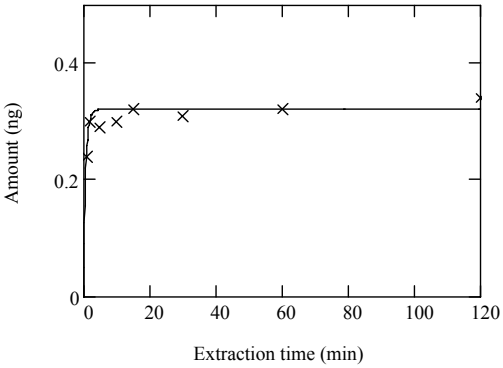

(b)

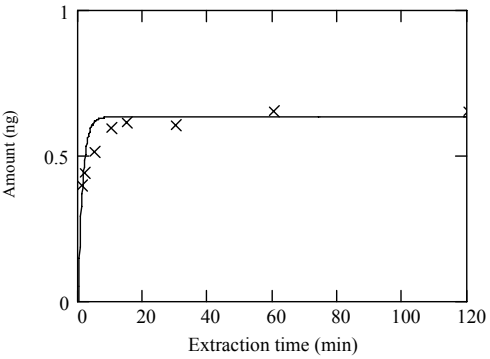

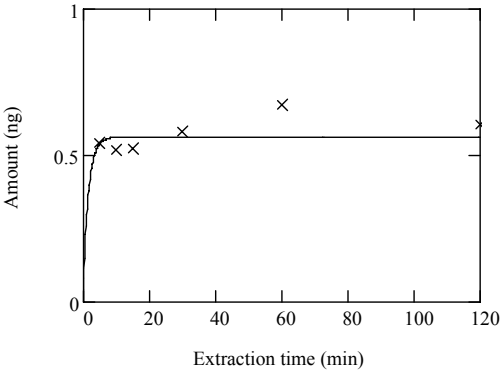

(c)

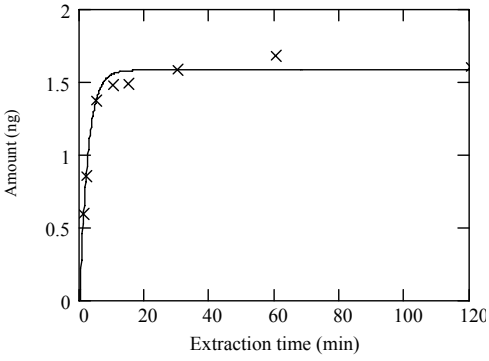

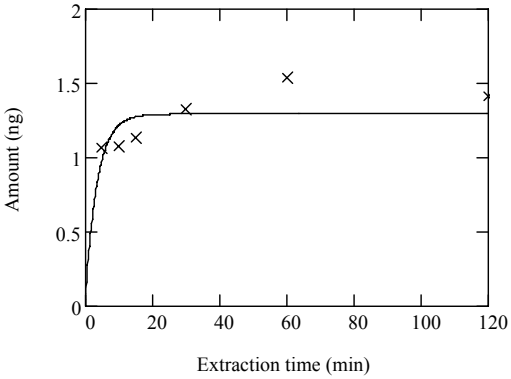

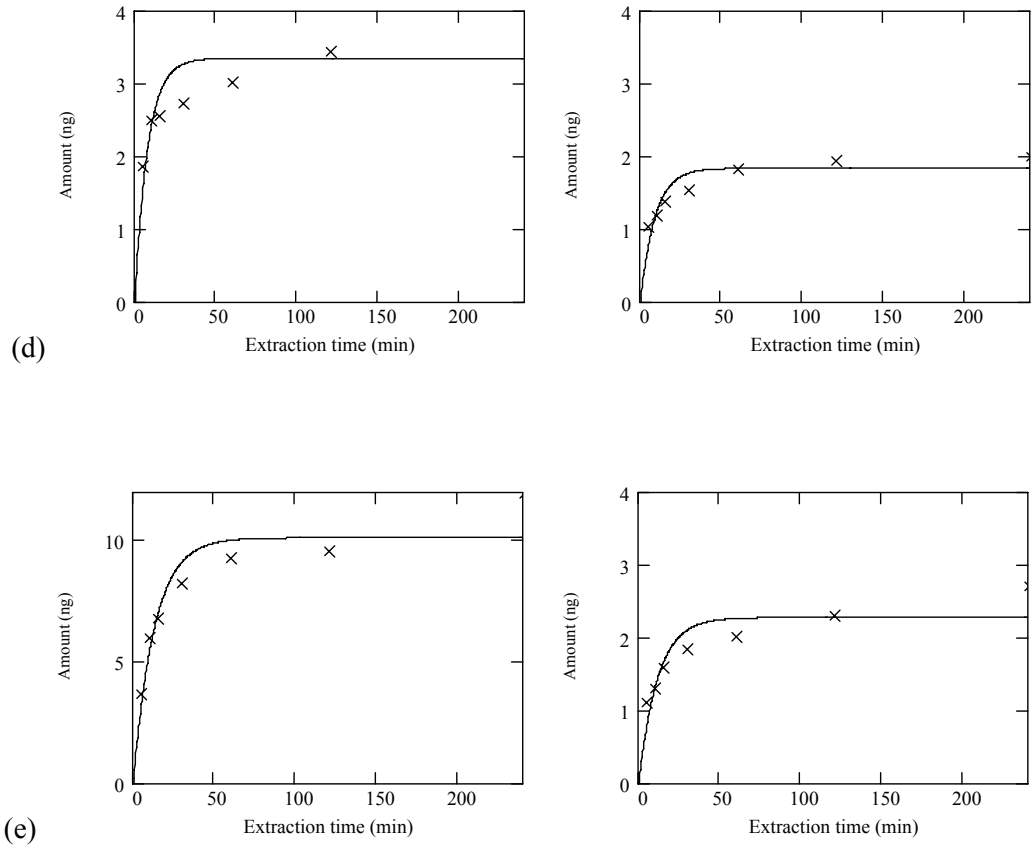

Appendix 1 Extraction profiles of PAH in aqueous solution with (right column) and without (left column) humic acid. (a) naphthalene; (b) acenaphthylene; (c) fluorene; (d) anthracene; and (e) pyrene.

(a)

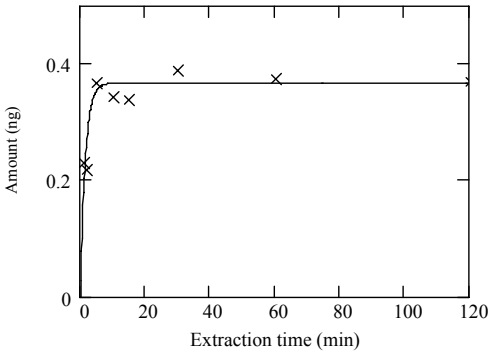
Amount (ng)
0
0.2
0.4
0 20 40 60 80 100 120
Extraction time (min)

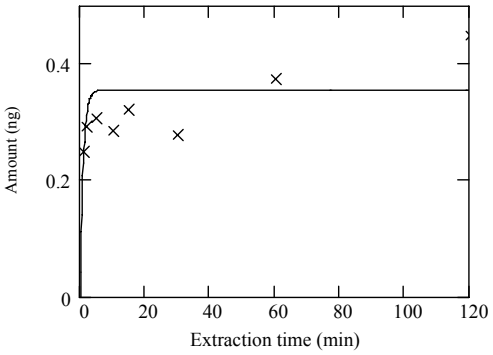
Amount (ng)
0
0.2
0.4
0 20 40 60 80 100 120
Extraction time (min)

(b)

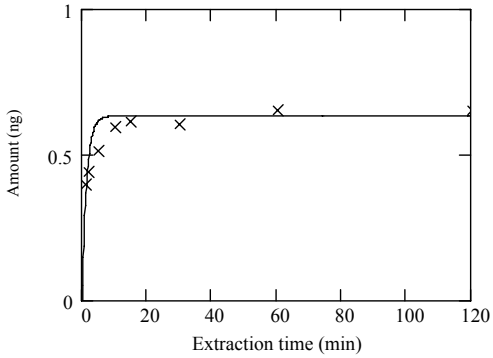
Amount (ng)
0
0.5
1
0 20 40 60 80 100 120
Extraction time (min)

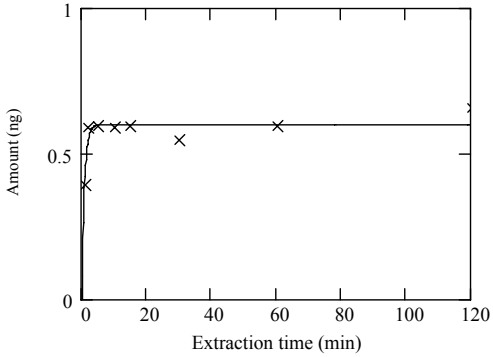
Amount (ng)
0
0.5
1
0 20 40 60 80 100 120
Extraction time (min)

(c)

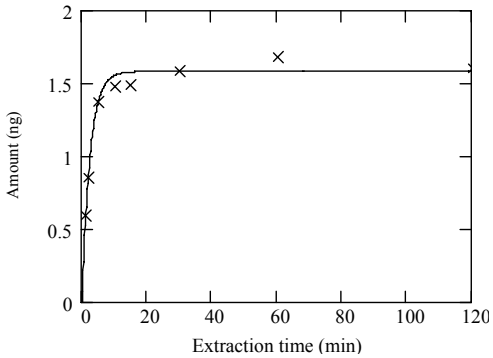
Amount (ng)
0
0.5
1
1.5
2
0 20 40 60 80 100 120
Extraction time (min)

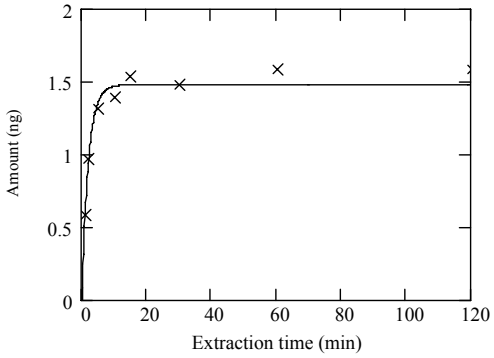
Amount (ng)
0
0.5
1
1.5
2
0 20 40 60 80 100 120
Extraction time (min)

(d)

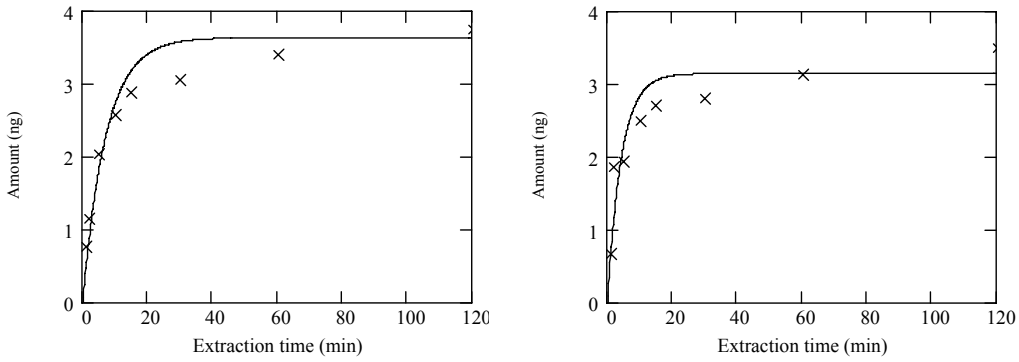

(e)

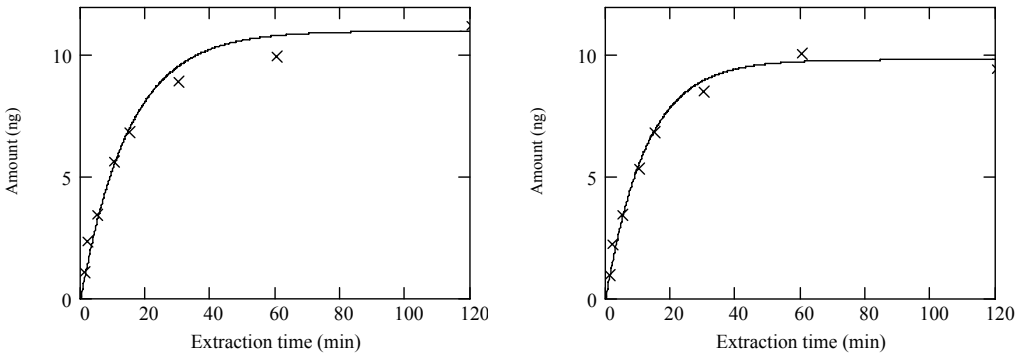

Appendix 2 Extraction profiles of PAH in aqueous solution with (right column) and without (left column) fulvic acid. (a) naphthalene; (b) acenaphthylene; (c) fluorene; (d) anthracene; and (e) pyrene.

(a)

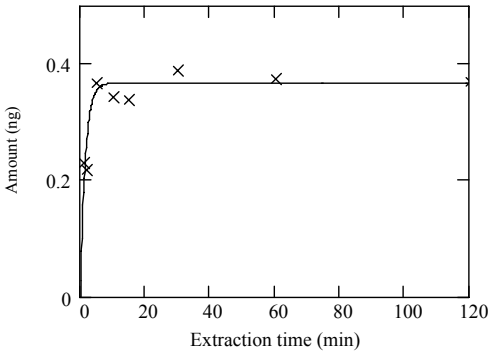
Amount (ng)
0
0.2
0.4
0 20 40 60 80 100 120
Extraction time (min)

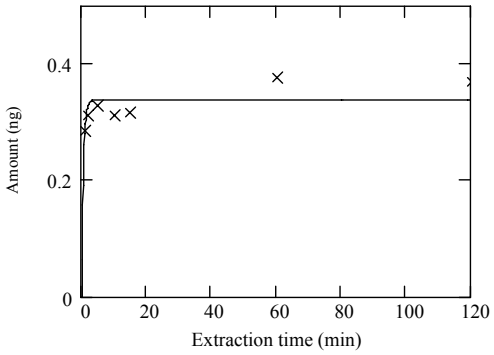
Amount (ng)
0
0.2
0.4
0 20 40 60 80 100 120
Extraction time (min)

(b)

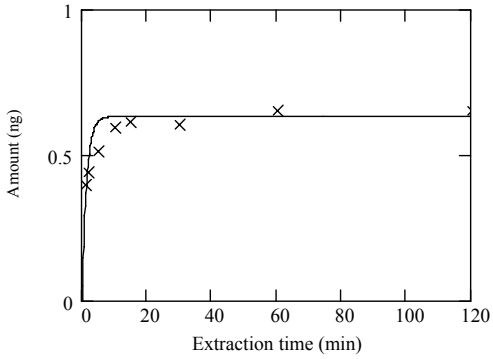
Amount (ng)
0
0.5
1
0 20 40 60 80 100 120
Extraction time (min)

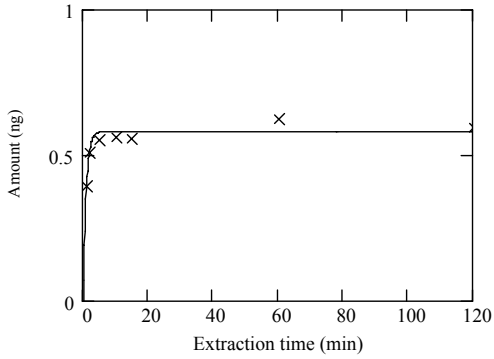
Amount (ng)
0
0.5
1
0 20 40 60 80 100 120
Extraction time (min)

(c)

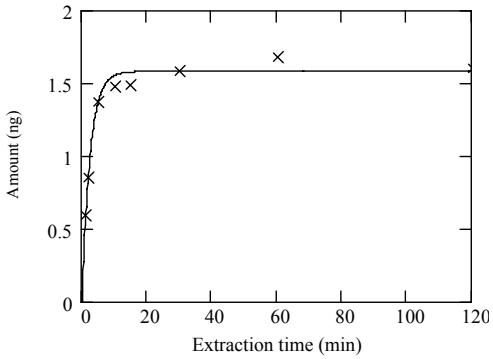
Amount (ng)
0
0.5
1
1.5
2
0 20 40 60 80 100 120
Extraction time (min)

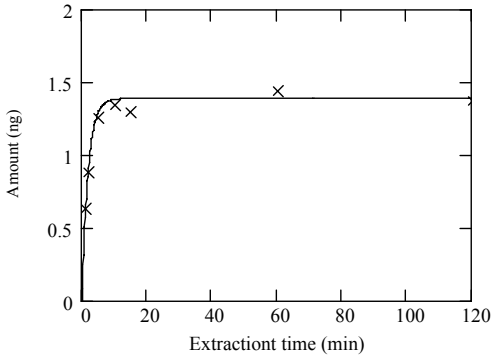
Amount (ng)
0
0.5
1
1.5
2
0 20 40 60 80 100 120
Extractiont time (min)

(d)

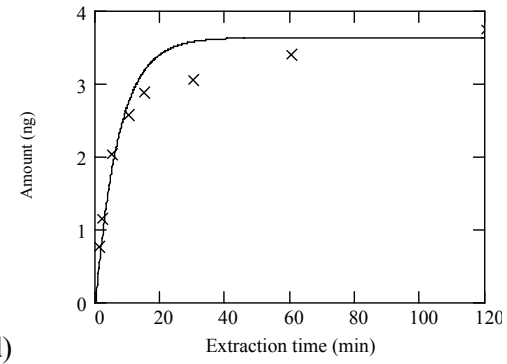

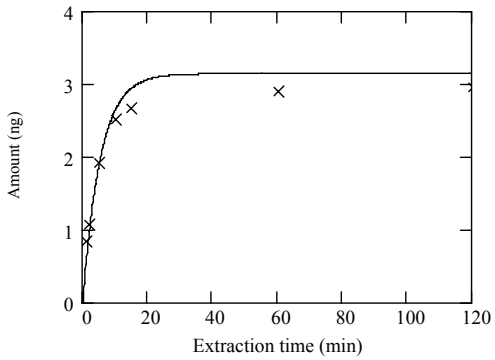

e)

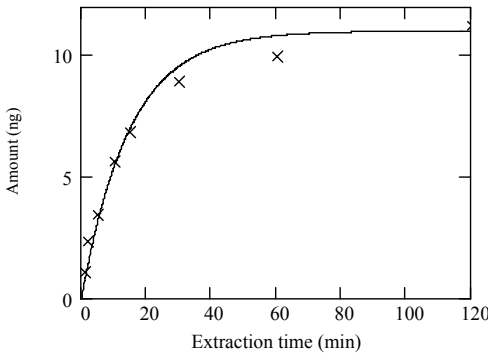

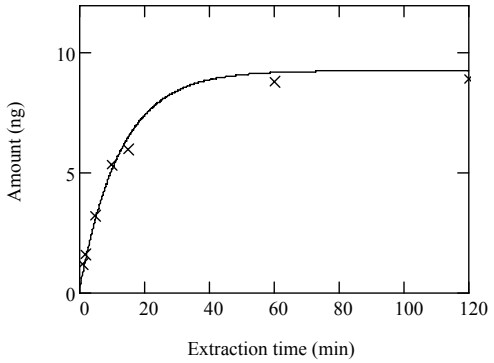

Appendix 3 Extraction profiles of PAH in aqueous solution with (right column) and without (left column) NOM. (a) naphthalene; (b) acenaphthylene; (c) fluorene; (d) anthracene; and (e) pyrene.

Glossary

a	Time constant
A	Surface area of a SPME fiber
b	Constant depends on Reynolds number
B_3	Geometric factor
BSA	Bovine serum albumin
BTEX	Benzene, toluene, ethylbenzene, and xylene
CAR	Carboxen
$\overline{C}$	TWA concentration
C_b	Binding matrix concentration
C_b^0	Total concentration of binding matrix
C_b^∞	Equilibrium concentration of analyte bound onto binding matrix
C_{bs}	Bounded analyte concentration
C_f	Analyte concentration in the fiber coating at the interface of the fiber coating and the boundary layer
$C_f^{'}$	Analyte concentration in the fiber coating at the interface of the fiber coating and the fused silica
C_f^∞	Equilibrium concentrations of analyte in the fiber
C_{HOM}	Concentration of HOM in the matrix
C_i	Analyte concentration observed in time period t_i
C_s	Analyte concentration in the bulk of the sample matrix
C_s^0	Initial analyte concentration

$C_s^{'}$	Analyte concentration in the boundary layer at the interface of the fiber coating and the boundary layer
C_s^{∞}	Equilibrium concentrations of the analyte in the sample matrix
d	Diameter of the fiber
D_f	Diffusion coefficient in the fiber coating
D_g	Gas-phase molecular diffusion coefficient
D_s	Diffusion coefficient in the sample matrix
D_w	Diffusion coefficient in water
DI-SPME	Direct immersed solid phase microextraction
DVB	Divinylbenzene
E	Constant depends on Reynolds number
$\mathbf{F}$	Body force
FID	Flame ionization detector
FLD	Fluorescence dector
GC	Gas chromatograph
h_f	Mass transfer coefficient in the fiber coating
h_s	Mass transfer coefficient in the boundary layer
$\bar{h}$	Average mass transfer coefficient
HOM	Humic organic matter
HPLC	High Performance Liquid Chromatography
HS-SPME	Headspace solid phase microextraction
IHSS	International Humic Substances Society
J	Mass flux
K	Distribution constant

K_a	Equilibrium binding constant between analyte and binding matrix
K_D	Sorption coefficient
K_{fs}	Distribution coefficient between fiber coating and sample matrix
K_{hs}	Distribution coefficient between headspace and sample matrix
k_{as}	Rate constant for the association reaction
k_{dis}	Rate constant for the dissociation reaction
L	Length of fiber coating
LFER	Linear free-energy relationship
LLE	Liquid-liquid Extraction
Log K_{ow}	Log Octanol/Water Distribution coefficient
M	Molar mass
M'	A large number defined as 10000 in this study
MS	Mass spectrometer
N	Magnetic stirrer speed in revolutions per second
n	Amount of analyte absorbed onto the fiber
n_e	The amount of analyte absorbed onto the fiber at equilibrium
nd-SPME	Negligible depletion solid phase microextraction
NOM	Natural organic matter
P	Pressure
PA	Polyacrylate
PAHs	Polycyclic aromatic hydrocarbons
PDMS	Poly(dimethylsiloxane)
PDMS/DVB	PDMS/divinylbenzene

PISCES	Passive *in situ* Concentration/Extraction Sampler
ppb	Parts per billion
ppm	Parts per million
q	Amount of standard desorbed from the fiber after sampling time *t*
q_0	Initial amount of standard extracted onto the fiber
Q	Amount of standard remaining on the fiber after sampling time *t*
QSAR-model	Quantitative structure activity relationship model
R	Pump sampling flow rate (volume/time)
r	Distance between the fiber and the center of the vial
R_s	Radius of the stirring bar
Re	Reynolds number
r_i	Fiber coating inner radius
r_o	Fiber coating outer radius
Sc	Schmidt number
SPE	Solid-phase Extraction
SPMDs	Semipermeable Membrane Devices
SPME	Solid Phase Microextraction
t	Sampling time
t_e	Equilibrium time, defined as the time required to extract 95% of the equilibrium amount of an analyte from the sample
TPR	Template resin
TWA	Time-weighted Average
u	Linear velocity
$\mathbf{u}$	Velocity vector

USEPA	United States Environmental Protection Agency
UV	Ultraviolet
v	Kinematic viscosity
V_f	The volume of fiber coating
V_s	The volume of sample matrix
Z	Diffusion path length
δ_f	The thickness of fiber coating
δ_s	The thickness of boundary layer
ρ	Density of the fluid
η	Dynamic viscosity